
# Assessing Sentinel-1 Imagery for Sea Ice Monitoring in the Denmark Strait

Melissa Arielle Peterson

**Faculty of Life and Environmental Sciences**
**University of Iceland**
**2017**

# Assessing Sentinel-1 Imagery for Sea Ice Monitoring in the Denmark Strait

Melissa Arielle Peterson

30 ECTS thesis submitted in partial fulfillment of a
*Magister Scientiarum* degree in Geo-information Science and Earth Observation for Environmental Modeling and Management

MS Committee
Ingibjörg Jónsdóttir
Rannveig Ólafsdóttir

Master's Examiner
Björn Erlingsson

Faculty of Life and Environmental Sciences
School of Engineering and Natural Sciences
University of Iceland
Reykjavik, June 2017

Assessing Sentinel-1 Imagery for Sea Ice Monitoring in the Denmark Strait
Mapping sea ice in the Denmark Strait using Sentinel-1
30 ECTS thesis submitted in partial fulfillment of a *Magister Scientiarum* degree in Geo-information Science and Earth Observation for Environmental Modeling and Management



Faculty of Life and Environmental Sciences
School of Engineering and Natural Sciences
University of Iceland
Askja, Sturlugötu 7
107 Reykjavík
Iceland

Telephone: 525 4000

Bibliographic information:
Melissa Peterson, 2017, *Assessing Sentinel-1 Imagery for Sea Ice Monitoring in the Denmark Strait*, Master's thesis, Faculty of Life and Environmental Sciences, University of Iceland, pp. 121.

Printing: Háskólaprent
Reykjavik, Iceland, June 2017

# Abstract

Widely-available Synthetic Aperture Radar (SAR) imaging from the Sentinel-1 constellation offers opportunities for sea ice mapping and monitoring. In order to establish the viability of independent classification of new ice formation areas in the Marginal Ice Zone (MIZ) where sea ice presents maritime hazards, an independent classification was done to manually identify and delineate areas of new sea ice formation as conditions cool in autumn and sea ice pack extends into the Denmark Strait. A second analysis incorporated the use of climate data to revisit digitized new ice areas and determine analysis confidence. The analyses were performed for the three autumns that Sentinel-1 has now been available: 2014, 2015, and 2016. Obtained areas were used to run an optimized hot spot analysis to determine areas of significant clustering, perform a spatial analysis to identify patterns, and examine climate preconditions for optimal new ice formation. Autumn 2014 and 2015 showed a similar spatial pattern, while in 2016 ice did not appear in the study area until a month later than normal. 2014 was the year of greatest new formation in the MIZ in the Denmark Strait, followed by 2015, and distantly trailed by 2016. While imagery was very useful for interpretation, the interpretation was much stronger with the addition of corresponding climate conditions which should be considered when developing automated classifications based on Sentinel-1 images.

Keywords: Arctic, sea ice, Denmark Strait, Marginal ice zone, Synthetic Aperture Radar (SAR), Sentinel-1, Mapping new ice, climate preconditioning, Optimized hot spot analysis.

# Útdráttur

Ratsjármyndir úr SENTINEL 1A og 1B gervitunglum Evrópsku Geimvísindastofnunarinnar bjóða upp á margvísleg tækifæri við eftirlit og rannsóknir á hafís. Markmið verkefnisins var að kanna hve vel myndirnar nýttust til að greina nýmyndaðan hafís við jaðar hafísbreiðunnar á Grænlandssundi. Myndirnar voru greindar og flokkaðar m.t.t. nýmyndunar, og niðurstöðurnar bornar saman við veðurgögn til að kanna trúverðugleika. Einnig var veður dagana fyrir nýmyndun skoðað sérstaklega. Þessi greining miðaðist við árin 2014-2016, eða það tímabil sem tunglin hafa verið á braut um jörðu. Haustmánuðirnir oktobér, nóvember og desember voru skoðaðir þessi ár, eða það tímabil sem hafís rekur úr norðri inn á athugnarsvæðið og mikil nýmyndun hefst. Dreifing nýmyndunarsvæðanna var einnig skoðuð, til að greina hugsanleg mynstur á milli ára eða mánaða. Í ljós kom að árin 2014 og 2015 eru nokkuð svipuð, en árið 2016 skar sig mjög úr þar eð hafísrek og –myndun hófst mánuði síðar. Mest nýmyndun greindist árið 2014. Mikilvægt reyndist að hafa veðurgögn til hliðsjónar við túlkun myndanna, og styrkti það mjög alla greiningu. Þetta er nokkuð sem þarf að hafa í huga er farið verður í að flokka ratsjármyndir sjálfvirkt.

Norðurslóðir, hafís, Grænlandssund, hafísjaðar, ratsjármyndir, SENTINEL-1, hafískortlagning, veðurfarsgreining, hitakort.

*Dedication*

*To the advocates of a planet in transition.*

# Table of Contents

# List of Figures

# List of Tables

# Abbreviations

ASCAT - Advanced Wind Scatterometer

CLASS - Comprehensive Large Array-data Stewardship System

DMI – Danish Meteorological Institute

EGC – East Greenland Current

EODIS - Earth Observing System Data Information System

ESA – European Space Agency

FY - First Year [Ice]

GHCN - Global Historical Climatology Network

IMO – Icelandic Meteorological Office

LANCE - Land, Atmosphere Near real-time Capability for Earth Observation System

MET Norway – Norwegian Meteorological office

MIZ – Marginal Ice Zone

MODIS - Moderate Resolution Imaging Spectroradiometer

MY – Multi-Year [Ice]

NIC – United States National Ice Center

NASA – National Aeronautics and Space Administration

NOAA – National Oceanographic and Atmospheric Administration

NSIDC – National Snow and Ice Data Center

SAR – Synthetic Aperture Radar

SNAP – SeNtinel Application Platform

SST – Sea Surface Temperatures

STAR - Center for Satellite Applications and Research

# Acknowledgements

I would like to thank Erasmus Mundus for accepting and funding me in this endeavor by way of the Eramus+ award. Thank you to the European Commission's Education, Audiovisual and Culture Executive Agency (EACEA) for confirming me as a scholarship recipient. I am deeply thankful that I was able to concentrate on my studies for the duration of the GEM program. I have the utmost respect for the European Union's dedication to education, and for including those outside of its borders.

Thank you to my supervisor, Professor Ingibjörg Jónsdóttir, for support during the thesis and for the inspiration to discover the immense importance of this topic. Your guidance throughout the project was indispensable. Thank you as well for the inclusion in Department activities, which were incredibly exciting for me and provided learning in an area that I had been eager to explore.

Thank you to Professor Rannveig Ólafsdóttir and Dr. Raymond Nijmeijer, for your coordination of the program and your kindly support and responsiveness with my many, many questions.

Thank you to all of my lecturers at Háskóli Íslands and at ITC, University of Twente, for guiding the way to further and deeper knowledge in geography and showing me how I can fit into other disciplines in the professional world. I am so thankful to have been exposed to so many great academicians in so many departments including the Department of Natural Resources and the Department of Earth Systems Analysis at ITC, and the Faculties of Civil and Environmental Engineering, Earth Sciences, and Life and Environmental Sciences at the University of Iceland. Special thanks to the many stand-out lecturers for exceptional teaching and support during my time as a GEM student.

Thank you to everyone on the coordinating end of the program for facilitating the school transitions.

Thank you to all of the scientific agencies that made this work possible. Access to openly available scientific data is of paramount importance because knowledge is power. The more analysis we can do, the better off we are as humanity. Thank you to the European Space Agency for the Sentinel-1 imagery, and thank you to NASA for the MODIS imagery. Thank you to NOAA for the climate records and imagery, the NSIDC for the ice index, the NIC for the ice records, and the Danish Meterological Institute for the ice charts. A big thank you to the Icelandic Coast Guard for a very informative flight. Climate data are so important and I am glad there are so many agencies collecting it and disseminating it for the public.

Last, but not least, a resounding thank you to my whole family. I am deeply thankful for the constant support and affirmation from my parents, Heidi and Scott Peterson, my amazing grandparents, Adam and Hilda Linz, my siblings, Amanda, Blake, and Chase, and my dearest friend, Thomas Bartee. You guys are my rock. A special thank you to my GEM friends for the love through the hard times, and to all my friends from home who gave support via video calling, I love you all and am so thankful to have extraordinary people like you in my life.

# 2 Introduction

The year 2016 has played host to some of the largest abnormalities in Arctic sea ice behavior since sea ice records began. It has followed suit of many recent years including 2012, 2011, 2008, and 2005 in setting historical lows for sea ice extent and thickness, and showed alarmingly slow rates of autumn growth (Beitler, 2016). Autumn 2016 saw sea ice extent in the Arctic trailing that of 2012, the year which holds the record for the lowest sea ice minimum since steady satellite monitoring began in 1978 (Fetterer, Knowles, Meier, & Savoie, 2016; Wadhams, 2000). According to the National Snow and Ice Data Center (Beitler, 2017), 2016 set the record minimum sea ice extent for every month from October 2016 to March 2017. The last three years have also broken the minimum records for winter-end sea ice pack maximum extent (Vizcarra, 2017a).

Many years in the last decade have lagged substantially behind the thirty-year climatology in terms of sea ice extent, thickness, and volume. Rising surface temperatures and Arctic sea ice extent are widely-used indicators of the state of the climate, and both have exhibited extreme trends in recent years with surface temperatures setting record highs (Potter, Cabbage, & McCarthy, 2017) and sea ice extent exhibiting record levels of retreat. Arctic sea ice extent at the yearly minimum has decreased by 13.4% per decade (Lynch, 2016).

Generalized warming in the Arctic has made it increasingly unlikely that a few cold years will help sea ice recover to its previous extents and thickness (J. C. Stroeve et al., 2012) because even when it is growing, sea ice is still lacking in extent (J. Stroeve et al., 2008). This is partially due to recent trends in temperatures (Bekryaev et al., 2010; Kumar et al., 2010; Rigor et al., 2002) which are becoming widely apparent as new warm records are set each year, with the first half of 2016 breaking the all-time half-year warm temperature record, since records began in the mid-nineteenth century (Potter, Cabbage, & McCarthy, 2017). Climatological feedbacks, such as the ice-albedo feedback, threaten the prevention of sea ice levels to return to what was recorded in the late twentieth century and amplify the warming effect in the Arctic (Vihma, 2014). It is therefore important to understand the behavior of sea ice in the past, sea ice behavior is quantified and analyzed, and how to increase accuracy of model inputs to aid in projecting what will happen in the future of the Arctic.

Changes in sea ice behavior are described through variables including spatial extent (in which internal open areas are included), actual sea ice-covered area, ice thickness (which are an input to the measure of sea ice volume), drift velocities, ice composition types, and concentrations. It is of increasing interest to study the behavior of sea ice because it has direct impacts on both human activities and future environmental processes in the Arctic Ocean and its peripheral water bodies. Monitoring sea ice is crucial for ensuring safety in maritime operations and for climate monitoring.

Where the North Atlantic Ocean and the Arctic Ocean meet is an area of interest regarding future sea ice behavior because of the effects sea ice can have on shipping, fish farming, and other marine activities in the area. This region is separated into the Greenland, Iceland, and Norwegian Seas, and is often referred to as the Nordic Seas or the GIN Sea. Sea ice has direct implications on human activity because even small ice floes can compromise safety of maritime operations, and ice conditions in the Nordic Seas can change rapidly in ideal sea ice formation conditions, or because of shifting winds or large storms. This area is also worth

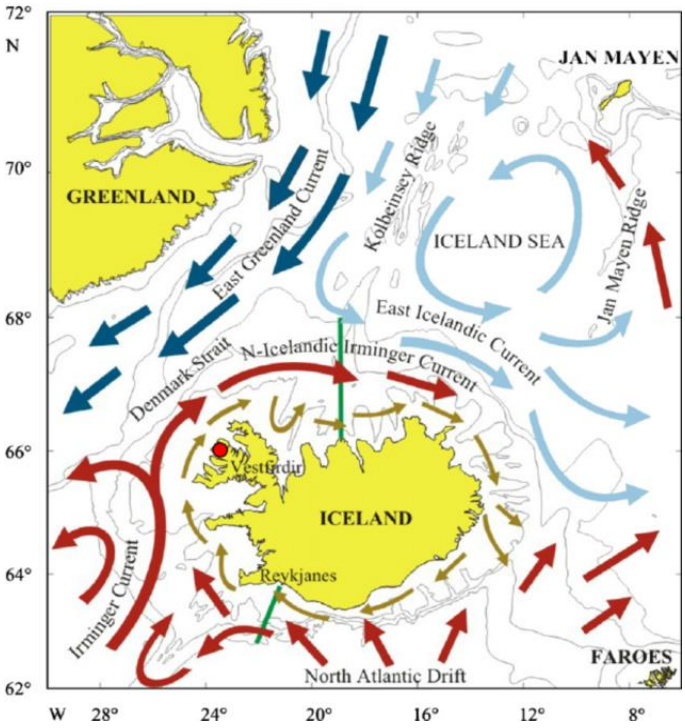


*Figure 1: Currents in the GIN seas. The East Greenland Current bears sea ice from the Arctic Ocean to the Denmark Strait. In the Denmark Strait, sea ice behavior is also affected by the Iriminger Current.* (Jónsson, 2017)

studying for environmental reasons, because it is an area of major oceanic convection, which cycles heat and nutrients through the planets oceans and plays a role in regulating the climate. Sea ice has a particular role in catalyzing oceanic convection, and the subsequent upwelling of cold, nutrient-rich water, which provides fodder for marine ecosystems and water that is unsaturated with carbon, and acts as a carbon sink. Ice enters the North Greenland Sea by way of the Fram Strait, the body of water between Greenland and Svalbard which connects the Arctic Ocean to the Greenland Sea. The area of greatest sea ice export from the Arctic Ocean's Transpolar Drift occurs at the Fram Strait, driven by winds (Wadhams, 2000), and has a strong correlation with atmospheric circulation (Strong & Magnusdottir, 2009; Vinje, Løyning, & Polyakov, 2002). The Fram Strait accounts for about 10% of the sea ice mass export from the Arctic Ocean (R. Kwok, Cunningham, & Pang, 2004), and also serves as the main connection of deep water transport that occurs between the Arctic and the rest of the oceans (Gerland et al., 2006). The sea ice that is exported from the Fram Strait is exported year round, but varies seasonally in flux and velocity (Vinje & Finnekasa, 1986; Widell, Osterhus, & Gammelsrod, 2003). The sea ice flux through the Fram Strait is considered a signal of ice advection in the Arctic (Hansen et al., 2013), and an indicator of ice thickness in the Arctic (Widell et al., 2003).

The ice is composed of multiple types of ice: ice that has formed within the last growing season and has not yet undergone a melt season, called first-year (FY) ice; ice which has survived at least one melt season, called multi-year (MY) ice; and icebergs. In recent years, the ratios of old and young ice have been changing, where the fraction of young ice is increasing relative to older ice (J. Stroeve et al., 2008). Sea ice exported through the Fram Strait primarily by geostrophic winds and the East Greenland Current (EGC) continues to drift southward, at increasing velocities in recent decades (Smedsrud, Sirevaag, Kloster, Sorteberg, & Sandven, 2011), along the coast of Greenland.

As shown in Figure 1, the EGC runs southwards along the coast of Greenland bearing the cold, relatively fresh water from the Arctic Ocean to the south. The Irminger Current brings warmer, saltier water from the North Atlantic up the western coast of Iceland. Where the currents meet can often be seen from remotely sensed imagery due to the sharp contrast in sea surface temperatures (SSTs). Ice export from Fram Strait affects the freshwater balance of the Nordic Seas, which affects oceanic convection (R Kwok, Cunningham, & Pang,

2004). In the cooler seasons, Arctic-borne sea ice survives to pass between the east Greenland coast and Jan Mayen (71.0318° N, 8.2920° W), an island of Norwegian dominion lying northeast of Iceland and east of Greenland. In autumn, as the ocean and the atmosphere cool and sea ice volume flux increases out of the Fram Strait, ice is transported further south, past Scoresby Sound, Greenland (70.5000° N, 25.0000° W), into the Denmark Strait. The Denmark Strait is the body of water between Greenland and Iceland which connects the Greenland Sea to the North Atlantic Ocean. It is greatly affected by sea ice because of its location as a shipping channel and fishing grounds for Iceland.

On its path through the Denmark Strait, sea ice is often captured in gyres adjacent to the coast of Greenland, spurred by currents. On the southwards journey ice is broken into smaller floes. The autumn is characterized by sea ice pack changes in the Denmark Strait, both in the breakdown of ice floes into smaller floes, and in new ice formation between older floes. Certain patterns of atmospheric circulation, in combination with ocean currents, can cause sea ice floes to drift further into the Strait, towards Iceland. As temperatures fluctuate with the coming winter, the southwards-drifting sea ice undergoes periods of freeze and thaw. When Arctic air surface temperatures begin to cool the surface layer of the ocean in the Autumn to -1.8° Celsius, new sea ice formation occurs between the pre-existing sea ice pack in the Denmark Strait. The less dense ice floats on the surface of the ocean and thickens on the bottom and sides through congelation freezing, and can incorporate floes from the Arctic. Freeze-up can occur rapidly, on the order of hours or days.

When conditions are less constantly cold in the Autumn, as has been the case in some recent years, such as 2016, the pack can return to melt conditions when it should typically be undergoing very rapid FY ice growth. The pack is weaker than it used to be with higher proportions of young or new ice (Itkin et al., 2016). Younger ice has undergone less thickening, which is a means of resistance to melt or to be deformed by other ice floes or the coast. This means that the ice edge can be rapidly modified by storms, which occur frequently in the Denmark Strait. Itkin et al., (2016) argues that weaker ice pack is less resistant to winter storms, and presented evidence that storms can irreversibly deform a weaker pack. While exposed ocean in the right autumn conditions can precondition sea ice freeze-up events, unfavorable conditions from variable temperature conditions can prevent the pack from recovering or induce a melt event.

Automated tools have been developed to monitor sea ice extent, concentration, and drift in order to more accurately model the complex mechanics of sea ice behavior. Sea ice extent is monitored in its entire spatial extent from various satellite platforms via optical and thermal imagery, as well as passive and active microwave remote sensing. Other characteristics are monitored by other ocean-based remote sensing techniques, such as buoy-monitored drift velocities (R Kwok et al., 2004; Rigor et al., 2002), and moored upward looking sonar-monitored ice thickness (Gerland et al., 2006). Sea ice is currently monitored by the Icelandic Meteorological Office (IMO) in collaboration with the Norwegian Meteorological Institute (MET Norway) and Danish Meteorological Institute (DMI) (Icelandic Met Office, 2017). The DMI publishes ice charts twice weekly describing the extent and concentration of the sea ice pack (Danish Meteorological Institute, 2017). The United States National Ice Center (NIC) releases daily sea ice pack extents, including the extent of the Marginal Ice Zone (MIZ). The NIC uses a combination of sensors, buoy data, weather and ocean conditions, and expert analysis (U.S. National Ice Center, 2017). The NIC also provides weekly and monthly analyses. There are many satellite-derived products, which provide detailed information on sea ice age, thickness, brightness temperatures, and concentration, such as

daily ice concentration maps from SSM/IS, the Special Sensor Microwave Imager/Sounder, and AMSR2, the Advanced Microwave Scanning Radiometer 2. Passive microwave imagers have built a long, reliable source of sea ice information (Wadhams, 2000). Sea ice has been monitored by use of passive microwave imagery since 1978, providing a thorough record of sea ice extent in the Arctic.

It is useful to investigate additional methods to improve sea ice monitoring in the Denmark Strait, south of Jan Mayen and Scoresby Sound, because that area is widely used in maritime operations, and is also interesting for monitoring changing conditions stemming from a changing climate. The Demark Strait is frequently traversed for shipping and fishing operations. Knowing how sea ice is modified as climate variables change, such as recent increases in air and ocean temperatures, is crucial to aid in safe navigation. While general patterns of sea ice behavior have been established, ideally, remotely sensed sea ice products could be derived automatically in near-real time from a wider array of sensors. As sea ice sees newly reduced extents, there are options for shipping and marine operations to carry on into the autumn season in the Denmark Strait and sea ice formation is delayed. Thus, investigating alternative monitoring methods is important, and would be worth developing further for application to the Denmark Strait for use in navigation and environmental monitoring, particularly in the autumn, when there is substantial interannual variability.

Imagery has been refined using additional electro-magnetic monitoring techniques, such as satellite-mounted active microwave remote sensing, which can provide imagery under more robust conditions than optical sensors, albeit at reduced spatial resolutions. Synthetic Aperture Radar (SAR) is an active imager that provides high resolution imagery regardless of atmospheric conditions or solar illumination. Past satellite-SAR imagers include ERS-1 and ERS-2 (European Remote-Sensing Satellite), RADARSAT (Radar Satellite), and ENVISAT (Environmental Satellite). In 2014, Sentinel-1 imagery, via the European Space Agency's (ESA) Copernicus Program, became available, and in 2016 a second satellite joined the Sentinel-1 constellation. Sentinel-1 imagery enhances the satellite record of sea ice extent, and provides additional details about ice type, extent, concentration, and local conditions that influence the sea ice pack. This mission is important because it provides SAR imagery in medium to high spatial resolution with wide spatial coverage, frequent temporal resolution, and images available in near-real time.

For sea ice monitoring, the structure of the sea ice pack itself is readily evident using SAR imagery. Ice bands, leads, and polynyas are all important features of the sea ice pack which can stretch of tens of meters to tens of kilometers in scale. Compacted and diffuse ice edges allow for wind direction interpretation. Ice fields, bights, and tongues are all identifiable from SAR imagery and speak to the nature of local conditions, including ocean currents and winds (Holt, 2004; Onstott & Shuchman, 2004). Wave action propagation in the ice field is also recorded. The position of the ice edge is additionally important, because it reveals the where the ocean and atmosphere are exchanging heat and moisture, and also provides hazard and safety information for marine operations which can be affected by rapid changes in the dynamic ice edge from high winds, shifting currents, and storms (Shuchman, Onstott, Johannessen, Sandven, & Johannessen, 2004).

SAR is not sensitive to atmospheric disturbances and precipitation, although it can monitor atmospheric interaction with the ocean surface, as well as rain cells (Holt, 2004), and is useful in marine applications for this reason. It is not sensitive to solar illumination, so the sensor is capable of acquiring information after sundown and during the winter season at the

poles, which is an advantage over optical imagers. As polar orbiters, SENTINEL-1 gives frequent coverage of remote areas which have been historically difficult to observe.

SAR imaging is unaffected by weather conditions, but it can show signatures of conditions at the time of image capture on the surface of the ocean. Some of the most frequent atmospheric conditions that are readily identifiable are surface roughening of the open ocean, gravity waves, and atmospheric boundary rolls (where frontal air masses meet and modify ocean backscatter) (Holt, 2004). While moderate winds can facilitate pre-conditioning of ocean water for freeze-up by cooling the surface ocean and creating a slurry of mixed ice particles (called frazil), moderate and high winds often prevent new sea ice from coalescing. High winds are visible on SAR imagery and can provide an explanation for a lack of formation on a certain day with ideal air and sea temperatures.

Sentinel-1 imagery is therefore an informative tool to study sea ice in the Denmark Strait. In order to investigate its utility in sea ice monitoring, new ice formation is investigated using the imagery. It is imperative to identify zones of new ice formation in order to understand how the magnitude of new ice formation may be changing over time, both contributing to the area of the sea ice pack and its mechanical weakness as young ice. SAR imagers offer the opportunity to monitor freeze up in the autumn, spatial hot spots of formation, deformation from storms, and optimal climate preconditions that spur freeze-up. This allows a more complete understanding of sea ice behavior in the Denmark Strait. Not only is new ice formation interesting from a climate perspective, but it also provides more information for marine vessels that make transit in the area during the highly-dynamic autumn period, especially in the MIZ. Testing Sentinel-1 imagery for sea ice monitoring purposes can aid in preparing models and can help indicate whether daily automated Sentinel-1-derived products are feasible for development.

## 2.1 Research Objectives

### 2.1.1 General Objective

To assess the potential of Sentinel-1 synthetic aperture radar imagery for sea ice monitoring applications in the Denmark Strait during the autumn season.

### 2.1.2 Specific Objectives

- To independently identify and map new sea ice formation areas in the Marginal Ice Zone south of 71° North using only SENTINEL-1 imagery.
- To compare mapped areas with other sea ice information products from the National Ice Center and MODIS imagery.
- To identify climatological pre-conditions for optimal new ice formation in the Denmark Strait.
- To determine hot spots of new sea ice formation in the Denmark Strait and to assess the significance of where ice forms.
- To compare how new sea ice formation areas vary spatially during 2014, 2015, and 2016.
- To independently track sea ice floes as they pass south of 71° North from SENTINEL-1 imagery to determine velocity.

### 2.1.3 Research Questions

- How well can new sea ice formation in the Marginal Ice Zone be mapped from Sentinel-1 imagery compared to optical imagery?
- How much ice is forming in the Marginal Ice Zone of the Denmark Strait in Autumn?
- What climate conditions are optimal for new sea ice formation in the Marginal Ice Zone?
- Where are new sea ice formation hotspots in the Denmark Strait?
- How does new sea ice vary on monthly, seasonal, and annual scales as mapped from Sentinel-1 imagery?
- How does sea ice behavior over the past three autumns compare to the preceding decade?
- How can the route of sea ice once it passes south of 71° North and associated velocities be manually tracked from Sentinel-1 imagery?

### 2.1.4 Hypotheses

- Sentinel-1 imagery can be used to map new sea ice formation areas in the Marginal Ice Zone.
- Sentinel-1 imagery will be more robust in the identification of new sea ice formation areas than available optical and thermal imagery.
- Sea ice behavior is changing in the study area.
- Sentinel-1 imagery can be used to make manual classifications of sea ice concentration, and to track ice motion and velocity.

# 3 Literature Review

## 3.1 Role of Sea Ice

The study of sea ice is necessary for a clear and quantifiable input to global climate models. Sea ice is a climate modulator because of its high albedo (Zege et al., 2015) and insulating characteristics (Vihma, 2014), and its behavior affects the climate of the northern hemisphere by influencing atmospheric circulation (Tang, Zhang, Yang, & Francis, 2013; Vihma, 2014). Sea ice spurs a positive feedback with temperature and further ice formation. Sea ice has a high albedo, so it reflects most incoming solar radiation back out to space which provides a cooling effect in the Arctic. Sea ice covers the much darker ocean water, so heat energy from insolation is prevented from absorbing into the surface ocean, helping to keep surface ocean temperatures cool. Sea ice also acts as a damper to ocean-atmosphere heat, energy, and moisture fluxes. The inhibition of these exchanges keeps the ocean cooler, even in a warming atmosphere, because it prevents heat transfer from the ocean back to the atmosphere (which would spur additional warming). Increased temperatures and reduced sea ice would therefore cause more energy transfer to the high latitudes. Sea ice catalyzes the development of more sea ice. When sea ice forms, brine is rejected through a series of drainage channels that form in the ice. The rejection of high concentrations of brine stimulates oceanic convection, and colder water is upwelled from the deep ocean. This surface upwelling encourages further ice formation as well providing fertility for marine ecosystems. Fishing in the ocean has provided a source of livelihood for Icelanders for centuries (Ogilvie & Jónsdóttir, 2000), and now an entire fishery industry depends on the fertility of the ocean around the island.

Changes in sea ice must be monitored because the climate, Arctic residents, and the Arctic ecosystem will all be impacted. Sea ice is a critical component of the Arctic ecosystem. According to (Stroeve et al., 2008), the food web depends on Arctic sea ice because it determines the Arctic cold pool. Fish and other marine animals, as well as mammals like walruses, seals, and polar bears, depend on sea ice and the Arctic cold pool for the basis of life. Indigenous Arctic peoples also rely on sea ice for hunting and travel to sustain their way of life. Many people continue to rely on fishing and fishery production economically.

Sea ice has not proven to be beneficial for everyone. Sea ice travels south along the coast of Greenland on the East Greenland Current, but shifts in weather patterns can cause sea ice floes to drift to the coast of Iceland (Ogilvie & Jónsdóttir, 2000). Historically, sea ice pack has made life difficult for Icelanders by impeding access to coasts, and causing economic livelihood hardship because of Iceland's reliance on access to fishing grounds (Ogilvie, Hill, & Jónsson, 2011; Viking Society for Northern Research, 1981). Sea ice behavior around Iceland has been recorded in various capacities for centuries through a variety of observational sources (Ingibjörg Jónsdóttir, 2006; Ogilvie et al., 2011) and proxy reconstructions (Cabedo-Sanz, Belt, Jennings, Andrews, & Geirsdóttir, 2016). Atmospheric and oceanic behavior can advect ice to the Icelandic coast (Ogilvie & Jónsdóttir, 2000). Sea ice inhibited trade because of hindered access to trade routes (Mann, 2002). Additionally, sea ice was often indicative of difficult springs and cold summers likely because of the relationship between sea ice and the associated atmospheric and oceanic conditions (Cabedo-

Sanz et al., 2016). Sea ice is connected to suppressed inland air and sea temperatures, inhibiting the grass crop (Ogilvie et al., 2009). These conditions were dangerous for Icelanders because farmers could run out of food stores for livestock causing starvation of livestock, and subsequently, people (Ogilvie et al., 2011). Icelanders endured major hardships during the Little Ice Age because of frequent sea ice pack in north and northwestern Iceland preventing trade with Europe and inhibiting fishing activities.

Sea ice has reached the coast of Iceland less frequently in recent years. The exception is the unusual icing of the occasional fjord, as occurred in 2007 due to a blocking high pressure system over Greenland which caused an ice band to drift away from the main pack to Iceland (I. Jónsdóttir & Sveinbjörnsson, 2007). The amount of ice which reaches Iceland is dependent on the quantity of ice in the Denmark Strait, ocean conditions, and atmospheric conditions (Icelandic Met Office, 2017). Coast guard flights are regularly taken to examine the extent to which Icelandic coasts and the Denmark Strait are affected by sea ice, since the ice invades fishing grounds and can make maritime operations treacherous.

The shipping and fossil fuels industries see great opportunities in fast-retreating sea ice. Further implications can come from the potential to exploit resources, such as oil reserves, which will be more accessible in the Arctic due to the retreat of the ice. Retreating ice also opens shipping routes to decrease distances for traded good to travel, however this has implications via increased, direct greenhouse gas and pollution emissions from shipping lanes. There is potential for direct emissions of black carbon soot which could exacerbate an already record-breaking melt scenario of Arctic sea ice (Arctic Circle Secretariat, 2016). Additionally, there is the possibility that shorter routes could stymy increases in route travel. Indirectly, drilling for fossil fuels will add to greenhouse gas emissions in both use and consumption, which will raise air temperatures further, and opens the Arctic to the environmental threat of oil spill disasters which would choke fragile Arctic ecosystems (Arctic Circle Secretariat, 2016). The Arctic already suffers from an amplification of the global rate of warming, so increased emissions directly to that region would have major implications.

## 3.2 Monitoring Changes

Kang et al. (2014) endeavored to learn more about the relationship between Arctic sea ice extent and ice surface temperature in an effort to connect atmospheric variability and interannual sea ice variation. They used the Terra MODIS (Moderate Resolution Imaging Spectroradiometer) sensor and looked for statistically significant relationships between sea ice extent and temperature to attempt to predict sea ice variability in upcoming seasons. A robust lag relationship was identified between sea ice extent and ice surface temperature between 2000-2013, with a one month lag showing the greatest significance.

Air surface temperatures in the Arctic have risen at rates nearly twice as fast as the rate of the rest of the Northern Hemisphere (Bekryaev et al., 2010). Kumar et al. (2010) merged data about from NOAA (National Oceanic and Atmospheric Administration) Land/Sea Merged Temperatures, United Kingdom Hadley Center HADCRUT3v, NCEP/NCAR-R1 reanalysis in a spatially interpolated grid for use in three global circulation models to examine how temperatures are amplified in the Arctic. They identified the contribution of anomalous sea ice conditions in amplifying observed surface-based Arctic ocean warmth.

They determined there is a spatial link between areas of amplifications and sea ice loss, and the pattern of amplification follows the pattern of ice loss.

Other studies have sought to monitor changes in sea ice extent, and what changes that incurs. In a study by Kwok (2014), deformation of sea ice was examined during the beginning of the growing season. Typically, MY sea ice will compose most of the remaining ice at the end of the melting season, but changes in atmospheric circulation in some parts of the Arctic Ocean have encouraged ice convergence, and thusly ridging, of FY sea ice. Typically, thicker ice has greater resistance to melting. This compaction however, opens up areas of low-albedo open water to solar absorption while temperatures are too warm for young-ice formation on the ocean surface, as would be seen in winter in leads and polynyas. This means there is ice attenuation instead of rapid new ice formation. Open ocean also leads to increases in ocean-atmosphere heat and moisture flux which can affect other variables such as air temperature, moisture, cloud cover, and stability in the troposphere, all of which affect atmospheric circulation (Vihma, 2014). These changes are even more perceptible in autumn and winter as the air temperature cools more rapidly than the ocean so the flux from ocean to atmosphere is larger.

Another crucial component requiring study regarding Arctic sea ice are measurements of sea ice albedo and a determination of the fractional cover of melt water ponds. Identifying meltwater ponds is important because as ice melts, its albedo decreases, which speeds up melting. The radiative balance changes as melt ponds form, and melt accelerates. When the ice disappears, open ocean is exposed which further accelerates ocean warming, air warming, and the melting of sea ice. Zege et al. (2015) sought to create an algorithm to continuously monitor sea ice albedo and the fraction of meltwater ponds through the use of satellite-derived data. They used ten wavelengths from MERIS (MEdium Resolution Imaging Spectrometer) and the associated solar and observation angles to create an algorithm which maps melt pond area fractions and the spectral albedo. Despite accuracy complications with determining the fraction of dark ponding on sea ice, the team created a tool which can be modified and applied to other sensors for continuous sea ice monitoring. The algorithm uses a bi-directional reflectance distribution function and atmospheric correction to obtain very high accuracy spectral albedo values. Algorithms which can be run continuously to interpret a constant stream of satellite data can improve the temporal resolution of sea ice albedo studies.

In sea ice monitoring, increased spatial resolution of satellite imagery products with frequent revisit times allows for more information to be extracted about the extent and nature of the sea ice pack. Ice drift can be monitored because the spatial resolution is high enough to identify specific MY ice floes by their surface characteristics, and the temporal resolution is high enough to follow them over a series of hours, days, or weeks to calculate their drift directions and velocities. The availability of more spectral bands increases the information that can be collected by adding additional information to that which can be garnered from only the optical-wavelength bands.

### 3.2.1 Multi-factor Variability

While studies vary greatly in their scopes and methodologies, several commonalities are readily addressed in the nature of sea ice interactions in the Arctic. Common factors mentioned in general discussions about overall impacts on sea ice characteristics include: changes in atmospheric and oceanic circulation, wind-driven variability, anomalous

temperatures, ocean-atmosphere heat flux, moisture and precipitation trends, and ice-albedo feedback. There is a school of thought among many of the authors that despite the complexities in monitoring Arctic sea ice and how its behavior is changing due to different factors, there is not any factor that can singularly explain sea ice behavior and the changes seen in recent years. Many articles directly discuss the links to greenhouse gas forcing, and all concede that this has set in motion interactions which are complex and multi-faceted, and which cannot be explained by natural variation alone. For instance, Kang et al. (2014) points to a combination of ice-albedo feedbacks from natural variability and atmospheric forcing by greenhouse gases to explain the recent behavior of sea ice extent. The effects of changing sea ice are considerable, because of the feedback mechanism that can drive the system to further decreased record low extents which will cascade effects to make the sea ice situation more severe. Itkin et al., (2016) points out the weakening of the material strength of the sea ice pack in massive deformation events which expose more sea water. Other studies and reviews ponder the effects of an altered atmospheric circulation on the northern hemisphere (Bader et al., 2011; Tang et al., 2013; Visbeck, Hurrell, Polvani, & Cullen, 2001)

The interactions described by the different articles vary temporally over seasonal, interannual, and decadal time scales, as well as spatially locally, across the Arctic basin, and remotely throughout the northern latitudes. Tang et al. (2013) discusses possible links between variable Arctic winter atmospheric circulation and mid-latitude climatic conditions. Other authors allude to feedbacks of influence within the Arctic sea ice regime as seen in ice-albedo feedbacks and greenhouse gas forcings (Kang et al., 2014; Wang & Overland, 2009). Vihma (2014) discusses how rapid climate warming in the Arctic has caused sea ice decline to accelerate, and how simultaneously the behavior of sea ice is responsible for amplifying the warming. This complements the statements of Kumar et al. (2010) which posit that sea ice is responsible for much of the variability in Arctic atmospheric circulation, and that circulation can be seen to follow the pattern of sea ice loss. All of the studies agree that some combination of factors in the Arctic are responsible for the short and long term variability being seen in sea ice over the past few decades, which is critical to understanding the system holistically. A main takeaway of this comparison is that all components are linked and a change in one factor will inevitably affect the others.

### 3.2.2 Modeling

With such a variety of interactions to consider, they should be combined in a fashion to examine how the various magnitudes of effects over varying time scales will possibly shape the future. Modeling is a tool used to project what will happen in the climate system. Models are incredibly complex, and a number of modeling approaches can be utilized to project future sea ice behavior. Overland & Wang (2013) compared various model types, including trendsetters and stochasters, to determine the range of uncertainty that can be expected in sea ice cover in the future. They have undertaken multiple studies in the past decade to project when to expect the first nearly sea ice-free summer, defined by coverage of less than one million square kilometers (Overland & Wang, 2013; Wang & Overland, 2009, 2012). They concluded that the first nearly sea ice-free summer would occur much sooner than expected in the models created by the Intergovernmental Panel on Climate Change (IPCC). Later updates to their CMIP5 (Coupled Model Intercomparison Project Phase 5) models, including more recent data, confirmed the expectation that the first sea ice-free summer could occur as soon as the 2030s. Other studies echo similar sentiments about how many sea ice projections tend to be conservative (Stroeve et al., 2008).

### 3.2.3 Further Studies

Throughout the literature, there are several needs identified for future research. The most common needs had to do with cloud radiative forcing. There is high uncertainty regarding the effects it has on radiation, and subsequent interactions with sea ice. Clouds are also responsible for difficulties making measurements in the Arctic because they can seriously inhibit the spatial and temporal resolution of optical sensors. In the study by Kang et al. (2014), 60 – 80% of daily observations per month were missed because of cloud cover. Cloud masking and haze was identified by Kang as one of the biggest challenges for ice surface temperature satellite estimations.

Another area in need of further research was identified by Kang et al. (2014). Changes in the spatial distribution of sea ice extent and thickness by use of remote sensing are required to gain better temporal and spatial resolution about the long-term variability in the Arctic. Better temporal resolution and longer study periods result in a greater number of observations and allow for statistical significance to be determined.

## 3.3 Synthetic Aperture Radar

SAR can overcome some of the challenges of limited observations due to the restrictions on visible sensors. It also has a higher spatial resolution than many passive imagers for sea ice observation. It is advantageous to use SAR as a means for marine observation, because as an active radar, it is very sensitive to phenomena at the ocean surface (Holt, 2004) which can provide ancillary information in addition to sea ice observations.

### 3.3.1 Interpretation of SAR Imagery

There are many different features besides sea ice that are evident in SAR imagery which are useful for determining the conditions and processes which drive sea ice movement and formation. SAR imagery reveals these phenomena at a variety of scales. As ice forms, ice-dependent upwelling can sometimes be observed. During mass freeze-up events, large quantities of brine rejection drive ocean convection, ventilating the deep ocean with oxygen, and providing and upwelling of deep-ocean nutrient rich, cold water (Wadhams, 2000). Often, the boundary layer of different water masses is visible in the vicinity of the sea ice pack (Shuchman, Onstott, Johannessen, Sandven, & Johannessen, 2004). Underwater topography and oceanic convection control the movement of the boundary, and it is closely associated with the behavior of the pack (Shuchman et al., 2004). Colder, fresher runoff from Greenland interacts with warmer, brinier sea water and can impact ice conditions. While SAR only penetrates the ocean surface a matter of millimeters (Holt, 2004) it is useful for identifying neighboring water masses.

One of the most obvious mesoscale features of the ice pack are the eddies of the East Greenland Current as it interacts with the Greenlandic coast and neighboring bodies of water. These large-scale eddies are immensely important because of their impact on sea ice as it travels south along the coast of Greenland. The eddies swirl the sea ice and causes the sea ice pack to deform, exposing open ocean to incoming solar radiation. The numerous processes that affect the ice pack in the MIZ are demonstrated in *Figure 2*.

To interpret microwave data, the signatures of different phenomena in the image must be understood. Radiometrically “cooler” objects appear darker and radiometrically “warmer”

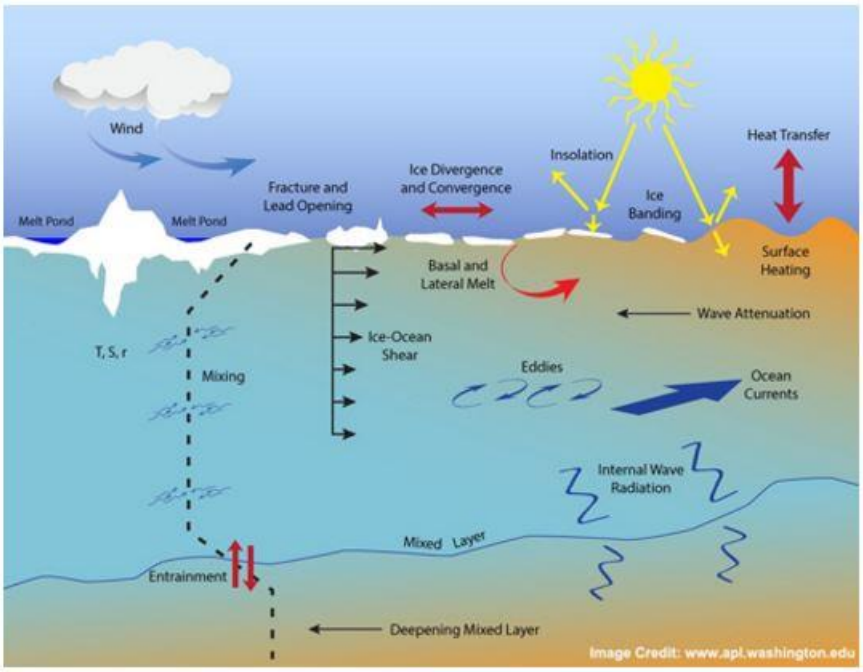


*Figure 2: Illustration of the complex phenomena that occur at the sea ice edge, many of which are visible in SAR imagery . (University of Washington Applied Physics Laboratory, 2017)*

objects appear brighter (F. D. Carsey, Barry, & Weeks, 1992). With active imagers, such as Sentinel-1, the radiometric temperature, or brightness, is based on the return of the signal from the target which is returned to the sensor after it emits a pulse (McCandless Jr. & Jackson, 2004). Radar detection of sea ice is dependent on roughness and the electrical properties of the ice. The dielectric properties of sea ice vary with the salinity of the ice (F. D. Carsey et al., 1992; Onstott & Shuchman, 2004; Wadhams, 2000). The roughness is highly dependent on the density of the ice which is modified with ice age (Onstott & Shuchman, 2004).

Density in sea ice is tied to salinity. Salinity and porosity of sea ice can vary with age and ice development (Wadhams, 2000). Therefore, a wide range of radiometric responses are possible. Ridging (sea ice vertical thickening through in-pack collisions and collapse of the weakest ice) and surface roughness also play a role in affecting the brightness temperature. MY ice (ice that has survived at least one melt season) tends to have stronger backscatter responses than FY ice, FY ice has a stronger response than young ice, young ice has a stronger response than new ice, and new (frazil/grease) ice has different backscatter response than that of open ocean. As sea ice ages, it tends to become less dense, and more porous in the upper layers, as it decreases in salinity via brine rejection, and it acquires vertical variation from accumulated ice deformation of the floe (Rigor & Wallace, 2004). Snow cover on top of the sea ice pack will also modify signatures, as can frost flowers (F. D. Carsey et al., 1992).

Informative atmospheric variables when considering the formation of new sea ice areas are air temperature, sea surface temperature, wind velocity, wind direction. Informative ocean variables for new sea ice formation include the thickness of the surface ocean layer, the freshness of the surface ocean layer, the temperature of the surface ocean layer, the presence of nearby sea ice (because of influence in water mass overturning), and ocean surface roughness. Sea ice can form in both calm and disturbed conditions, with different characteristics (Wadhams, 2000). Conditions that are too rough will prevent freeze-up, but turbulence may pre-condition it for when conditions calm slightly by cooling the surface ocean. These variables have implications on where and how much new sea ice can form, and

are highly dependent on prevailing atmospheric and oceanic conditions and variability. Sea ice formation is also affected by the underlying bathymetry because of how it causes the water masses to interact.

# 4 Methodology

## 4.1 Study Area

The Denmark Strait is the body of water between Iceland and Greenland. The area of interest borders over 750 kilometers of the Greenlandic coast. The uppermost bound of the study area is 71° North, and the sea ice pack is followed south until 67° North, flush with the coast. The longitudinal extent varies with the extent of the ice pack between these two latitudes, primarily between 18° West and 33° West for the duration of the study. The sea ice pack typically descends south of the Scoresby Sound sometime in October as colder temperature stimulate ice production in the Arctic and as ice is exported via the Fram Strait. It will also move eastwards due to the Jan Mayen current

The time of interest is the astronomical autumn season, defined as September 21st to December 21st, for the years 2014, 2015, and 2016. These are the years for which SENTINEL-1 has been operational and has collected data in the autumn season.

The topography of Greenland often stimulates katabatic winds which blow through the study area, affecting the sea ice pack. The bathymetry of the Denmark Strait is made up of the continental shelf from Greenland which eventually drops off into a deeper channel, before decreasing in depth in a shelf off the Icelandic coast, as seen in *Figure 3*. The Greenland Sea, in combination with the Labrador and Norwegian seas, produce most of the oceanic deep water for the northern hemisphere (Shuchman et al., 2004), and are thought to act as a driver of the global thermohaline convection, which is driven by heat and salinity differences (Wadhams, 2000). Wadhams (2000) points out that there has already been a noticeable weakening of convection in the Greenland Sea.

The study area is characterized by highly variable phenomena. It is known for the interaction of several water masses, primarily the East Greenland Current. It is known as an area of high activity of deep ocean convection. Additionally, the area study area crosses the Arctic Circle, at 70 ° North. The Arctic climate is harsh, characterized by cold, storminess, and intense wind activity. There is extreme variability in the weather over the course of the Autumn season, and periods of storminess and calm play a major role in dictating sea ice behavior. There is also a lot of variability from year to year.

This area is of great interest because of the extremely variable climate and ocean conditions that characterize it normally, as well as suspected changes in the normal phenomena, possibly due to changes in the climate system. It is important to monitor the Denmark Strait for changes, because sea ice can move drastically over a period of hours, days, or weeks, which is hazardous for shipping, fishing, and other marine operations which are carried out frequently in the Denmark Strait. Even small MY ice floes can present significant hazards to ships. Therefore, it is important to characterize and quantify sea ice behavior in the Denmark Strait, so that it can be better mapped and modeled in the future.

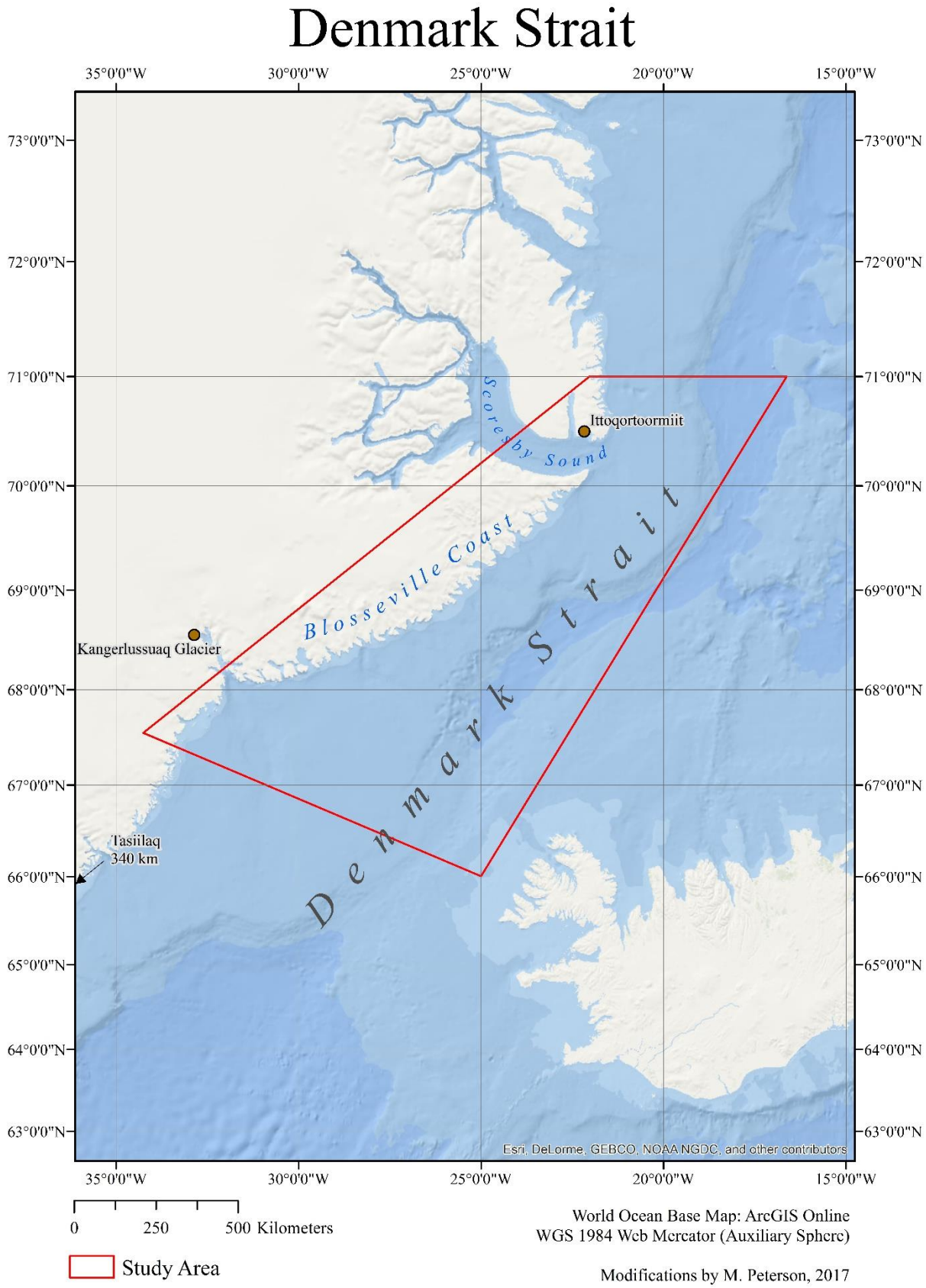


*Figure 3: Map of the location of the Denmark Strait and its underlying bathymetry.*

## 4.2 Data

The European Space Agency's Copernicus Program offers access to SAR imagery of the planet via the Sentinel-1 imager, with most frequent coverage over the poles. Data is accessible through the Copernicus Program Science Hub in four collection modes, and multiple polarizations. Swaths are compiled and mosaicked on the back end, and end-user products are geometrically corrected and geo-referenced.

SAR imagery is ideal for monitoring sea ice because of its cloud-penetrating ability and its independence from solar illumination for imagery capture. In polar regions, optical imagery is difficult to use for certain applications because of frequent cloud coverage and wintertime darkness. The autumn season is the period of interest for this study, and towards the end of the autumn season, and optical imagery, such as from MODIS (Moderate Resolution Imaging Spectrometer) Aqua and Terra, Landsat-8 (Land Remote Sensing Satellite), and AVHRR (Advanced Very High Resolution Radiometer), loses optical coverage of the study area. Even when solar illumination is not an issue, frequent storminess and cloudiness in the Arctic and sub-Arctic regions decrease the number of observations usable in a sea ice study (thermal bands are still available). The Denmark Strait is often clouded as many storm systems make transit across this area making optical imagery not ideal for the study despite high resolution, frequent images of the study area.

SAR is an active imaging technique, and its wavelength is cloud and atmosphere-penetrating. SAR imagery is recorded in swaths as the imager passes the target in a global circuit. SENTINTEL-1 collects images in the C-Band in four polarizations. The polarization used in this study was the dual horizontal (DH) polarization, which is a combination of the Horizontal-Horizontal (HH) and the Horizontal-Vertical (HV) bands. Medium-resolution Ground Range Detected imagery was available for the study area (GRDM) (European Space Agency, 2017). The revisit period for the study area is between one to two days, but varies orbit slightly. The more southerly areas have less coverage because of slightly less frequent coverage. Gaps between images greater than two days occur in the study area, but it is not clear why. Beginning in 2016, more images were made available by the launch of a second imager, SENTINEL-1b (S-1b) to complete the pair with SENTINEL-1a (S-1a) which has been operational since 2014. Imagery in the study is therefore only from S-1a until 2016, when a combination of S1-a and S1-b imagery became available.

SAR imagery is collected in four modes, Stripmap, Interferometric Swath, Extra-Wide swath (EW), and Wave. Level-1 (processing level) GRDM EW imagery was used in this study because it is already geo-referenced and is the primary imaging mode for Sentinel-1 over the study area. EW images are acquired in 5 swaths, and the large spatial coverage has a trades-off lower spatial resolution. Grid spacing in the medium-resolution EW is 40 meters by 40 meters (European Space Agency, 2017). SAR imagers collect in both nadir and side-looking bursts, but the Level-1 GRDM EW images are pre-processed, geo-referenced, and projected. SAR returns are processed, swaths are mosaicked, and ground control points are assigned. For this study, downloaded imagery did not require pre-processing by the user although substantial SENTINEL-1 pre-processing options are available through a free software from the European Space Agency (ESA) called SNAP (SeNtinel Application Platform).

Currently, daily sea ice extents and concentrations are made available by the Danish Meteorological Office and daily extents of the sea ice and the MIZ are made available by the

National Ice Center. The measurements from the National Ice Center combine measurements from buoys, imagers, and sea ice experts and are offered in a variety of formats, including shapefiles for use in ArcGIS. This is an additional tool used in the analysis to determine which new ice formation areas occurred in the MIZ. The National Ice Center shapefiles provide classification based on ice concentrations. The sea ice pack is classified where the sea ice concentration is above 80%. The MIZ is defined by the NIC to be between 10% and 80% concentration of sea ice (U.S. National Ice Center, 2017).

Additional data availability comes from optical imagers, such as MODIS Aqua and Terra which offer high resolution imagery on non-clouded days. MODIS and NOAA (National Oceanographic and Atmospheric Administration) AVHRR are useful imagers for tracking sea ice drift and verifying sea ice parcel movements. However, for the new ice study, optical imagery was not utilized because it is unavailable during part of the study area because of wintertime darkness in the Arctic around the end of November. Much of the study period was also cloud covered, so bright, cloud-free days were rare and often did not coincide with the capture dates of the available SAR images for the Denmark Strait.

Passive microwave imagery makes up the bulk of the remotely sensed sea ice record, most recently with SSMIS (Special Sensor Microwave Imager Sounder), SSM/I (Special Sensor for Microwave/Imaging), and SMMR (Scanning Multi-channel Microwave Radiometer). Derived products include sea ice concentrations at varying spatial resolutions. 25-kilometer spatial resolution data from SSM/I AMSR-E (Advanced Microwave Scanning Radiometer - Earth Observing System) sea ice concentration product were considered in MIZ identification.

During the astronomical autumn season (September 21 to December 21), C-band SAR imagery was collected through the Copernicus Sci-Hub portal. Acquired images were those in the study area, during the study period, where the ice had passed south of 71° North (similar latitude to Jan Mayen). SAR images were sought for every available date in the study period in the study area bounded by 71° North and 67° North, which is just north of Scoresby Sound, southwards along the Greenlandic Blosseville Coast to a degree of latitude south of the outlet of Kangerdlussuaq glacier. Temporal coverage is typically every two to three days, however there are several periods for which images of the area were available had smaller and larger time gaps. The number of images acquired for each season will be addressed in Results.

The autumn season is of interest because it is often covered less thoroughly in the literature. However, with decreasing sea ice thicknesses and extents, it is interesting to explore how autumn climate conditions may be changing the timing of the winter freeze-up or where the freeze-up is occurring.

# 4.3 Methods

## 4.3.1 Mapping New Ice Formation

SAR images were compiled for the completion of this study, and are freely available upon registration with the Copernicus Sci-Hub web portal. SAR images were acquired from the Copernicus Sci-Hub web portal using search queries for the spatial extent of the study area, between 71° North and 67° North latitude, adjacent to the coast of Greenland. Searches were

conducted for all imagery during the time periods as follows: September 21 – December 21, 2014, September 21 – December 21, 2015, and September 21 – December 21, 2016. These are the three years for which Sentinel-1 was available for the astronomical autumn season. Only Sentinel-1 images were queried, and were queried based on acquisition date. Several image footprints were available from routine revisits along the satellite travel path, and these commonly traversed footprints, which showed both the Greenlandic coast and the edge of the ice pack, were acquired. In the cases where the footprint did not include both the coast and the pack, adjacent imagery would be acquired, where available. Primarily, on any given date, the entire sea ice pack in the study area would not be visible, but much of it would be. There were several dates where the satellite acquired images directly over the pack and would allow for adjacent or overlapping images for the same date to be acquired. Where images overlapped for the same date, they would typically have a timestamp twelve hours later than the first image.

A decision was made to use Extra-Wide (EW) images in the Horizontal-Horizontal, and Horizontal-Vertical polarizations. Medium-resolution Ground Range Detected images were the most readily available image product for the study area. Images for each available result were previewed using the preview tool, and assessed as to whether sea ice was present south of 71° North. For dates where sea ice presence in the study area was questionable, the images were acquired and analyzed as to whether they met the spatial criteria of the study with the rest of the image batch.

All available images of the study area during the study period with sea ice presence were compiled into monthly series of images. Sentinel-1 images downloaded from Copernicus Sci-Hub were procured in two polarizations, the HH and the HV bands. The raster bands are packaged as separate images within the Measurement folder of the .zip file from the Copernicus site. Each file was approximately 490 megabytes unzipped. Files were unzipped in file trees, which were organized by year. 76 Sentinel-1 images were acquired for autumn 2014, 77 Sentinel-1 images were acquired for autumn 2015, and 60 images were acquired for autumn 2016. Bands were added manually to ArcMap because they were nested in pairs within the unzipped folders. To combine the two bands for a single date into a single image, the Composite tool was used from the Image Analysis window. This step enhances the image by increasing the information that is readily interpretable from the image by adding colorization to the bands to simulate depth. Composite images were stored as temporary files in .mxd map documents which were maintained by year to reduce the processing power required in each document and to assist with image organization. Raster mosaics were not used because there is no option for Sentinel-1 imagery, and it became tedious to add the separate dual-bands individually. To have added composites, bands would have needed to be added to the document and exported as new files. Instead, the temporary files were used for the duration of the study at no noticeable computational expense. Composite images were stored without their original bands in the map document and were organized into monthly groupings, in chronological order.

To display the bands with minimal spatial distortion, the projection NSIDC (National Snow and Ice Data Center) Sea Ice Polar Stereographic North was chosen. This projection uses the geographic coordinate system GCS Hughes 1980. The projection was assigned to the data frame and the composite images were projected on-the-fly.

Images were assessed to ensure that the ice pack had passed south of 71° North latitude. A grid was displayed in Layout mode over the study area. A shapefile was created and named 71 North

and the 71° North latitude line was digitized in an edit session to about halfway to Jan Mayen. This shapefile was used in each map document as the northernmost boundary of the study area. The southern boundary of the study area was less concrete, because ice formation would not begin until the end of the season, but the study area terminated at 67° North. The only lateral extent consideration for the study area was what could be considered the MIZ, which varied by image. Latitudinal formation extents were the main focus, so long as they were in the MIZ and not the main sea ice pack. Images that did not have sea ice pack that met the spatial criteria were excluded from the study. All days that had imagery with sea ice pack in the study area were considered for analysis.

Initially, each image was analyzed independently from other images, and independent of other data sources. This independent analysis was intended to reveal how much detail could be acquired from a single image by an analyst. The analysis entailed first defining the MIZ so that user-created criteria could be specified for delineating. Many definitions for the MIZ exist. Woods Hole Oceanographic Institution (Jayne, 2015) defines the MIZ as the area where ice cover is sparser, more heterogeneous, more susceptible to deformation, and more mobile. The Marginal Ice Zone Program focuses more on the features of the ice pack, such as banding, eddies, internal waves, and mixing (University of Washington Applied Physics Laboratory, 2017). Some classify the MIZ based on concentration percentage (National Snow and Ice Data Center, 2017; Sea Ice Atlas, 2017; Strong & Rigor, 2013). The NSIDC also adds the following, "…a part of the seasonal ice zone that varies in width (100 to 200 kilometers) that extends from the ice edge into the pack, where waves and swells affect the ice, often characterized by highly variable ice conditions."

The analyst used a certain set of use-defined criteria (*Figure 4*) in order to make the study most useful for the maritime operations. The criteria were self-defined based on the many definitions, and on the indirect objective of the study: maritime safety. Thus, if a ship would be at risk from accessibility to sea ice pack edge in a certain area, it would be considered marginal ice. Isolated sea ice bands do occur, and they were considered as marginal ice. If the parcel of ice was susceptible to open water and wave action, it was considered marginal. Waves disturbing parcels of ice somewhat internally would be considered of the MIZ, if it was clear the concentration of the pack was less than 8/10. Less than that proportion, it was deemed better to air on the side of over-digitizing main pack, than neglecting areas that may seem less hazardous from the ocean surface. Decisions were made with caution and uncertainties were mark instead of left undigitized because in maritime safety, even small ice floes can present a serious hazard. The MIZ and the ice edge are also extremely variable, both in location and in behavior. Overall, sea ice extent is of interest for climatological purposes, but daily imagery provides planning abilities for marine activities that need to occur in the area. Vessels can become trapped in ice because of the high spatial variability of sea ice because of wind changes and frequent storms. The ice edge is responsive to dynamic mechanical processes, such as the movement of ice or deformation events, as well as thermodynamic processes such as ice formation, ablation, or melt. Where the wind blows towards the ice pack it forms a compact, edge where the ice is pushed against the pack, and where the wind blows off-pack, a diffuse edge forms which can make MIZ identification more difficult. This is because a diffuse edge will scatter ice to lower concentrations and reduce the brightness signature.

Once the MIZ was distinguished, it was necessary to determine if there appeared to be new ice formation in or near the MIZ. This requires knowledge of features that are often present in SAR imagery and the variety of backscatter effects that are present in the imagery.

## Criteria

**Marginal?**

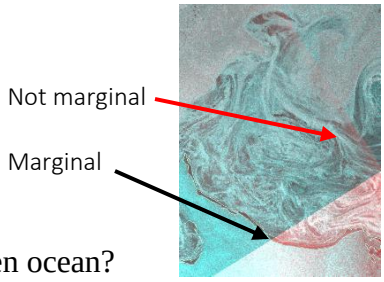


- Is the new ice patch subject to wave action?
- Is there a direct line-of-sight to open ocean?
- Is the patch sheltered between two larger ice gyres?
- Is there are clear band of ice separating the ice from open ocean?

**New ice?**

- What is the color contrast with the surrounding areas?
- Is the pattern typical for new ice formations? Streaky, thin, and dark?
- Is it occurring near or on the edge of an eddy or the ice pack?
- Is there clear signage that the patch is being affected by weather or may actual be an artefact of the weather?

**Size?** **|← 500 m →|**

- Is the patch diameter greater than 500 meters in more than two directions?
- Is a small size patch likely part of a nearby cluster? Is it near enough for inclusion? Is it the same color and texture?

*Figure 4: Specific criteria designated for digitizing new ice in the MIZ in this study.*

Radar backscatter occurs because of roughness differences of the target and differences in the dielectric properties of the target. For sea ice and open ocean applications, there is a clear difference in backscatter between the land and the ocean with the land (the coast of Greenland) backscattering brightly, and the ocean returning as darker. Sea ice has a distinctive appearance on SAR imagery which is why SAR is an excellent choice for sea ice monitoring purposes. The pack appears as a variety of returns, brighter than the ocean, and flush with the coast. When there is snow on both the land and the ice, it was more difficult to discriminate the exact boundary; however sea ice has temporal variation in backscatter, and will vary on smaller scales.

Surface roughening of the ocean is a common feature when there are high winds over the imaged ocean area. Frontal movements, advection, katabatic winds, and lee waves are all identifiable

because of footprints on the imagery. While SAR only measures the first few millimeters of surface ocean, cold and warm water boundaries can often be identified. Indeed, weather systems can also be identified as they move through the area because of long linear impressions that are left with clear surface roughness differences on either side.

*Figure 5: An example of new sea ice formation adjacent to a pre-existing ice band. Sentinel-1 image, October 12, 2014. European Space Agency.*

Backscatter returns to the radar sensor vary widely based on the dielectric properties and roughness properties of the ice surface. These properties change substantially as ice ages, with MY ice appearing differently that FY ice, young ice, or nilas/frazil/grease/new ice. New sea ice formation has properties very near that of sea water, such as high brine concentration, but appears darker because of the dampening of Bragg waves that occurs with new ice formation (Onstott & Shuchman, 2004). New ice formation in calm ocean conditions versus new ice formation in disturbed ocean conditions have markedly different manifestations on the SAR imagery; but both new ice formation in calm and disturbed conditions bear much darker returns than their surrounding areas. Older, MY ice has undergone the formation of brine drainage tube formation, and likely the flushing of much remaining saline with melted snow pack and surface ice. Because MY ice has been flushed of brine in the surface layers, they are more porous and less dense. MY floes are also distinguishable from having acquired a hummocky topography from cumulative deformation and melt. The amount and type of deformation a parcel of sea ice has undergone is also visible from SAR imagery because it will alter the backscatter to the sensor. MY ice exhibits surface volume scattering as opposed to FY ice. New sea ice and FY sea ice have more lossy (where electrical information dissipates) returns to the imager (Shuchman et al., 2004). Considering topography alone, FY ice formations are flat and smooth, in comparison to MY formations which can tower several meters in height. The presence of snow on sea ice can also drastically change the backscatter from a specific parcel.

Deformation of FY versus MY ice will result in differing topographies, and subsequent backscattering. FY ice is the deformation of flat, smooth ice. When pressures increase enough as ice parcels are converged by wind, surfaces rupture in long, linear edges. FY ridges protrude from the ocean surface and the sea ice pack as jagged ridges and are easily distinguishable from MY ice floe ridges, because MY floes have been subject to melt and weathering. Melt pools form on ice during the summer, and melt will reduce the height and jaggedness of ridges. Surviving floes are considered MY ice and are identifiable by undulating, hummocky topography. These characteristics were considered in the analysis, because signatures of different kinds of ice will vary based on daily conditions, and can make independent classification difficult. The various responses within the pack were differentiated from new ice areas in the classification and were

used to locate sea ice pack edges, because new ice often forms near the pack edge, as demonstrated in *Figure 5*. On images where the contrast was low, attention was paid to the specific structures in the pack to ensure that dark backscatter responses were new ice, and not recently frozen young ice, or surface melt signatures.

In the composite imagery in ArcMap, the specific backscatter of new ice formation areas would appear as deep, cherry red, almost black expanses of water. These returns indicate areas of very calm, very cold, water. The new ice formation in calm conditions begins as grease ice, and there is very little backscatter to the sensor, which accounts for the dark appearance of new ice areas. The physical reason for this phenomenon is that Bragg waves are diminished in grease ice, reducing backscatter returns to the sensor. As grease ice turns to frazil ice, and as frazil ice turns to nilas, which, through congelation growth, thickens to FY ice, there are gradually more backscatter returns to the radar. The backscatter returns to the radar increase as the ice thickens on the bottom and widens on the edges. Additionally, new ice formations will have increased returns as they mature from grease ice to pancake ice because of newly formed raised edges as they expand into larger ice pans, as used to occur often in the Odden ice tongue. During analysis, dark returns in the MIZs, near ice bands edges, and in between ice gyres were sought after.

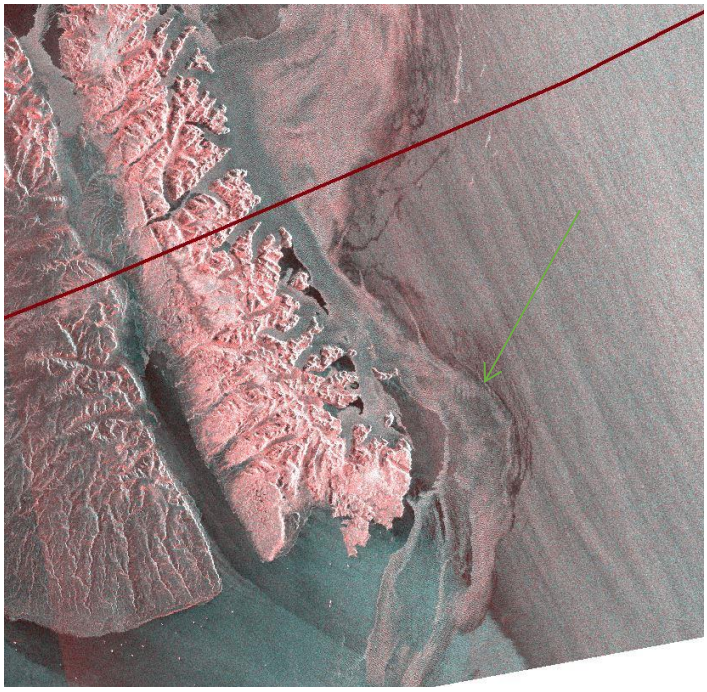

*Figure 6: A Sentinel-1 image with ice formation during conditions where the ocean is disturbed. The red line is the northern bound of the study area at 71 ° North. The ice pack is indicated with an arrow. October 21, 2014. European Space Agency.*

However, new ice can also form in disturbed conditions, but appears differently because the ice will form differently in agitated conditions, as seen in *Figure 6*. Oftentimes, the wind will disturb the upper surface of the ocean causing the surface to appear bright, an uneven turquoise and cyan in Composite. New ice bands were characterized by roughly linear, jagged, often branched tendrils reaching out into open ocean, typically bright red in composite. When temperatures increase and there is melt on the pack, signatures decrease in range and the contrast of the resulting image decreases as well. Often, these conditions are too warm for new ice formation and very little, or no, new ice formation can be found in images in which this occurs. In this stage of the analysis, this was only inferred from the image backscatter, as were other potential false positive features such as weather fronts, atmospheric turbulence signatures, and adjacent water masses.

One shapefile was created for each raster composite image pair. Specifications for the shapefiles were made in the NSIDC Sea Ice Polar Stereographic North projection. Once the dark patches met the appropriate classification criteria, they were digitized in the corresponding daily shapefile, as

seen in *Figure 7*. A text field was added in each shapefile called "Confident" with the purpose of attributing the level of confidence in that specific digitized parcel being a new ice area in the MIZ. New ice areas could be expansive and extend for tens of kilometers in either tendrils or massive pools. If new ice returns seemed to match the surrounding ocean conditions, they were marked with a Confident attribute. A "Y" for Yes was assigned for parcels in which all criteria were met and there was certainty in the parcel's classification. A "N" for No was assigned for parcels in which the backscatter was unclear, but the surroundings seemed to reflect the appropriate criteria, the signal was obscured by the merging of swaths, or if it was unclear whether the parcel was in the MIZ. These classifications were revisited later in the study in the secondary analysis. A third classification, "N-Coast" was reserved for parcels that appeared to have new ice conditions, but were located immediately adjacent to the coast of Greenland. These cases could be lee-formation from katabatic winds blowing off of the land, and would thus have a different reason for formation and were classified separately. However, where the parcels occurred in the MIZ, they were considered confident, and thus included in subsequent analyses because they would add to ice formation that could prove a hindrance to marine operations.

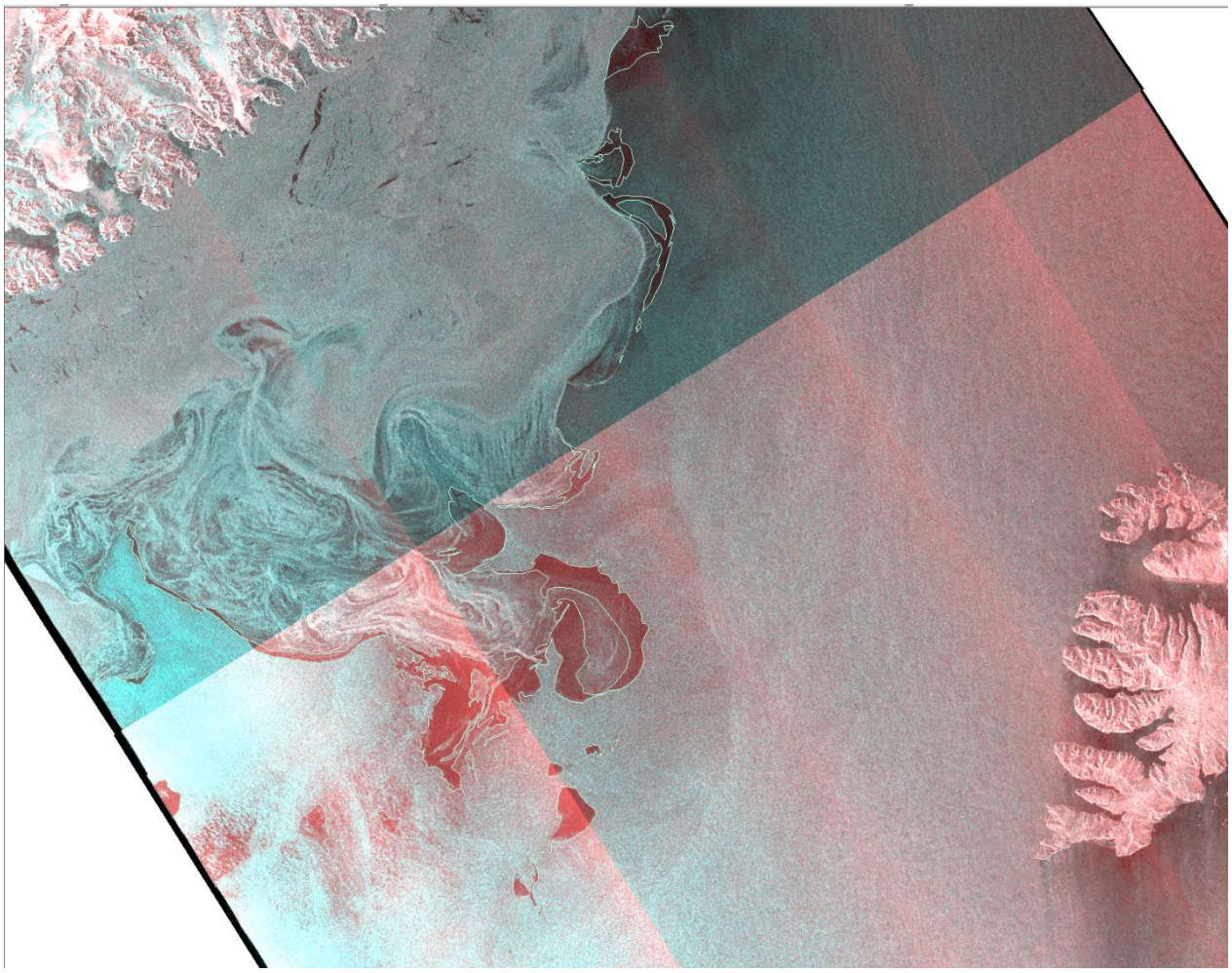

*Figure 7: Example of how parcels were digitized. New ice was digitized with a light green border at the edges of the ice pack. Sentinel-1 image, Dec. 5, 2016, European Space Agency.*

Of particular interest, is the possibility of algae-excreted biogenic oils, which exhibit backscatter similar to that of new sea ice forming in rough conditions, albeit with a different spatial pattern. The pattern appears more squiggly and condensed than that of new sea ice bands. These possible algae areas occur in early October 2015, and are of interest, because algae often bloom in September as ocean overturning accelerates with the southwardly-descending sea ice, which catalyzes an upwelling of nutrients to the Greenlandic Coast. However, October is a much later time than the algae would still usually be present. This is a potential area to consider further, as air and sea surface temperatures, as well as oceanic convection timing may be changing. Areas in October 2015 were thus marked as not-Confident, despite displaying the typical backscatter signal near likely new ice formation patches.

There are other marine phenomena that are important to recognize in interpreting sea ice from SAR imagery. These include cell and roll vortices, such as atmospheric boundary layer rolls. These appear on imagery as long, dark, uneven streaks. This can often appear through marginal areas of the ice pack because they show areas of high air and sea interaction. The dark backscatter returns can be misinterpreted as new ice areas. Karman vortex streets occur when wind blows evenly over topography and exhibits vortices downwind of the topography. More often, atmospheric gravity waves and lee waves appear in the study area, and indicate coastal atmospheric turbulence. Lee waves form perpendicular to the direction the wind is blowing, whereas boundary layer rolls form parallel to the direct from with the wind is blowing. Small waves can also be observed in the ice pack, albeit on much smaller scales than atmospheric gravity waves or boundary layer rolls.

The EGC and coastal gyres will swirl the pack ice, and oftentimes create formation conditions within the pack. This happens both in the main pack and in the MIZ. In the MIZ, new ice formation areas can vary widely in shape and extent, however. In many cases, new ice returns will be too small to be considered significant formations, and so these were considered separately in the analysis with below-threshold point placeholders in shapefiles that were created for each month using the same spatial reference as the polygon new ice area shapefiles.

It is worth noting the first ice dates in the study area occurred in October of both 2014 and 2015. First ice did not occur in 2016 until November, and thus there are eight months of analysis. No sea ice pack had descended into the study area by September of any of the three study years for which Sentinel-1 was available. Thus, the study was broken into 8 monthly sections, instead of the expected 9.

After the completion of the analysis, the Data Management merge tool in ArcMap was used to created monthly aggregate shapefiles as a supplement to the daily shapefiles, so that further processing options would be more manageable, where a fine temporal resolution was not required. These were used as an input for the initial round of Hot Spot analysis.

Once the first round of new ice classification and analysis was completed, a secondary round of confirmation analysis was undertaken. Each SAR image and new ice shapefile pair were revisited with additional data sources to create a more robust analysis. In an ice center, multiple data sources are combined to create sea ice analyses. In this study, parcels were confirmed to be both in the MIZ and as indicative of local conditions. Polygon features in the new ice shapefiles were marked as Confident if the conditions were agreed with the backscatter response.

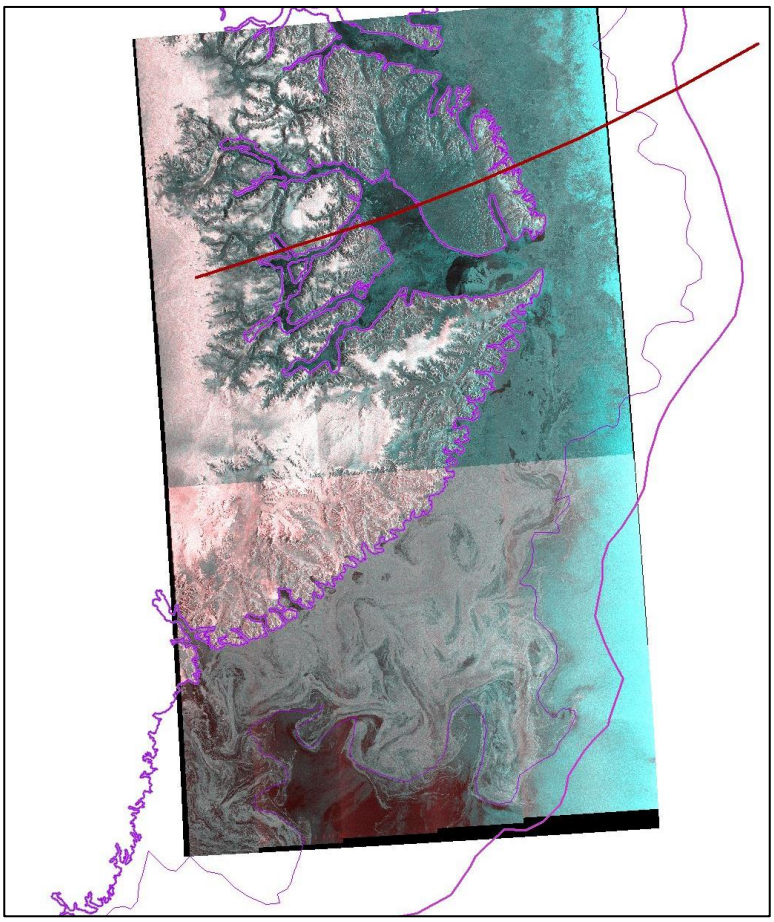

*Figure 8: An ArcMap display of Sentinel-1 image overlaid with the ice edge/MIZ product from NIC (purple) for that day (November 24, 2015).*

To confirm feature locations in the MIZ, daily shapefile products of the ice edge and the marginal ice zone were downloaded from the United States National Ice Center. Shapefiles were queried by image date through the NIC "Products" web page. The specific product selected in the query was the "MIZ Shape" for the Arctic. Shapfile packages were extracted before being imported into the corresponding ArcMap yearly maps. Once the NIC data were added to the maps, they were displayed with the corresponding Sentinel-1 imagery, as seen in *Figure 8*. The imagery was projected on-the-fly and displayed with outline-only symbology to determine areas of agreement between the NIC shapefiles and the initial MIZ new ice formation analysis. Symbology was modified to display to the two classes of the shapefile differently in order to quickly discern the main sea ice pack from the MIZ. For each daily image, the Marginal Ice Zone overlay was scrutinized for ice patches which were not included in the NIC file (as seen in *Figure 9*), and climate conditions for the day, including wind direction and velocity, sea surface temperature, and air temperature were used to confirm the boundary.

Digitized new ice formations that were greater than 1000 meters from the zone were re-evaluated. The 1000 meters threshold was chosen for consistency purposes, to allow for error on the part of the NIC shapefile where conditions did seem consistent with new ice formation, and to allow for slight spatial offset due to projection inconsistencies between the data types. Areas outside of the threshold were evaluated with conditions and were deleted where, upon further inspection, they were not consistent with the climate conditions or the NIC daily shapefile. Where areas seemed consistent with the conditions, but were not in agreement with the NIC MIZ specifications, they were marked as Not-Confident, if the parcel appeared to meet all other criteria. In combination with additional data availability from optical sensors and wind data, further decisions were made in order to refine the parcel boundaries and to ensure Confidence where it was assigned. Specifically, if a boundary was unclear, an image would be acquired from MODIS Terra or Aqua, or AVHRR, dependent on availability due to solar illumination or cloud cover. MODIS images were accessed from the LANCE (Land, Atmosphere Near real-time Capability for Earth Observation System) MODIS Arctic imagery subset, and from the NASA (National Aeronautics

and Space Administration) EODIS (Earth Observing System Data Information System) Worldview web portal.

Optical images were displayed side-by-side with the SAR imagery to make a comparison, as seen in *Figure 10*. Optical images were useful where conditions were very low in contrast, and would confirm whether wind roughening was occurring because of a meteorological system passing through the study area. ASCAT (Advanced Wind Scatterometer) 25-kilometer wind velocities and directions from METOP-A (Meteorological Operational satellite) were obtained through the NOAA STAR (Center for Satellite Applications and Research) web archive and would be compared side-by-side with the SAR imagery for the closest time stamp. ASCAT wind maps are available two times per day, on most days. Sea surface temperatures were collected for use, particularly in the beginning of the autumn, to confirm whether ice formation was possible in certain locations. NOAA CLASS (Comprehensive Large Array-data Stewardship System) was queried for 50-kilometer archived sea surface temperatures in a dataset that has been discontinued from July 2016 from National Environmental Satellite, Data, and Information Service (NESDIS). The NOAA daily Global Historical Climatology Network (GHCN) was queried to obtain daily archived air temperatures from Tasiilaq and Ittoqqortoormiit when they were available. Wind velocities and directions, sea surface temperatures, and air temperatures were recorded in an Excel spreadsheet for use in the climate pre-conditions section of the analysis. Data of unconfirmed quality were omitted from the study, despite eliminating many days of air temperatures. This was done to prevent possible errors that may come from temperature fluctuating above and below the freezing point.

The optical imagery and the ASCAT wind data would confirm where and when a system passed through, which assisted in identifying features which could be confused with new ice formation, such as boundary rolls and gravity waves. These atmospheric signatures often occupy the same

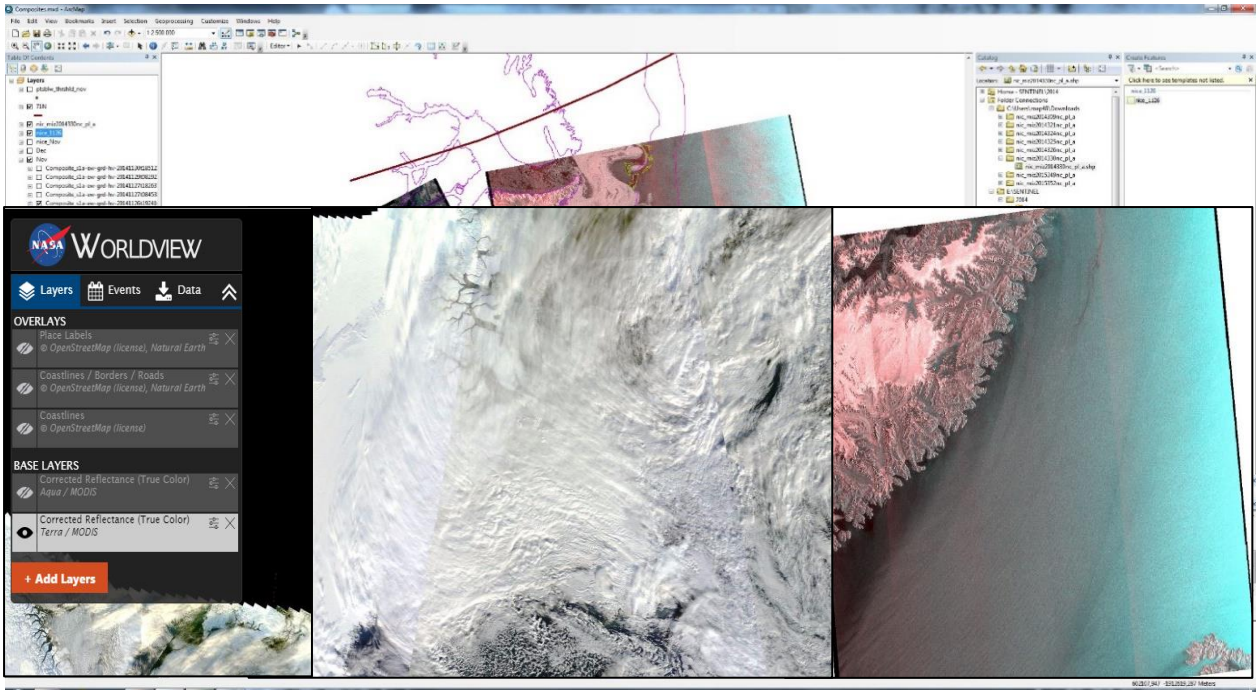


*Figure 10: Using optical imagery from MODIS to confirm storminess, as evidenced by ocean surface roughness, in the Sentinel-1 image. October 19, 2014. Courtesy of NASA and ESA.*

backscatter signals in SAR, so during the initial, independent analysis they were digitized and marked "N". During the secondary analysis "N" classifications were revisited and confirmed or removed by use of the weather data and optical imagery. Temperature data aided in expelling potential formation areas caused by weather, where there could not have been formation because air and sea surface temperatures were too high. The goal was to ensure that the confident parcels would be as accurate as possible in area calculations. For each date, a qualitative log was kept of local conditions versus the observed ice formation.

Later, the edited shapefiles were used as inputs in the climate analysis to determine what climate conditions seemed to spur the most new ice formation. The final daily shapefiles were merged using the Merge tool in the Data Management toolbox in ArcMap for input into the confirmed Hot Spot analysis. Merges were made for each month of daily polygons, for each season (labeled annually), and were combined into a shapefile including all formation areas from all formation days across the three autumns. Exact areas were calculated in kilometers by adding a field to each monthly shapefile's attribute table, in the "Double" data type and Calculating Geometry for area. Statistics were retrieved from the attribute table Statistics function.

Over the three years, 2,138 polygons were digitized (*Figure 11*). Of those, 1,651 were confident, not including the coastal formations. When the below threshold formation areas were added in, there were 3,416 digitized features over the course of the three autumns.

### 4.3.2 Hot Spot Analysis

The density of the digitized new ice areas is of interest, because it will indicate which areas are most productive, given certain climatic conditions. This information can be an input to a model or used to inform safety decisions for marine operations in the Denmark Strait. Furthermore, the extent and locations of new ice formation areas can be used to describe variations in sea ice behavior south of Scoresby Sound. Historically, sea ice south of Scoresby Sound is extremely variable which had had profound effects on marine operations. However, with changing climate conditions, this area is interesting in order to gauge oceanic response to atmospheric changes. The Fram Strait is the area of greatest sea ice volume export, and thus is used as a barometer of Arctic sea ice production. Similarly,

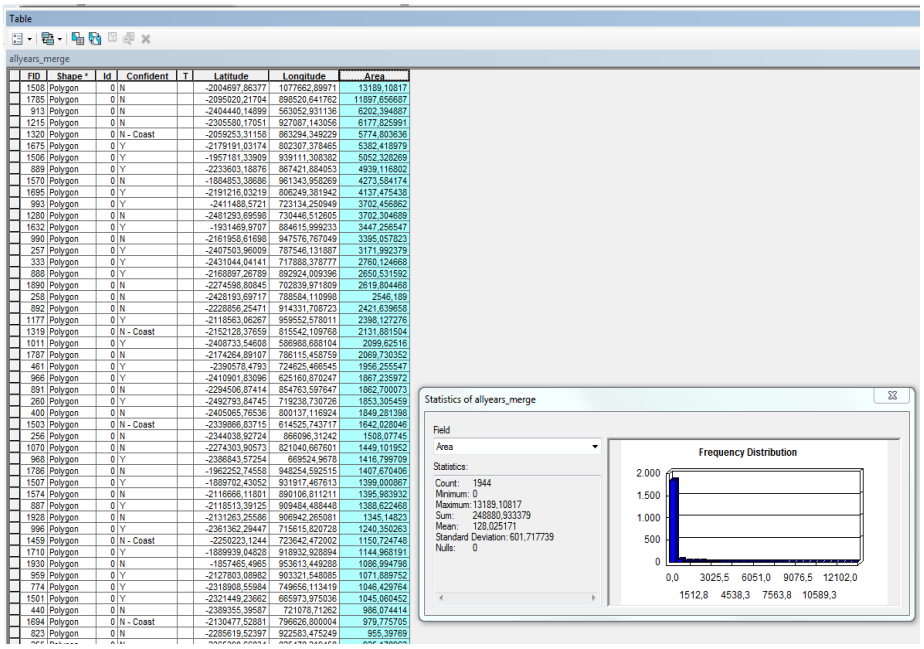


*Figure 11: Table, histogram, and summary statistics of the area of new ice formation for all years from ArcMap .*

the Denmark Strait can be used as a barometer for climate-dependent ice production south of the Arctic.

A heat map expresses the density of a phenomenon in a certain location. In the case of this study, the heat map would express which areas saw the most formation over the three autumns. This would be a density surface. However, in the case of the heat map, the statistical significance of the clustering is overlooked. Heat mapping differs from a hot spot analysis, because a hot spot analysis accounts for spatial autocorrelation of presence and absence.

The Hot Spot Analysis tool in ArcMap aggregates the data (incident data in either points or polyons), chooses an appropriate scale for analysis, measures data clusters based on neighborhoods or instances, and applies corrections for biased sampling or false discoveries (for instance due to multiple testing and spatial dependence) (ESRI, 2017). Using the Getis-Ord $G_i^*$ statistic, spatial association and the statistical significance of that association (Getis & Ord, 1992) is determined and displayed in confidence intervals, called Gi-bins in ArcMap. The output also adds z-scores and p-values to the attribute table. The Getis-Ord $G_i^*$ Statistic is examined in *Figure 12*.

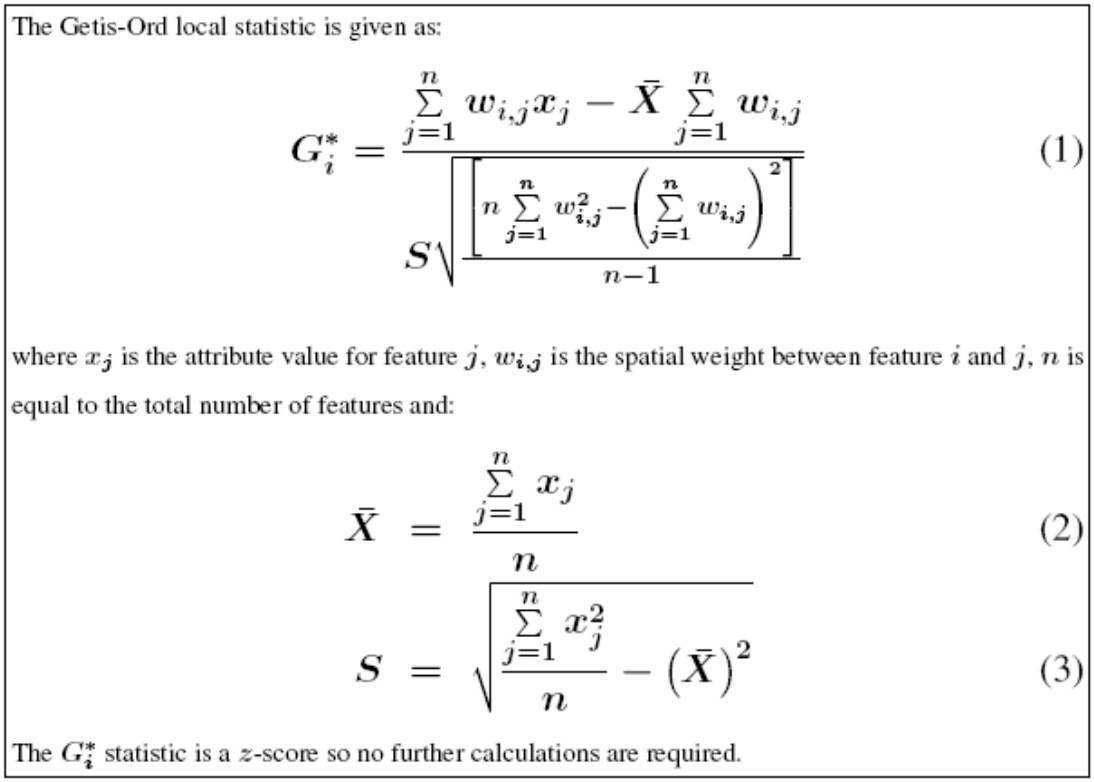

The Getis-Ord local statistic is given as:

$$G_i^* = \frac{\sum_{j=1}^{n} w_{i,j}x_j - \bar{X}\sum_{j=1}^{n} w_{i,j}}{S\sqrt{\frac{\left[n\sum_{j=1}^{n} w_{i,j}^2 - \left(\sum_{j=1}^{n} w_{i,j}\right)^2\right]}{n-1}}} \quad (1)$$

where $x_j$ is the attribute value for feature $j$, $w_{i,j}$ is the spatial weight between feature $i$ and $j$, $n$ is equal to the total number of features and:

$$\bar{X} = \frac{\sum_{j=1}^{n} x_j}{n} \quad (2)$$

$$S = \sqrt{\frac{\sum_{j=1}^{n} x_j^2}{n} - \left(\bar{X}\right)^2} \quad (3)$$

The $G_i^*$ statistic is a $z$-score so no further calculations are required.

*Figure 12: Explanation of the Getis-Ord Gi* statistic, courtesy of ESRI.* (ESRI, 2017)

Significantly high, positive z-scores are show clusters of high value, incident data and are considered hotspots. Significantly small, negative z-scores are considered cold spots and show clusters of low value incident data. Z-scores in the range between are either considered somewhat significant or not significant. These are classed into bins in the ArcMap output and bins are displayed with interval symbology. The Optimized Hot Spot Analysis tool was chosen from within the Spatial Statistics toolbox within ArcMap. The input for the Optimized Hot Spot Analysis tool

is a point feature shapefile, whereas the output from the new ice analysis was a polygon feature output. To convert the polygon feature class to a point feature class, the attribute tables were modified for all of the monthly merged polygon shapefiles. In each attribute table, two fields were added (with data type "Double" specifications). They were named latitude and longitude, and using Calculate Geometry, the Y-coordinate was calculated for latitude and the X-coordinate was calculated for longitude. The attribute tables were then exported, and added to the map document. The centroids were displayed as event layers using Display XY data (*Figure 13*). Event layers were exported to feature classes for permanent use.

Three options are offered for incident data without an Analysis Field in the Optimized Hot Spot Analysis tool. The COUNT_INCIDENTS_IN_FISHNET_POLYGONS was chosen for the Hot Spot Analysis for the study because it gives a straightforward representation of where and how much spatial clustering happens with a more spatially continuous polygon result, whereas the snapping to nearby points gives a result in discrete points and removes information from where it was originally located for the clustering. For this analysis option, at least 60 features must be available for aggregation, with thirty features remaining after aggregation, and the data must have sufficient variation. This means that for most days, an optimized hotspot analysis would not be ideal for analyzing clusters. However, on a weekly or monthly time scale, the feature count was sufficient.

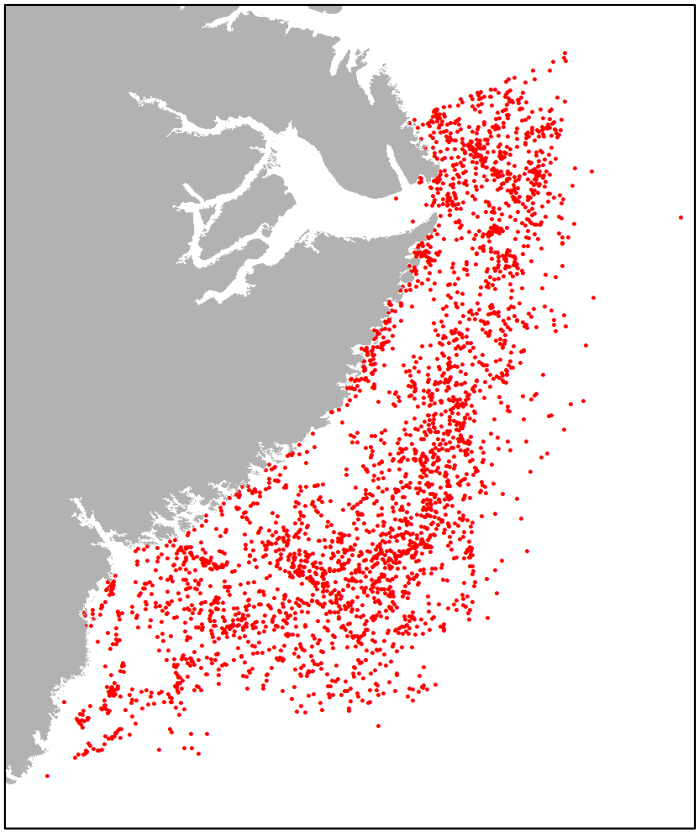

*Figure 13: Polygon centroid displayed as XY point data for new ice areas in the MIZ for all years.*

The COUNT_ INCIDENT_ IN_ FISHNET_ POLYGONS option works to aggregate incident data to use as the analysis field. Coincident points are collapsed and nearest neighbor measurements are made (for average and median distances). The greater of those two values is used to set the initial cell size to capture all incident point data in a fishnet polygon mesh. A count is made of incident data that falls in each polygon cells. Cells of 0 incidents are removed from the output. Next, spatial autocorrelation is accounted for using Global Moran's I. If there are more than 500 incident points, as in the case of annual and whole-study shapefiles, distances to a "K" number of neighbors (between 3 and 30) are calculated so that each point has a relationship with its neighbors. This is the input for the scale portion of the Getis-Ord $G_i$* statistic. As described, the significance results are displayed in classified bins based on statistical significance. Attribute tables with significance values were produced as an output from the tool. The process is visualized in a series of maps in *Figure 14*.

The Optimized Hot Spot analysis was carried out for each month, each season (Autumn, 2014-16), and for the total duration of the study (the 3 autumns combined). In the all-year analysis, below-threshold point data were included to give a comprehensive view of where new ice formation occurs most significantly.

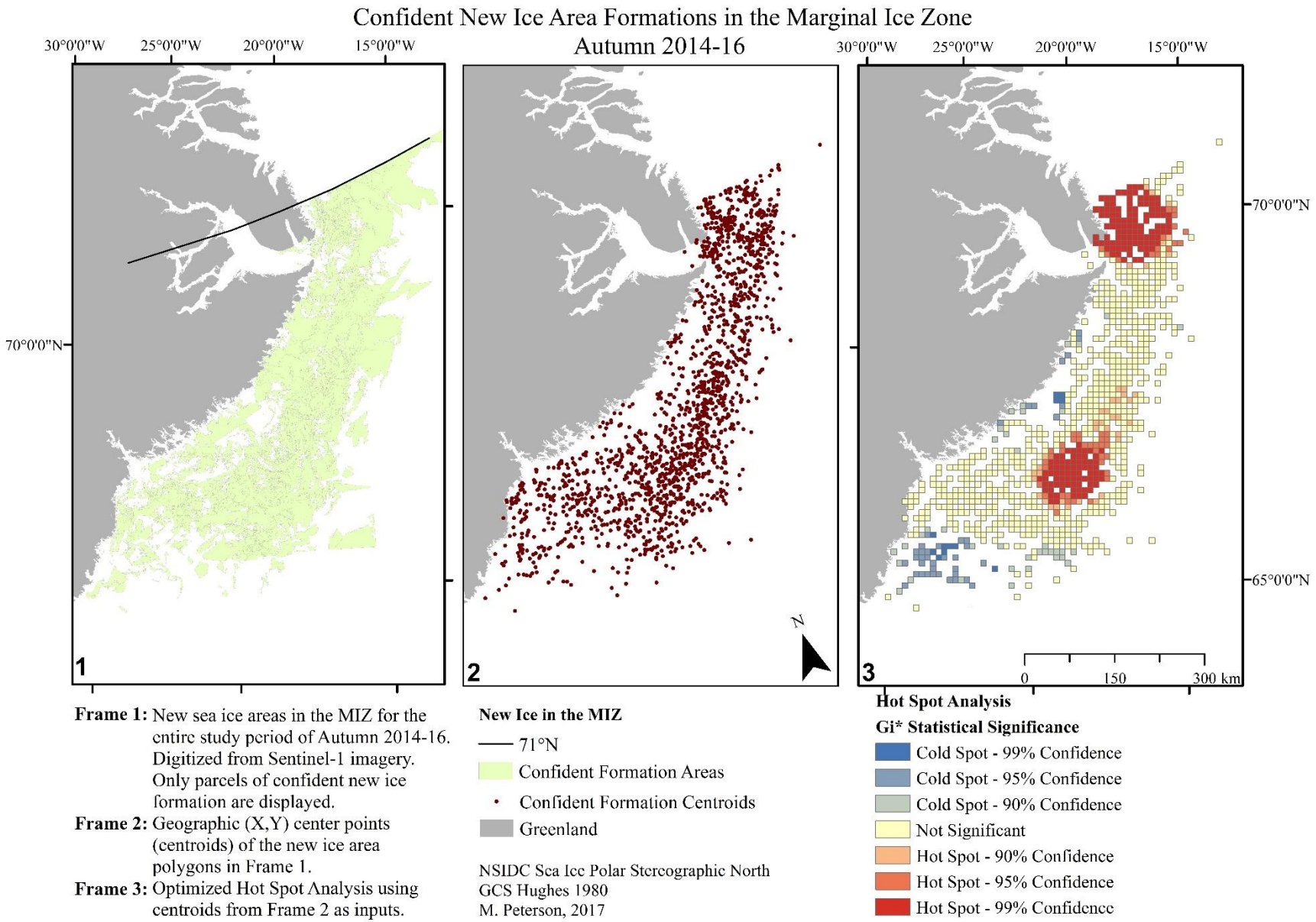


*Figure 14: Maps of the process to take MIZ new ice area polygons to an Optimized Hot Spot (Getis-Ord Gi*) Analysis.*

### 4.3.3 Spatial Analysis

Another way to assess the spatial variation and coincidence of the new ice formation areas was to perform spatial analysis. Spatial analysis was undertaken in the study by way of overlay operations, specifically intersections in ArcMap. The purpose of this analysis was to identify which areas were coincident between months and years. It is important to identify which months had the most formation in common in the same areas so that climate conditions could be investigated that may lead to main drivers of spatial variation of new ice formations in the Denmark Strait. Because of variation in the sea ice pack extent, the formation in the MIZ will also vary in extent. The spatial pattern of the different years was visualized in a series of maps, but spatial analysis allows for a more concrete description of what months had the most similar formation.

Daily polygon shapefiles were merged into monthly shapefiles using the Data Management toolbox during the new ice analysis phase. Monthly pairs were determined between the three years, and thirteen monthly pairs were chosen for the analysis using a matrix with analysis months on each axis. The thirteen monthly intersection pairings are as follows:

- October 2014 – October 2015
- October 2014 – November 2016
- November 2014 – November 2015
- November 2014 – November 2016
- November 2014 – December 2016
- December 2014 – December 2015
- December 2014 – November 2016
- December 2014 – December 2016
- October 2015 – November 2016
- November 2015 – November 2016
- November 2015 – December 2016
- December 2015 – November 2016
- December 2015 – December 2016

Months were paired with neighboring months of other years as well as their own unique month (e.g. comparing November 2015 and December 2016, instead of just Novembers to only other Novembers) because from first glance, the spatial variation was pronounced across all years. 2016's sea ice pack formation did not begin until the month after the first two years' pack formation first descended into the study area. Thus, it was considered important to attempt to quantify the differences in sea ice pack behavior over the three years.

The Intersect tool from the Overlay toolset from the Analysis toolbox in ArcMap was used to perform the intersect operations on the 13 monthly combinations. Each merged monthly shapefile was used as an input. Intersections were performed in the pairs, and area fields were added in the resulting attribute tables. The new fields were used to calculate geometry for the Areas of the intersecting polygons. Intersections only report exactly where there was feature overlap in the same location in both polygon shapefiles.

The area of each pair's intersection was recorded in an Excel spreadsheet and ranked by largest to smallest area. The six-monthly pairings with the most overlap were mapped to show where the areas have the most commonality. Additionally, intersects were performed for unique months over the three years.

Another notable spatial phenomenon was that of ice edge extent changes due to weather events. The extent of the sea ice pack in the Denmark Strait can be reduced rapidly due to deformation from weather conditions. It is often the case that after large freeze-up events which drastically extend the extent of the ice pack, storms and other mesoscale weather patterns will blow ice towards the coast of Greenland, and the thin, weak, young sea ice of the newly extended pack will deform against itself and against MY ice resulting in large amounts of deformation and extent coverage reduction. Sea ice concentrations where the pack extent remains will increase, however open ocean will be re-exposed to the atmosphere allowing for ocean-atmosphere interaction and heat exchange.

Using the notes that were recorded during the secondary new ice analysis, storm days were identified and images were compared side-by-side from the same footprint in order to compare the width difference in the ice edge before and after storms to get a sense of ice deformation. The measurement tool was used to measure along grid parallels to indicate the sea ice pack width before and after a storm.

In the temporal scope of seasons, because sea ice extent has reduced in the recent past for the Arctic as a whole, it was of interest to map the ice edge for the end of the season (December 21$^{st}$) over the course of the three years. Ice Edge shapefiles for December 21 of each year was queried on the NIC web portal where the MIZ can be obtained. Observing changes in the ice edge is interesting because changes in the ice edge indicate changes in the location of the MIZ. New ice formation in the MIZ is the focus of the study, so comparing the three year end-of-season ice edge extents was interesting to compare to new ice formation behavior, and weather and ocean conditions over the course of the entire season.

Additionally, ice edge shapefiles were also compiled from the NIC from 2006 to 2016 and were mapped together without fills to show how the movement of the ice edge changing over the last decade. This is informative as to changes in where new ice was forming over a longer time period, particularly considering the pronounced weakening observable in the sea ice pack since 2007. However, the Sentinel-1 record does not begin until 2014, so previous to 2014, other sources of sea ice data would be needed to quantify new ice areas in the study area.

### 4.3.4 Climate Pre-conditioning

One major point of interest in the study is to determine what conditions in the ocean and atmosphere spurred the most new ice formation. To do this, during the secondary new ice analysis, other sources of data were analyzed alongside the ice parcels of appropriate backscatter to determine if the area was in agreement with local conditions at the time of their observation. A qualitative log was kept as a record of the wind conditions and whether formation was expected and present.

Climate data was compiled from NOAA STAR (for ASCAT winds, seen in *Figure 15*), NOAA CLASS (for Global Sea Surface Temperatures, seen in *Figure 16*), NOAA GHCM (for air temperature records), optical imagers such as AVHRR, MODIS, Landsat-8 (for mesoscale weather

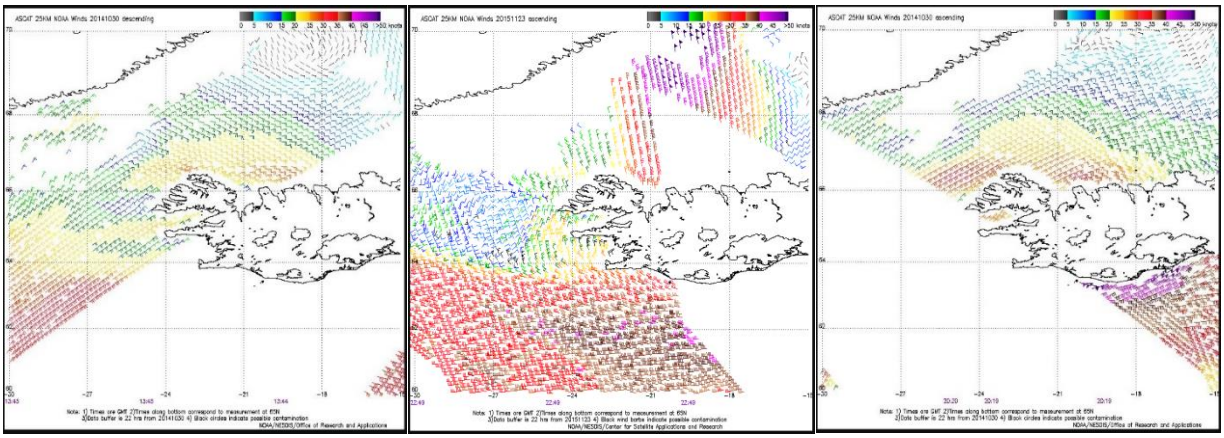

*Figure 15: Examples of ASCAT wind maps analyzed for the climate analysis.*

systems), and tabular data, such as sea surface temperature, air temperatures, and wind speeds and vectors were recorded in Excel spreadsheets for each image date. Information extracted from optical imagers, such as storminess and cloud cover, were noted in the qualitative log.

The days of greatest ice formation by month were determined by Area geometry calculations on the shapefiles in ArcMap. These days were manually compared to the climate conditions present on those days to determine what the most optimal formation conditions were for new ice in the MIZ during the study period in the study area. *Figure 17* is an example of a pre-conditioned day.

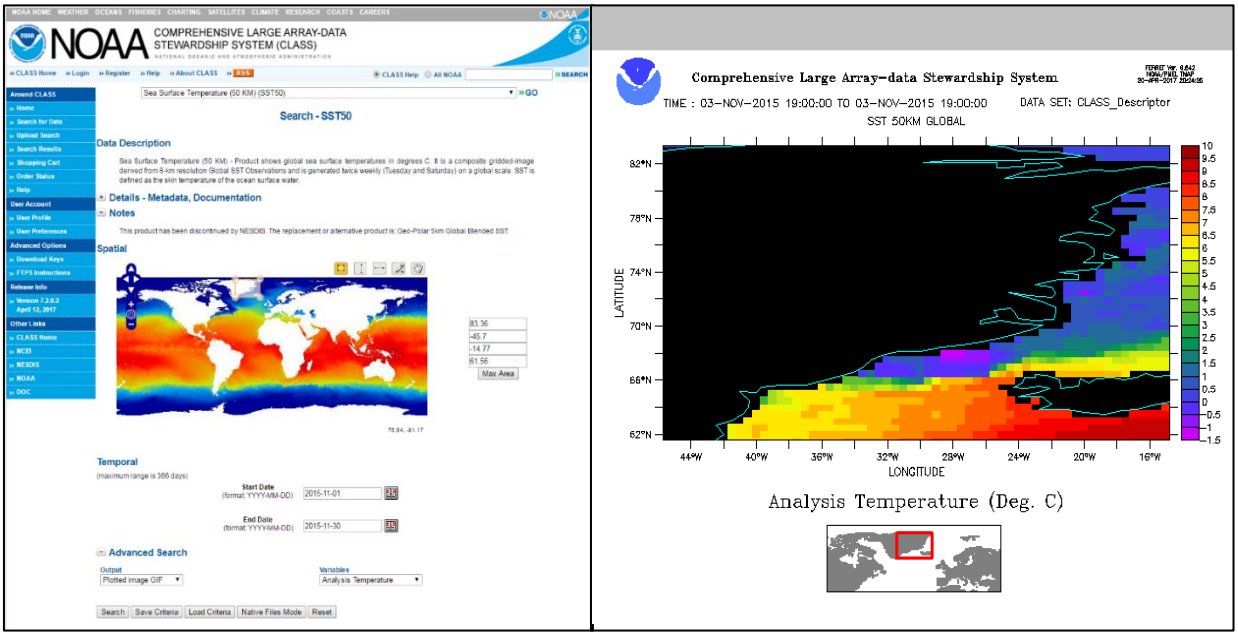


*Figure 16: NOAA CLASS Global Sea Surface Temperature map example, and retrieval from the CLASS database.*

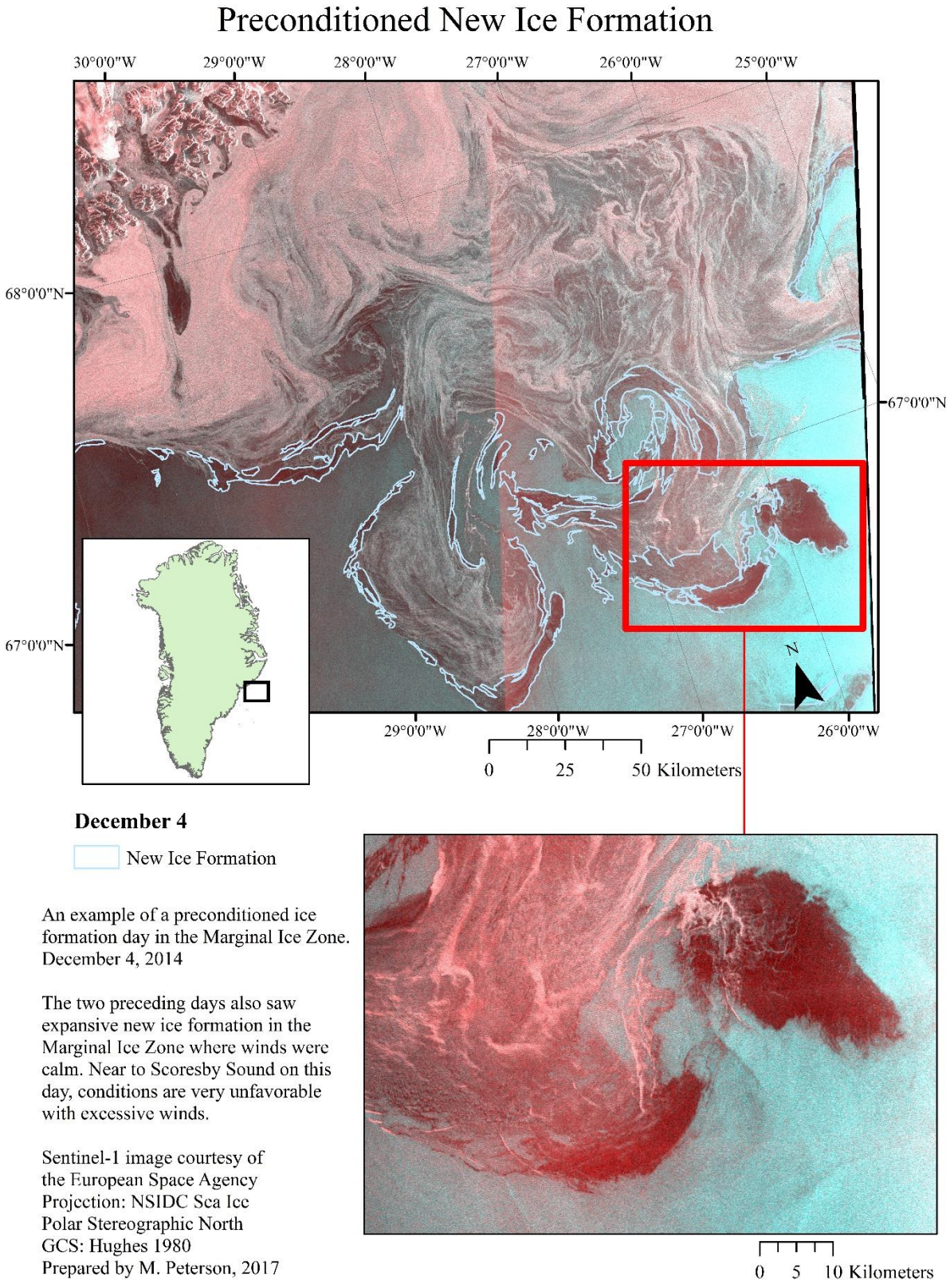


*Figure 17: Example of ice pre-conditioning and subsequent new ice formation in the MIZ.*

where freeze-up areas in the MIZ are large and clear.

### 4.3.5 Drift

Sentinel-1 image pairs were sought from consecutive days of observation in each month. One image pair was chosen from each month. The study area was scrutinized for distinctive MY ice floes with unique characteristics. Image symbology was modified to make small details clearer by enhancing the contrast, modifying the gamma stretch, and changing the resampling technique used in the display.

When MY floes were identified in both images of the image pair, a vector would be digitized, using a distinct marking feature on the floe as the line vertices. Distances were measured and divided by the time between images to obtain a drift rate.

Once the SAR imagery was downloaded, images were unzipped and imported into ArcGIS for processing. Images were combined using the Image Processing toolbar. Each set of corresponding HH and HV polarizations were combined into a single image using the Composite tool. For the purpose tracking sea ice drift, HH and HV bands were used separately to identify specific parcels of ice with better precision. However, for the identification of new ice formation areas, the two polarizations were used as a single composite image.

# 5 Results and Analysis:

## 5.1 Mapping New Ice Formation

In a comparison of the locations of autumn new ice area shapefiles between the years 2014, 2015, and 2016, there are some differences between the months of the different years, as can be seen in *Figures 18, 19,* and *20,* respectively. 2014 and 2015 tend to be consistent in the spatial extent of patches of new ice formation. They are consistent between October, November, and December, and also exhibit similar areal extents of formation areas.

In October, the MIZ new ice formation areas hover near Scoresby Sound as the main sea ice pack makes its journey southward. The sea ice pack moves southward with the increased ice flux out of the Fram Strait and the EGC moves the ice down along the coast of Greenland. Scoresby Sound and the coastline see most of the formation for October. While most of the formations are small, later in October, larger expanses of ocean begin to freeze and formation occurs in the study area. By November, the main sea ice pack has descended southwards of Scoresby Sound and continues to travel down the Blosseville Coast to the Kangerdlussuaq Glacier outlet. MIZ formations are separated from the coast by a thick sea ice pack of young, FY, and MY ice. Large freeze-up days occur several times a month. Some of the most expansive new ice patches are seen in November. There is more variability in the spatial extent of November 2015 compared to November 2014.

By December, the main sea ice packed has moved southwards of the Kangerdlussuaq Glacier outlet, and continues down the coast towards Tasiilaq. There are many small formation patches, and the variability in lateral extent is high. There is more variability in the spatial extent of December 2015 than in December 2014.

2016 varies wildly from 2014 and 2015. Firstly, there is no sea ice pack passing into the study area past the 71 ° North parallel in October 2016. November 2016 varies widely from the two preceding years in both area and extent. The sea ice pack in November 2016 exhibits spatial extent resembling that of Octobers in 2014 and 2015, more so than the Novembers of 2014 and 2015. Indeed, the ice was so delayed in October 2016, there are no plotted new ice areas for that month. Interestingly, the spatial extent of December 2016 more closely mimics that of November in the two preceding years more closely more than the preceding Decembers. However, new ice formation in December 2016 seems to lack the areal coverage of any of the other Novembers or Decembers. *Figure 21* shows how the formation over the three autumn seasons overlapped.

To demonstrate how variable sea ice pack can be between years, *Figure 22* compares the formations for a single week in the autumn of each year, the first week in November. 2014 and 2015 have rather expansive formations from sustained cold air temperatures which have been dominating for several weeks at this point in the season. Both years have benefited from the high reflectivity and likely deep ocean upwelling from a sea ice pack that has been present for the better half of a month by the first week in November. Conversely, 2016 expresses almost no new MIZ ice formations, and is the first week conditions were suitable for any new ice formation at all. This is a clear difference in freeze-up behavior across the very short study period, and begs the question of how much later freeze-up in the study area could be postponed if climate conditions in the Denmark Strait become warmer or more variable in the future.

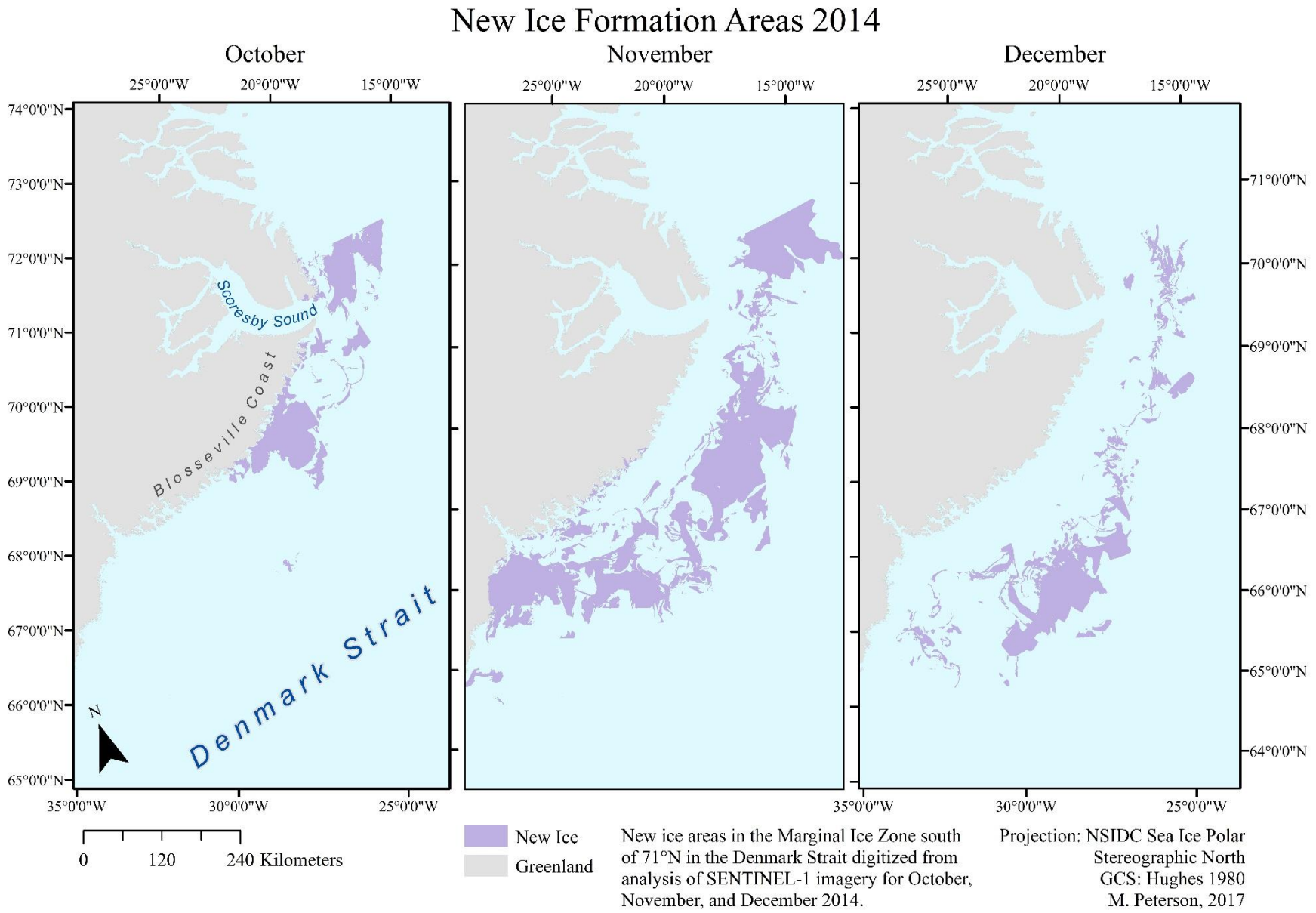


*Figure 18: MIZ new ice areas over the course of Autum 2014.*

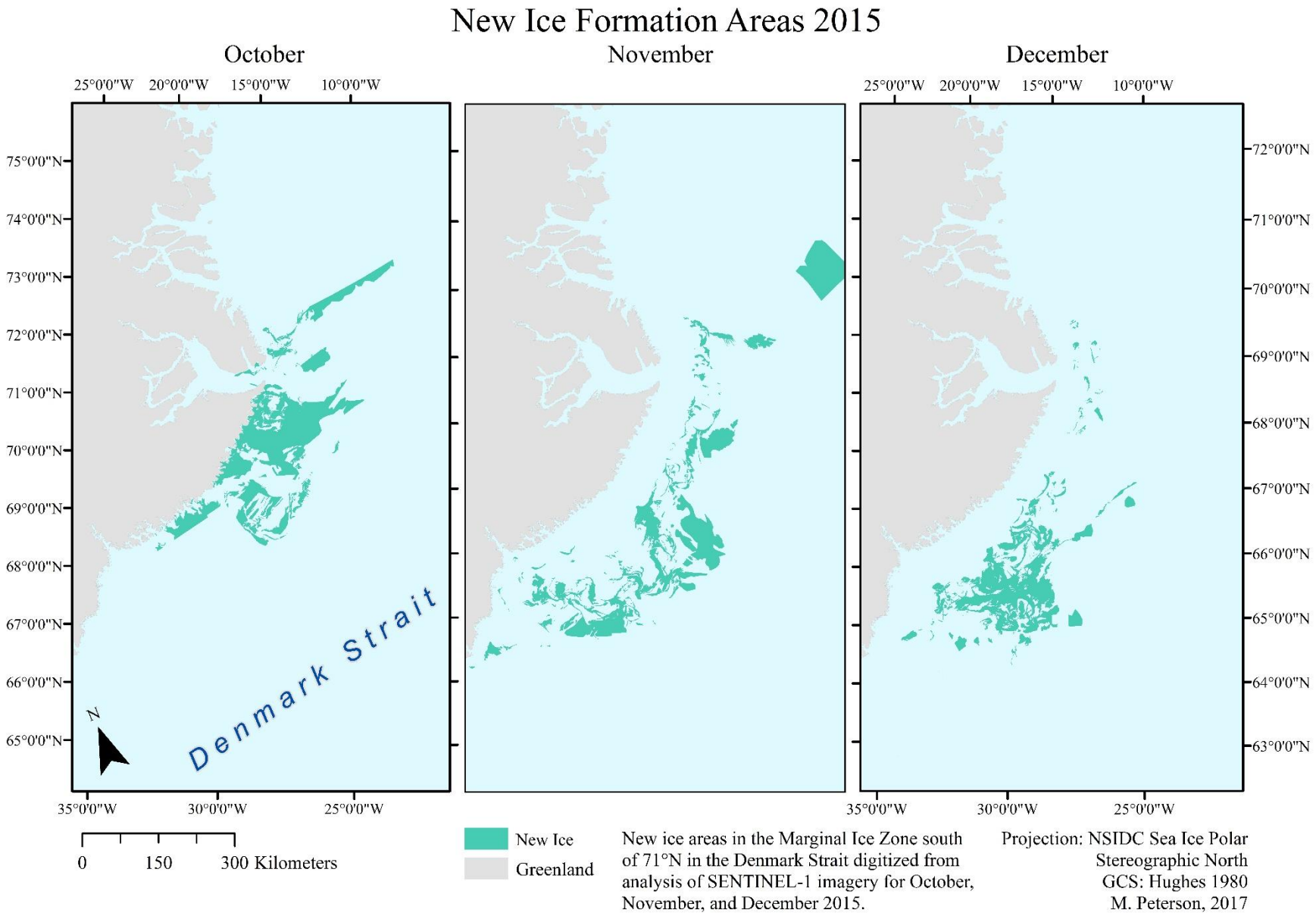


*Figure 19: MIZ new ice areas over the course of Autumn 2015.*

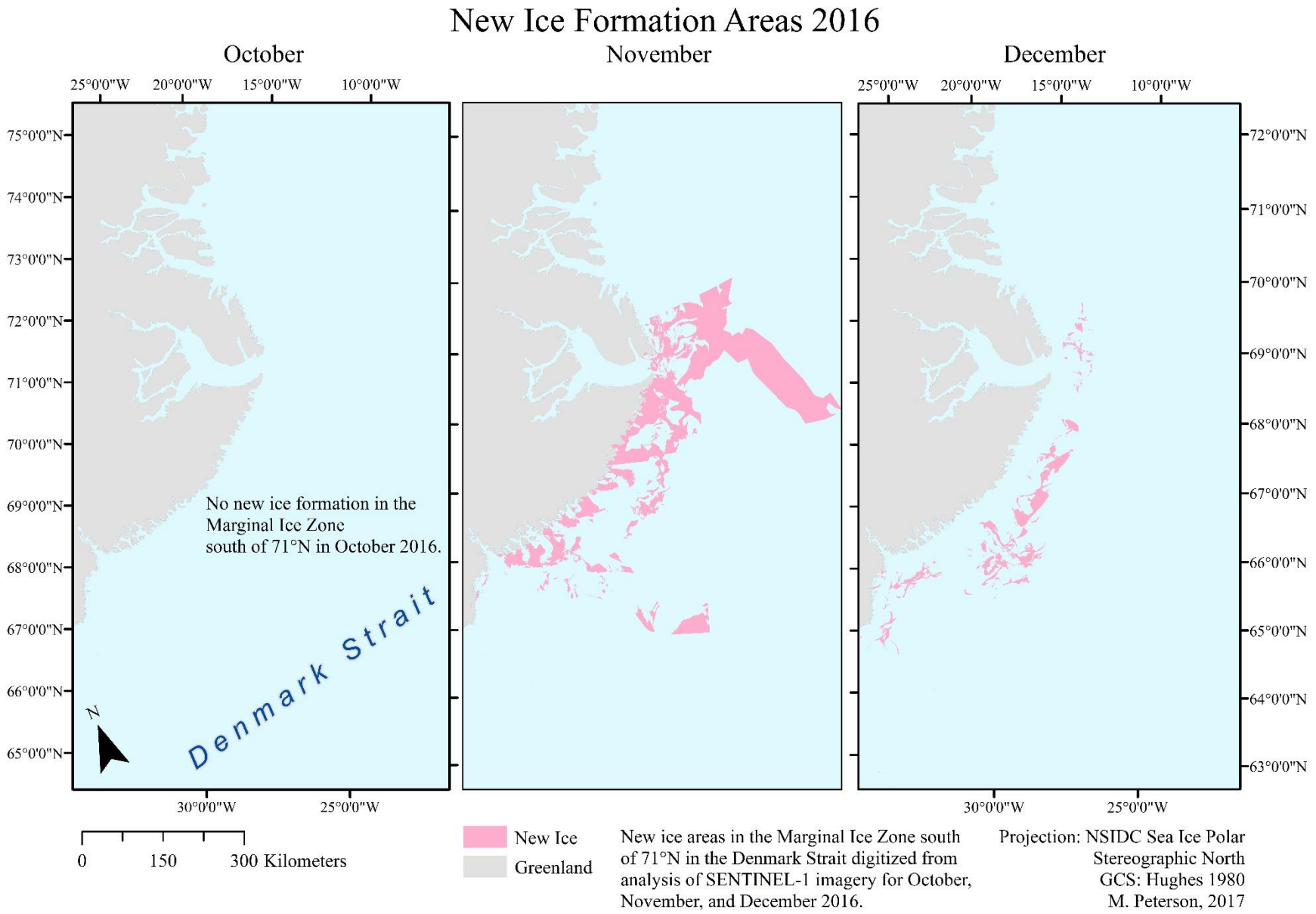


*Figure 20: MIZ new ice areas over the course of Autumn 2016.*

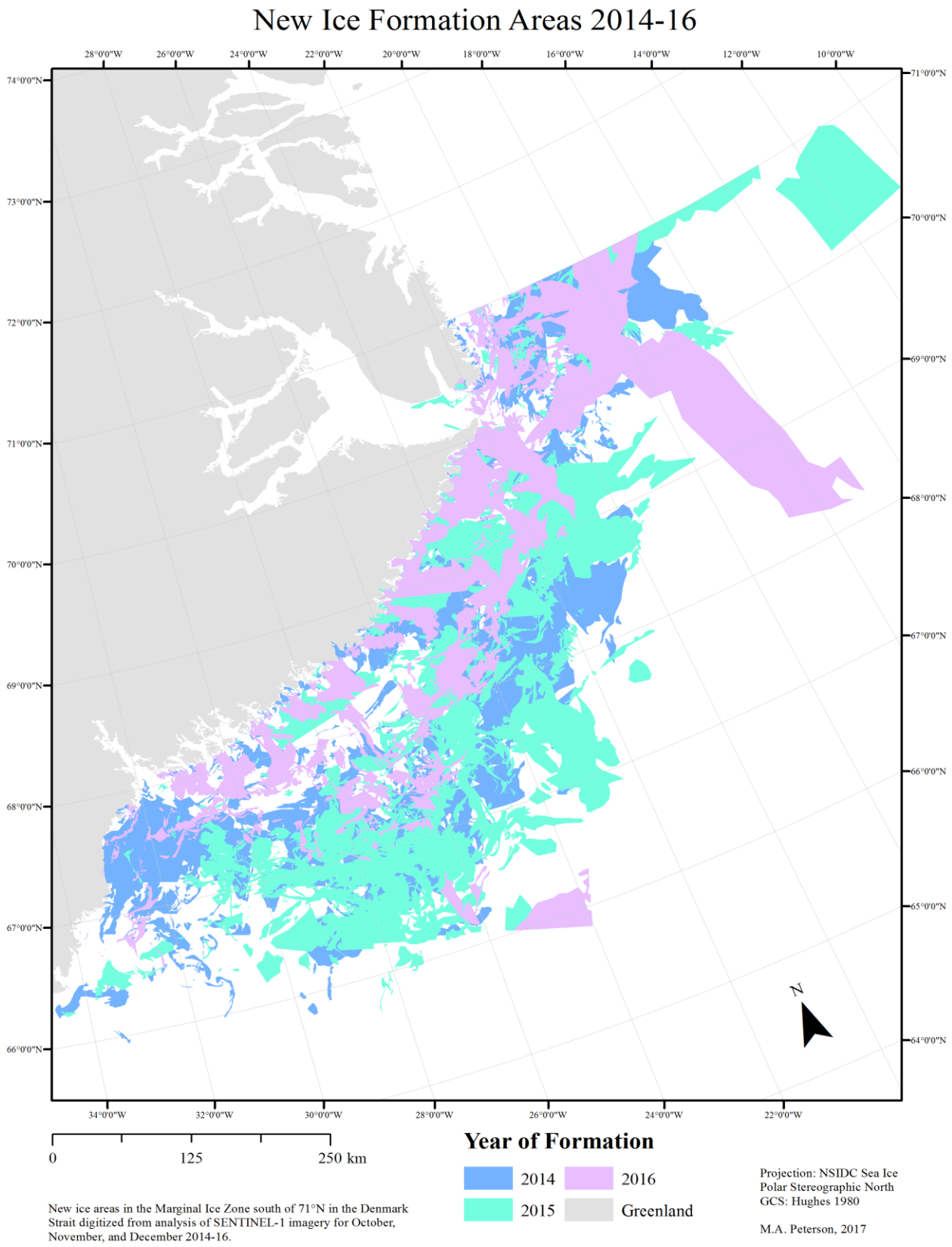


*Figure 21: The variation in MIZ new ice formation over the course of the three autumn seasons.*

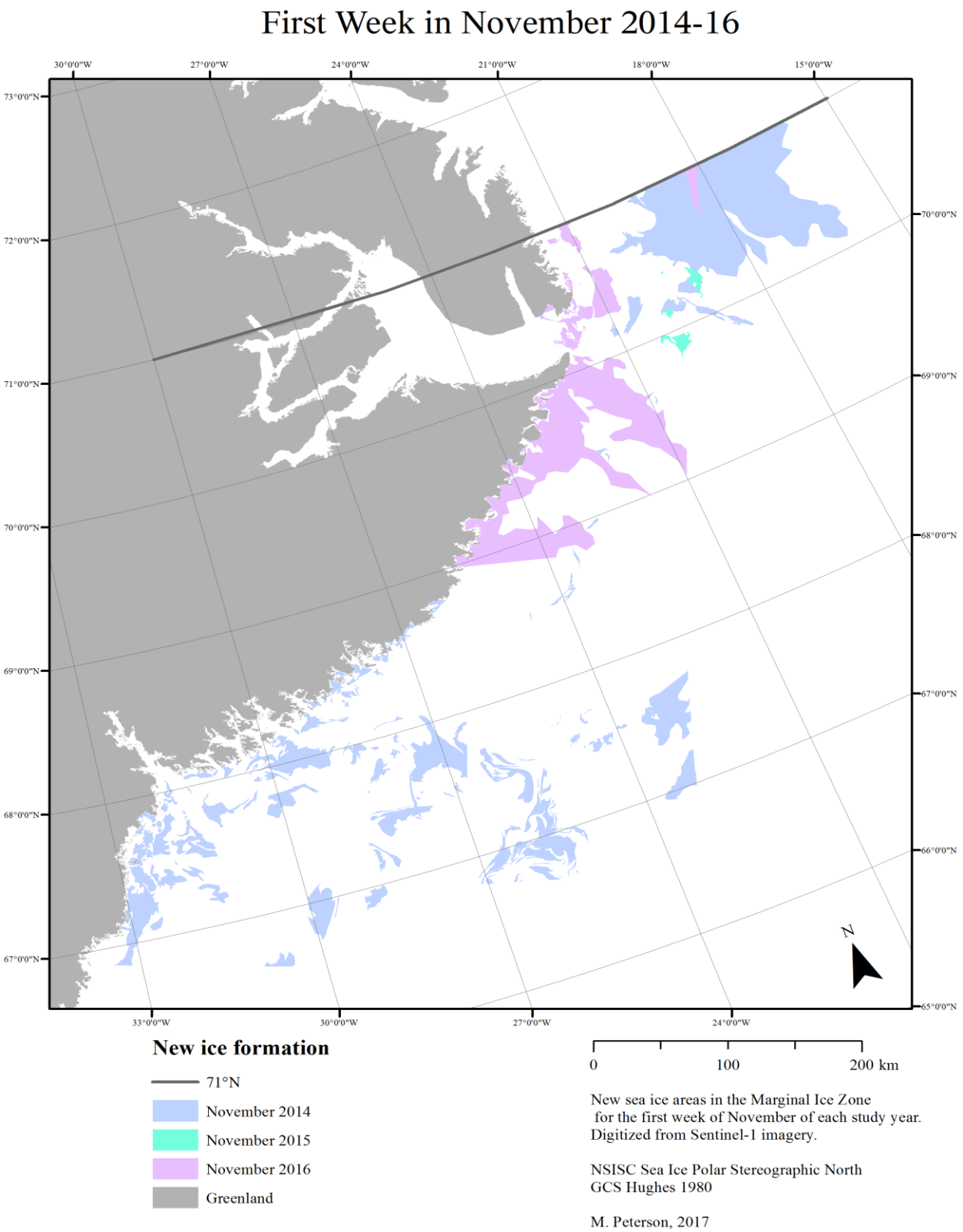


*Figure 22: Variation in the locations of new sea ice formation in the MIZ over the three autumns for the first week of November.*

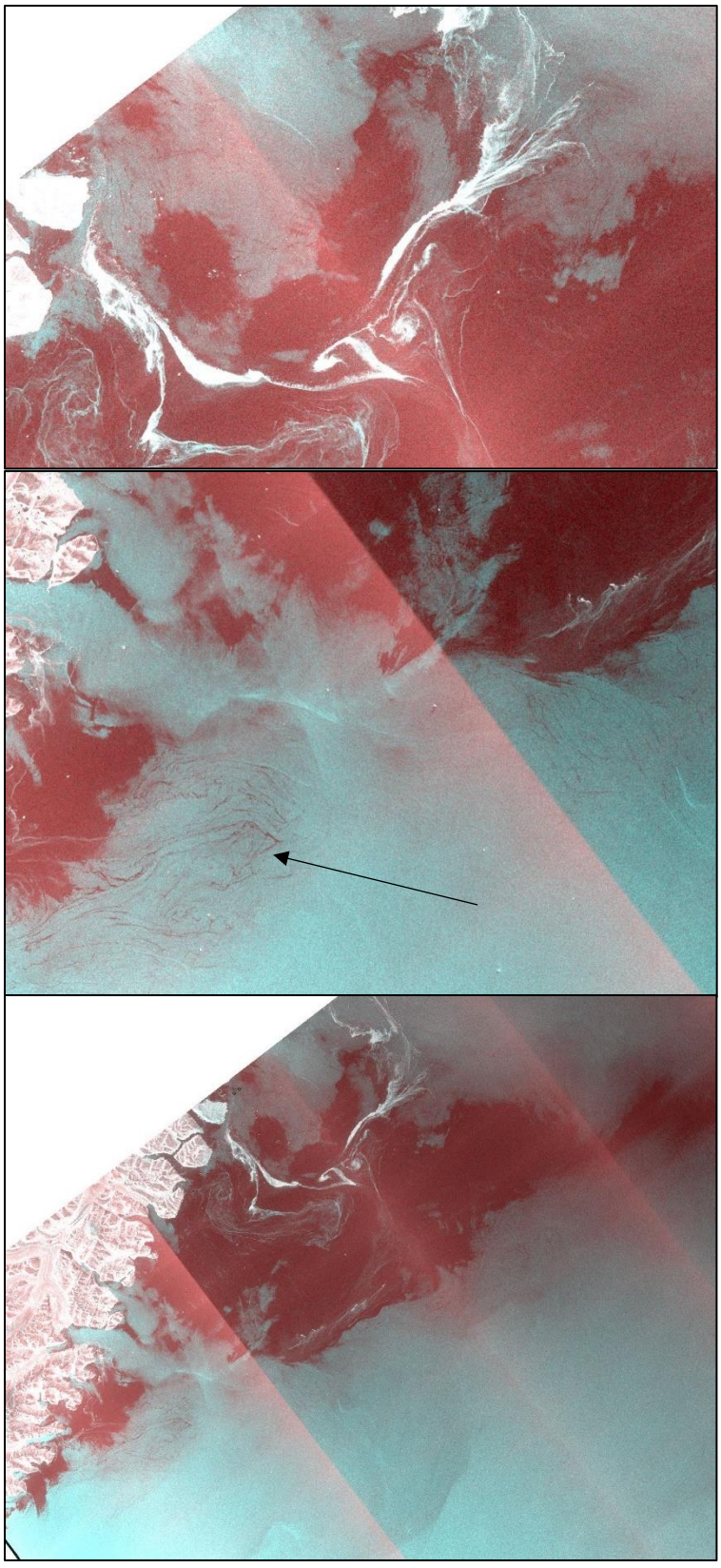

*Figure 23: A potential algal bloom in areas that may be new ice formation in early October, 2015. Usually, algal blooms occur one month earlier, at the latest. The arrow indicates the unusual formation.*

Generally, 2016 had new ice formation in the MIZ with the furthest distances from the coast, however they were few in number and we not marked confidently. 2015 had the farthest formation extents that were marked confidently. 2014's furthest extents for formation were several kilometers closer to shore, however the formation tended to be more clustered, and less scattered in its distribution.

There is an interesting day in early October 2015, in *Figure 23*, where there appears to be large formation in the study area. However, upon closer inspection, there is a possibility that the widespread formation may indicate a late algal bloom. When compared to sea surface temperatures for that date, October 3, 2015, temperatures adjacent to the sea ice park hover around 0° Celsius, approximately -0.5° Celsius at the coldest. However, sea ice formation occurs at -1.8° Celsius, which is not reached south of Scoresby Sound. North of the Scoresby Sound, sea surface temperatures are in the freezing range, but south of Scoresby is less likely on this date. Therefore, the formations seen could possibly be an algal bloom at the edge of the sea ice pack, or otherwise very cool, calm water, with perhaps minimal formation happening locally. The resolution of the CLASS SST Global dataset is 50 kilometers, so it is also possibly missing localized colder formations, so ice formation cannot be ruled out. Instead of deleting the potential formation areas, those that showed a sea ice like pattern were marked "N" and unusual looking areas were left unmarked.

In *Table 1*, the secondary analysis new sea ice areas of the MIZ are visualized. The digitized polygons were corroborated with climatological evidence to make more of a case for where new ice formation was likely in areas of favorable backscatter.

The counts are not significant, because the areas of the parcels are not uniform, they are included for clarity. In some cases, larger new sea ice areas were broken up into smaller clusters based on localized textures. Also, one very large area counts the same as one very small area just above the minimum size threshold. The maximum statistic references the polygon of the largest size for the given month, season, or all three autumns.

*Table 1: Quantities of new ice formation in the MIZ by month and by season, and associated statistics. October 2016 saw no new sea ice formation.*

| Analysis 2 - Area of New Ice in MIZ (square kilometers) | | | | | | |
|---|---|---|---|---|---|---|
| **Year** | **Month** | **Count** | **Maximum** | **Sum** | **Mean** | **Standard Deviation** |
| 2014 | October | 106 | 5391.82 | 22281 | 210.21 | 756.1 |
| 2014 | November | 323 | 8289.59 | 72855 | 225.56 | 768.43 |
| 2014 | December | 338 | 3171.99 | 32745 | 96.88 | 298.45 |
| 2014 | **Season** | 767 | 8289.59 | 127882 | 166.73 | 608.9 |
| 2015 | October | 285 | 10131.66 | 41936 | 147.14 | 679.14 |
| 2015 | November | 297 | 6812.4 | 41743 | 140.55 | 601.29 |
| 2015 | December | 226 | 2760.12 | 31849 | 140.92 | 344.45 |
| 2015 | **Season** | 808 | 10131.66 | 115528 | 142.98 | 573.39 |
| 2016 | October | 0 | 0 | 0 | 0 | 0 |
| 2016 | November | 319 | 13189.1 | 55563 | 174.18 | 909.54 |
| 2016 | December | 244 | 2519.02 | 10375 | 42.52 | 168.09 |
| 2016 | **Season** | 563 | 13189.1 | 65938 | 117.12 | 696.59 |
| All Years | October | 391 | 10131.66 | 64217 | 164.24 | 701.4 |
| All Years | November | 939 | 13189.1 | 170162 | 181.22 | 774.42 |
| All Years | December | 808 | 3171.99 | 74970 | 92.78 | 283.54 |

The most telling statistic of the table is the Sum, which combines all polygons for a given time period to give one overall area. November 2014 was, by far, the greatest ice producing month. It produced more MIZ new ice formation than the entire production of the Autumn 2016 season. The 2014 season outproduced the other two seasons, 2015 by 116% and 2016 by 142%. December 2016 was the lowest producing month (besides October 2016, which yielded nothing), which is surprising, because the previous two Decembers saw at least 30,000 $km^2$ formation, and December 2016 produced just over 10,000 $km^2$.Total production for 2014 and 2015 seemed similar, but the production in 2016 was much lower with 2016 being the only of the three years to not break 100,000 $km^2$ of new MIZ sea ice area.

Where the sea ice does not cover the open ocean, the ocean continues to absorb incoming solar radiation and ocean atmosphere interaction and exchange of heat and moisture remains higher. With larger areas of open ocean, sea ice is inhibited from cool the ocean and atmosphere, which in

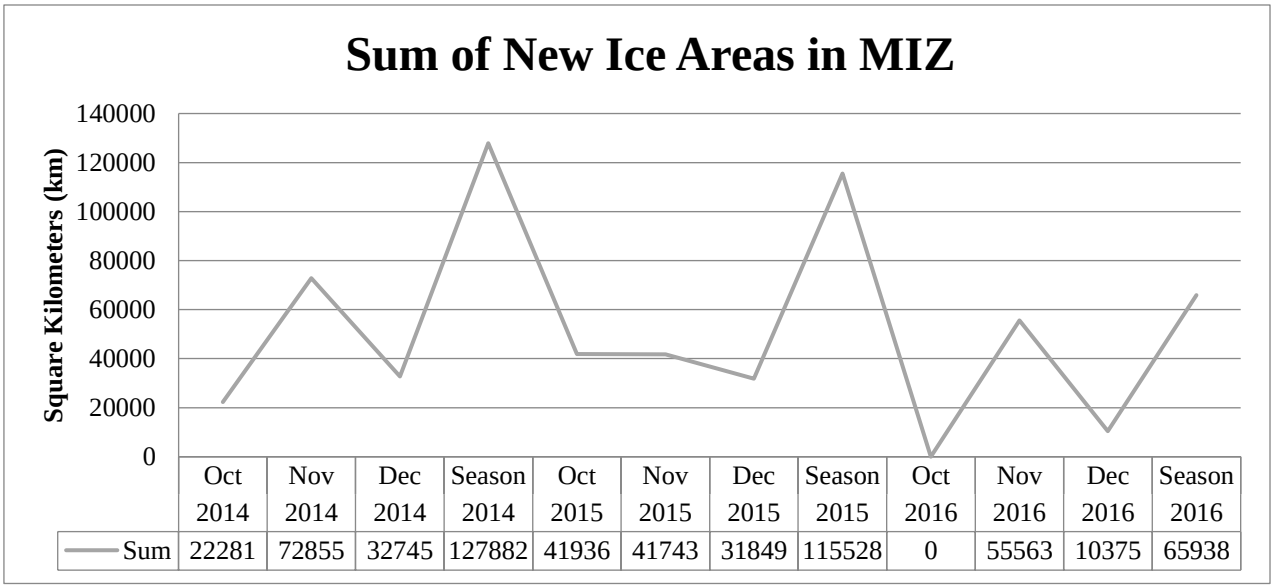


| | Oct 2014 | Nov 2014 | Dec 2014 | Season 2014 | Oct 2015 | Nov 2015 | Dec 2015 | Season 2015 | Oct 2016 | Nov 2016 | Dec 2016 | Season 2016 |
|---|---|---|---|---|---|---|---|---|---|---|---|---|
| Sum | 22281 | 72855 | 32745 | 127882 | 41936 | 41743 | 31849 | 115528 | 0 | 55563 | 10375 | 65938 |

*Figure 24: Variations in new ice areas in the MIZ, summed from polygons digitized across the months, are shown over the course study period.*

turn, catalyzes more warming. Later sea ice entry to the study area also slows cooling and freeze-up conditioning for the season. *Figure 24* shows the quantity of formation across the study period, and how significantly 2016 new ice formation in the MIZ lags behind that of the 2014 and 2015, according to classification of Sentinel-1 imagery with auxiliary climate information.

*Table 2* shows the difference between the first and secondary analyses in retrieving new sea ice area. Analysis 1 was carried out independently from climate data and ice extent information. Both analyses including a function for the confidence of each polygon truly representing new ice formation. Analysis two increased the proportion of polygons of confidence because additional data was incorporated to rule out climate conditions and out of MIZ areas. Also, overlooked parcels could be included. The secondary analysis added 60,470 $km^2$ of Not Confident new ice formation area, and 87,755 $km^2$ to the Confident new ice formation areas. This represents a major change in ice area classification due to a change in robustness of the classification technique. Over 30% more area was marked Confident with the addition of auxiliary climate information.

*Figure 25* shows the changes in the polygon classifications between the initial and final analyses. There is a large change in the total area and in the Confident areas between the two separate analyses. The second analysis benefits from external sources, which allows for better interpretation of the Sentinel-1 imagery based on conditions alongside backscatter. These findings suggest that isolated analysis of Sentinel-1 SAR imagery for new sea ice area identification may not be the optimal method of new ice classification in the MIZ.

*Table 2: Compares the areas digitized between the first, independent analysis of new sea ice in the MIZ to the secondary analysis which adds information from other sensors and climate archives.*

| **Digitized Area Comparison** | | | **Analysis 1** | | | | |
|---|---|---|---|---|---|---|---|
| | | | **Count** | **Maximum** | **Sum** | **Mean** | **Standard Deviation** |
| | | | | | | | |
| Not Confident | All Years | All Months | 1944 | 13189.1 | 248880 | 128.02 | 601.71 |
| Confident | All Years | All Months | 1434 | 5774.8 | 142515 | 99.38 | 399.7 |
| | | | **Analysis 2** | | | | |
| | | | **Count** | **Maximum** | **Sum** | **Mean** | **Standard Deviation** |
| Not Confident | All Years | All Months | 2138 | 13189.1 | 309350 | 144.69 | 620.82 |
| Confident | All Years | All Months | 1896 | 10131.66 | 230270 | 121.45 | 497.89 |

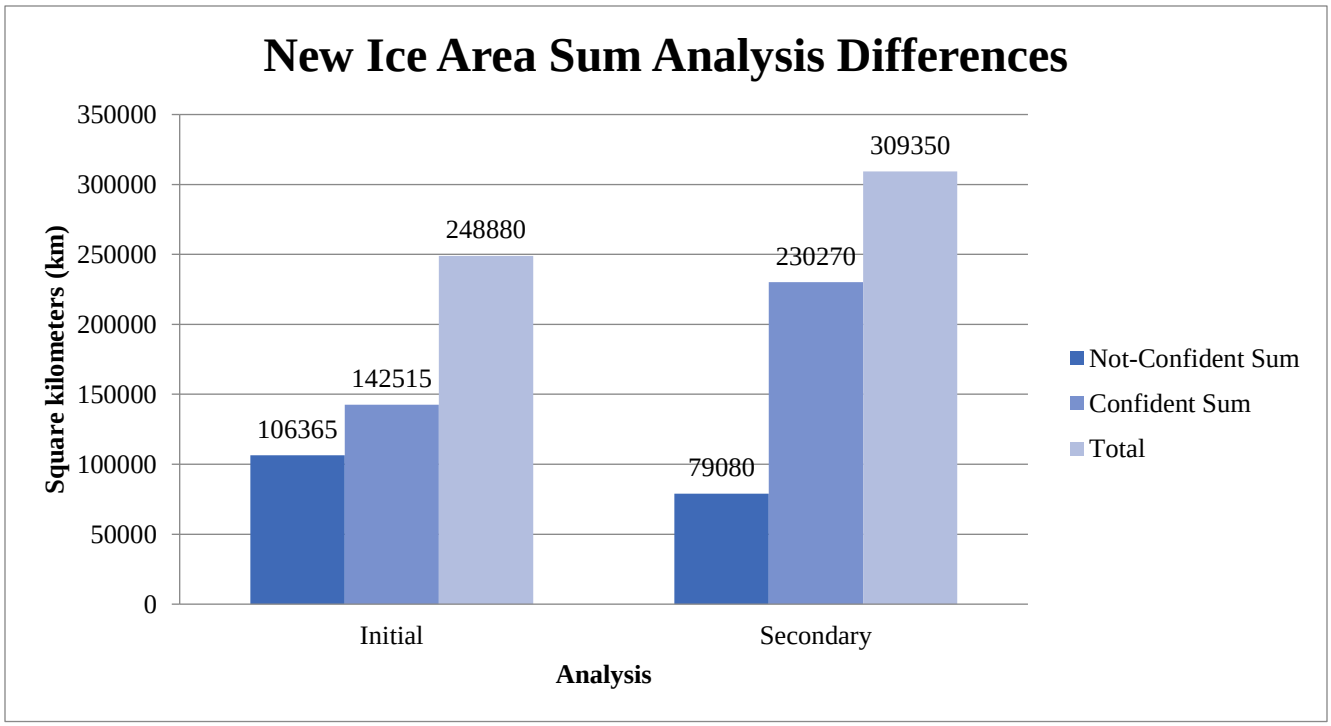


*Figure 25: Chart comparing the sum of the digitized areas between the initial and secondary analysis, and the proportion of the classified areas that were considered "Confident"by the analyst.*

## 5.2 Hot Spot Analysis

### 5.2.1 Analysis 1

Hot Spot Analysis was carried out on the Analysis 1 data for both the Confident and Not-Confident digitized polygons. At the start of the study, both the Count_Incidents_ Within_Fishnet_Polygons and Snap_Nearby_Incidents_ To_Create_Weighted_Points were tested to determine which feature would better represent the clustering in the study area. *Figure 26* and *27* are the products of the Snap_Nearby_Incidents_ To_Create_Weighted_Points option with the Confident and Not-Confident polygons, respectively. *Figure 28* is the product of the Count_Incidents_ Within_Fishnet_Polygons option including both the Confident and Not-Confident polygons from the first analysis.

In the second analysis, the Count_Incidents_ Within_Fishnet_Polygons option was chosen over the Snap_Nearby_Incidents_ To_Create_Weighted_Points option because the output is more readable because it appears more continuous. The data examined is not continuous, but the snapping option gives the appearance of neglecting the polygons that would fall in between those points. While those polygons are considered in the analysis, it is clearer to have a continuous fishnet polygon mesh, even though clustered instances may be arbitrarily separated by the scale of the fishnet.

Hot spot clustering seems to dominate at the northern tip of Scoresby (where all ice must pass through into the study area) and around 25 ° West and 68 ° North, where the ice edge seems to occur in each year, give or take deformation from storms or preconditioning further out in the open ocean. The cluster might represent the boundary of two water masses, perhaps the dynamic interaction of the EGC and the North Atlantic Irminger Current which define the ocean and atmospheric interactions in that region, and would also define the dynamic ice edge.

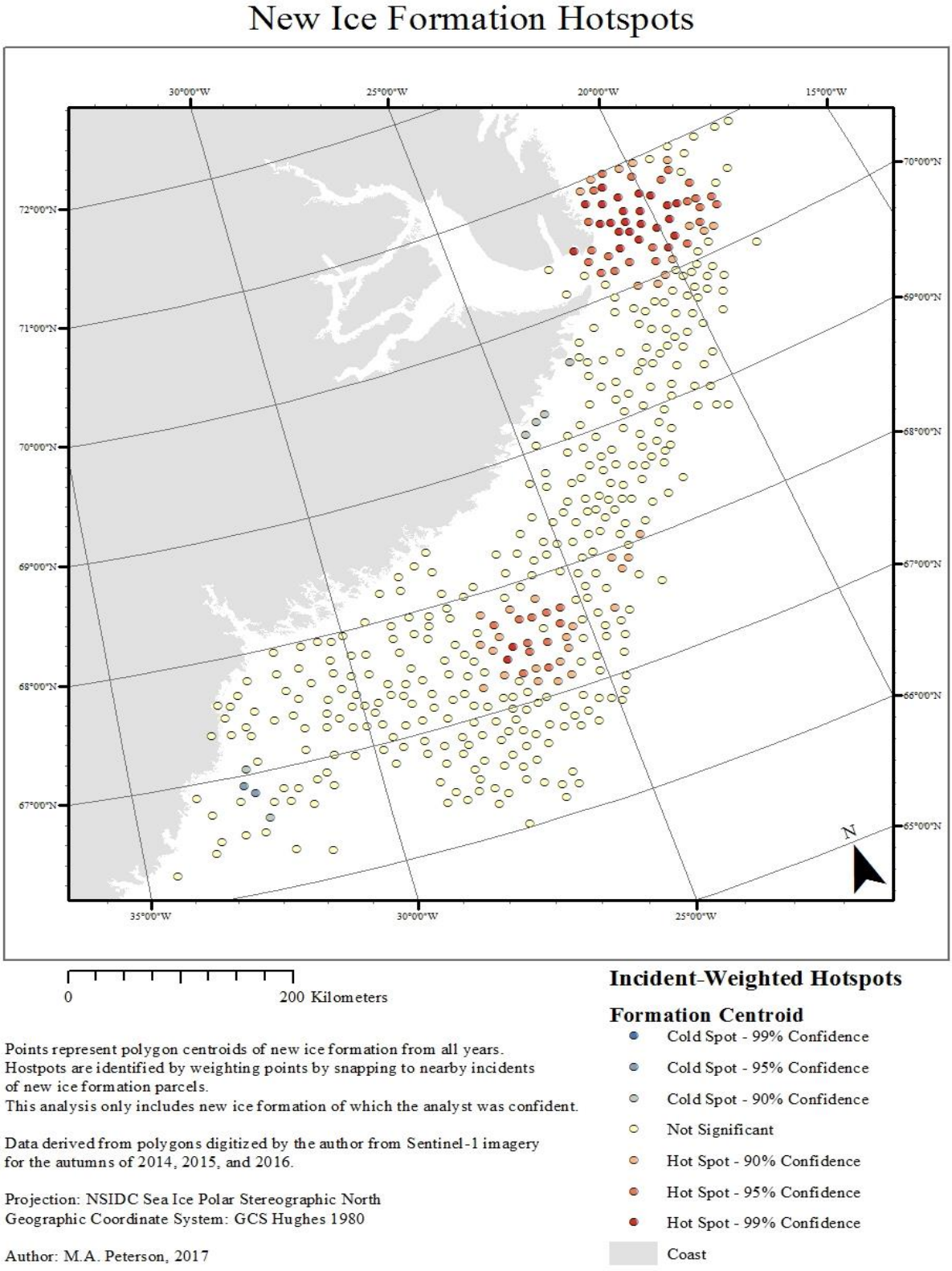


*Figure 26: Testing of the "Snap Nearby Incidents to Create Weighted Points"option of the Optimized Hot Spot Analysis in the initial analysis.*

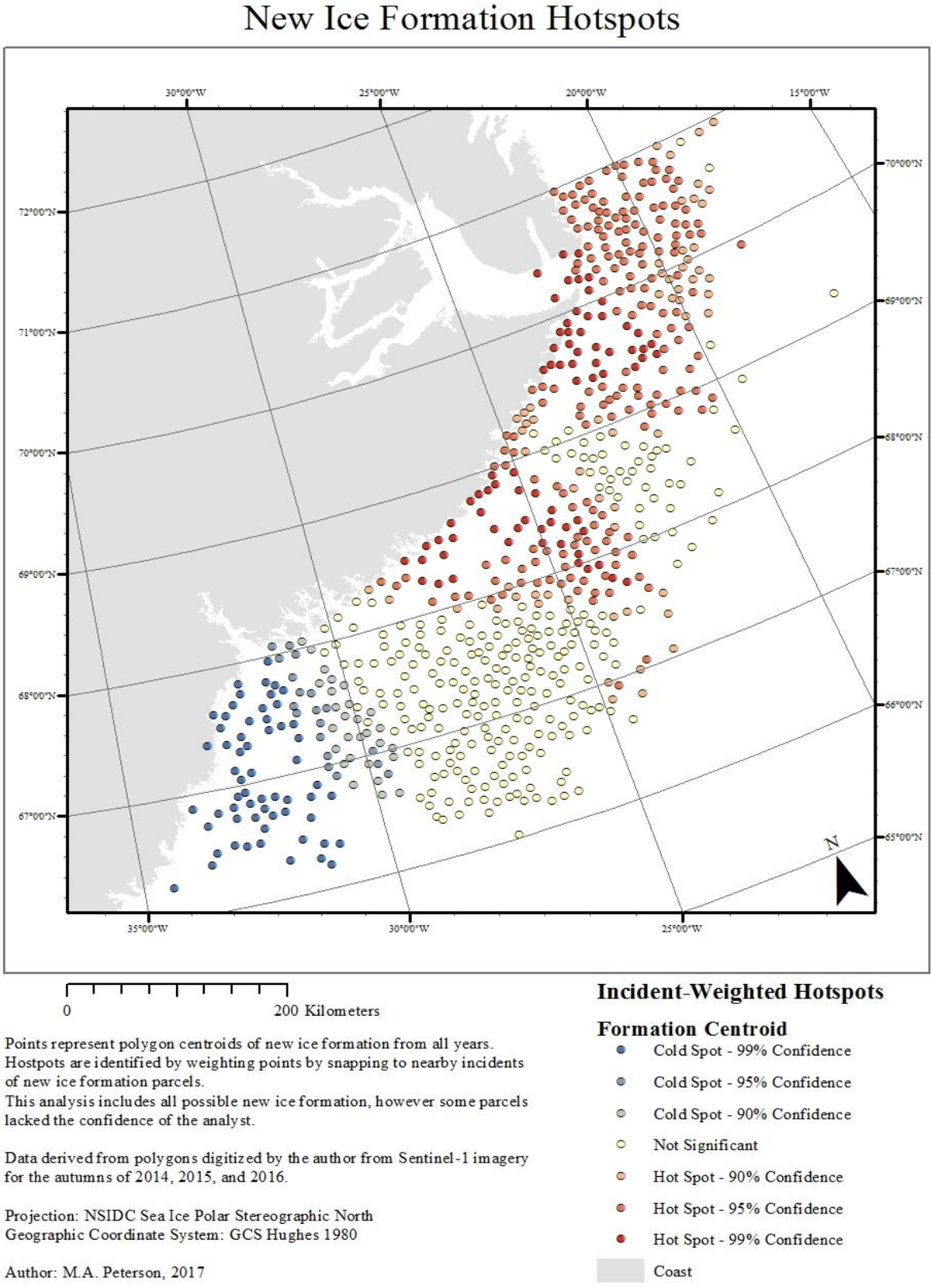


*Figure 27: Optimized Hot Spot Analysis using the "Snap Nearby Incidents to Create Weighted Points" option with all formation centroids from the initial analysis.*

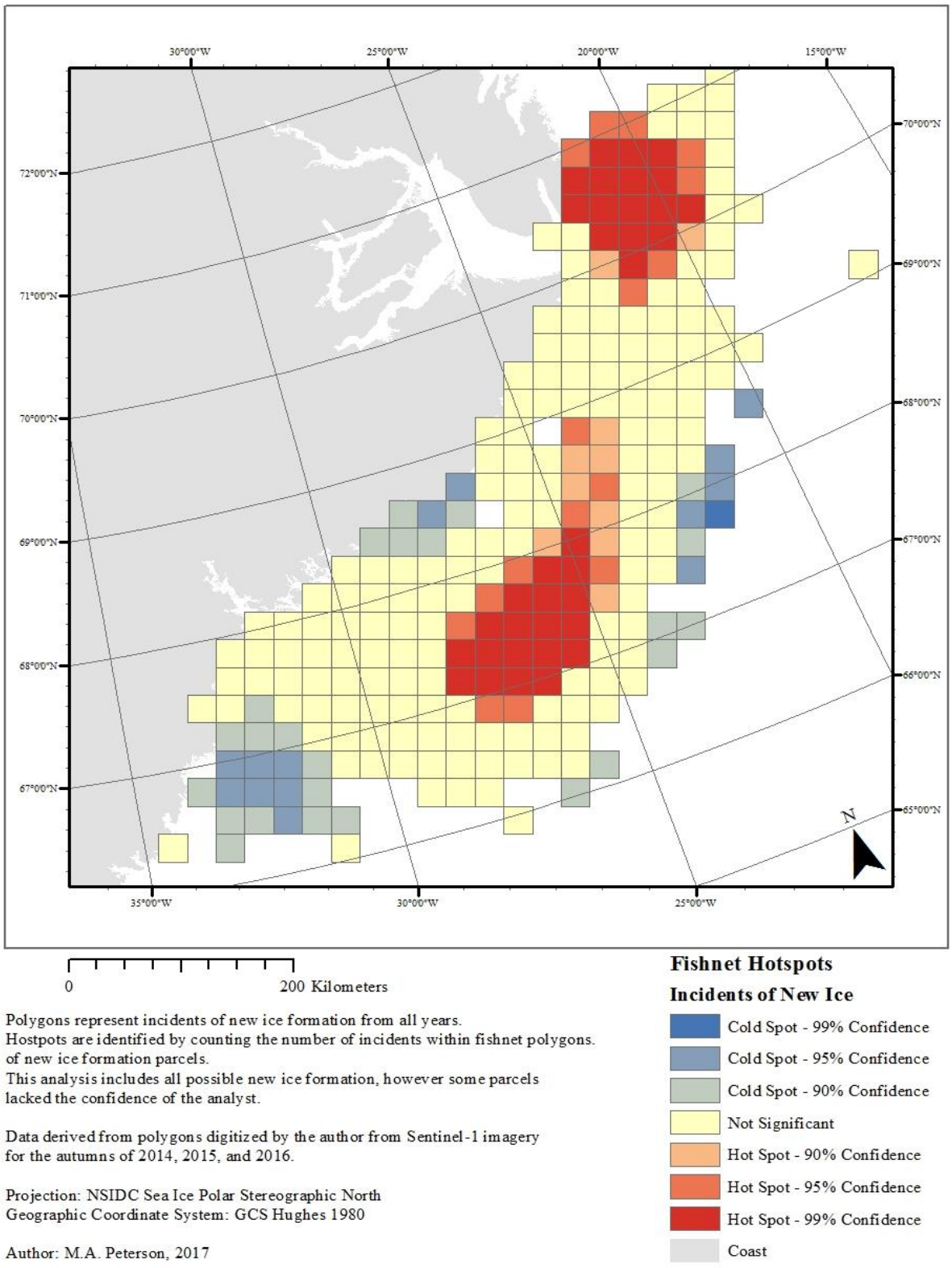


*Figure 28: Optimized Hot Spot Anlaysis using the "Count incidents within fishnet polygons" option, for the first analysis.*

### 5.2.2 Analysis 2

In the secondary analysis, solely the the Count_Incidents_Within_Fishnet_Polygons option was used. In *Figure 29*, all polygons for all years, both Confident and Not-Confident, and all below-threshold point features were used as the input. This allows for a general observation of where new ice is likely, but neglects the areas of the new ice formations.

The spatial resolution of the polygon fishnet mesh is automatically determined by the Optimized Hot Spot Analysis tool. The scale is finer in the secondary analysis than in the first because of testing done by the tool to determine neighborhood distances. This means that average distances and median distances in the secondary analysis are much smaller, and is likely due to additional samples being provided.

The clusters themselves appear more defined and another Hot Spot becomes apparent. There is significant clustering in addition to the Scoresby cluster and the 68N/25W cluster that are still present in Hot Spot Analysis of the secondary analysis polygons. The third hotspot occurs at 69N/25W, flush with the coast of Greenland. This is likely due to the inclusion of coastal new ice areas, and this area sees a lot of new MIZ formation as the sea ice pack descends in October and November. Cold spots dominate at the edge of the analysis field, and at the outlet of the Kangerdlussuaq Glacier. High winds tend to come off of the glacier through the southern edge of the Blosseville Coast, so this is not an unexpected feature of the analysis. It is difficult for new ice to form in very disturbed ocean conditions, which frequently occur in this location.

The cold spots at the ice edge are likely explained by the variability in the pack edge from year to year. Because the fishnet is present (and signifies presence and absence), there were instances occurring at some point in those locations. However instances of new ice formation in those areas may be rare or very infrequent because they may have been caused by abnormal weather or ocean conditions. Not significant areas show the areas where ice occurs, but without significant clustering. Areas without fishnet polygon mesh cells did not see ice formation at all in the duration of the three-autumn period.

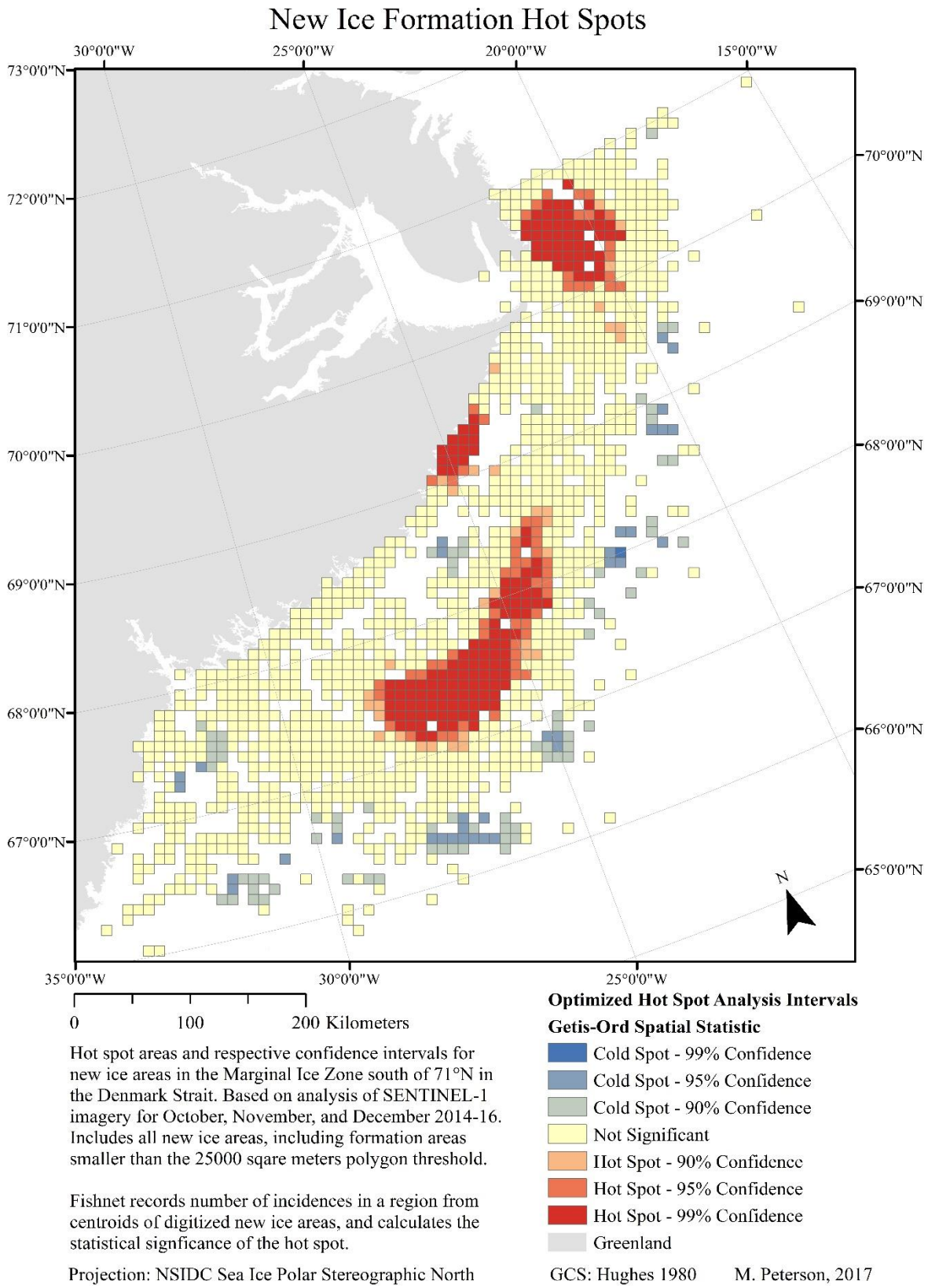


*Figure 29: Hot Spot Analysis using the fishnet polygon option with the final results from the secondary analysis, combining climate information and additional imagery resources for a more accurate classification of where new ice forms in the MIZ.*

*Figure 30* demonstrates the clusters across the three seasons of analysis, except for October 2016, culminating in eight separate analysis maps with seven of the eight demonstrating statistically significant clustering. The most pronounced and widespread clustering occurs in November 2015. 2015 saw very favorable climate conditions, which could explain why there would have been more formation and more clustering in this year than in the other years.

Another observation is that the spatial pattern of the hot spot clustering is typically near Scoresby when the ice first descends, then moves southwards along the coast, before moving laterally out into the open ocean as the sea ice pack extends later into the autumn season. The new ice formation areas are consistent with the behavior of ice, but the strength of the clustering varies between months and years.

December sees the least significant clustering of all the months in each year. December 2016 shows no significant clustering whatsoever, which is interesting because climate conditions were not optimal for sea ice growth that autumn. The lack of significant clustering could be, in part, due to the fewer instances of new ice in the MIZ during autumn 2016, which is likely attributable to less favorable climatic conditions than in the previous two autumns.

A critique of the Optimized Hot Spot Analysis tool, is that the functionality of the tool does not allow for polygons to be considered and then output in an automatically-scaled fishnet. The user must provide a fishnet of appropriate scale via manual means, use the polygons in the actual shapefile for the analysis, or use centroid points and completely neglect area as an analysis field. The specific issue for this study with the Hot Spot Analysis, is that the presence and absence function can only be considered at one point. Where there are substantial areas of new ice formation, it would be interesting to see where all of the overlaps are, not just the overlaps or neighborhoods of the polygon geographic center points. Future work could be done for this particular analysis to manually determine a fishnet of appropriate size and then to use the polygons layers as inputs for the tool. The tool itself is very useful in plotting the areas of significant clustering which adds depth to a density/heat analysis.

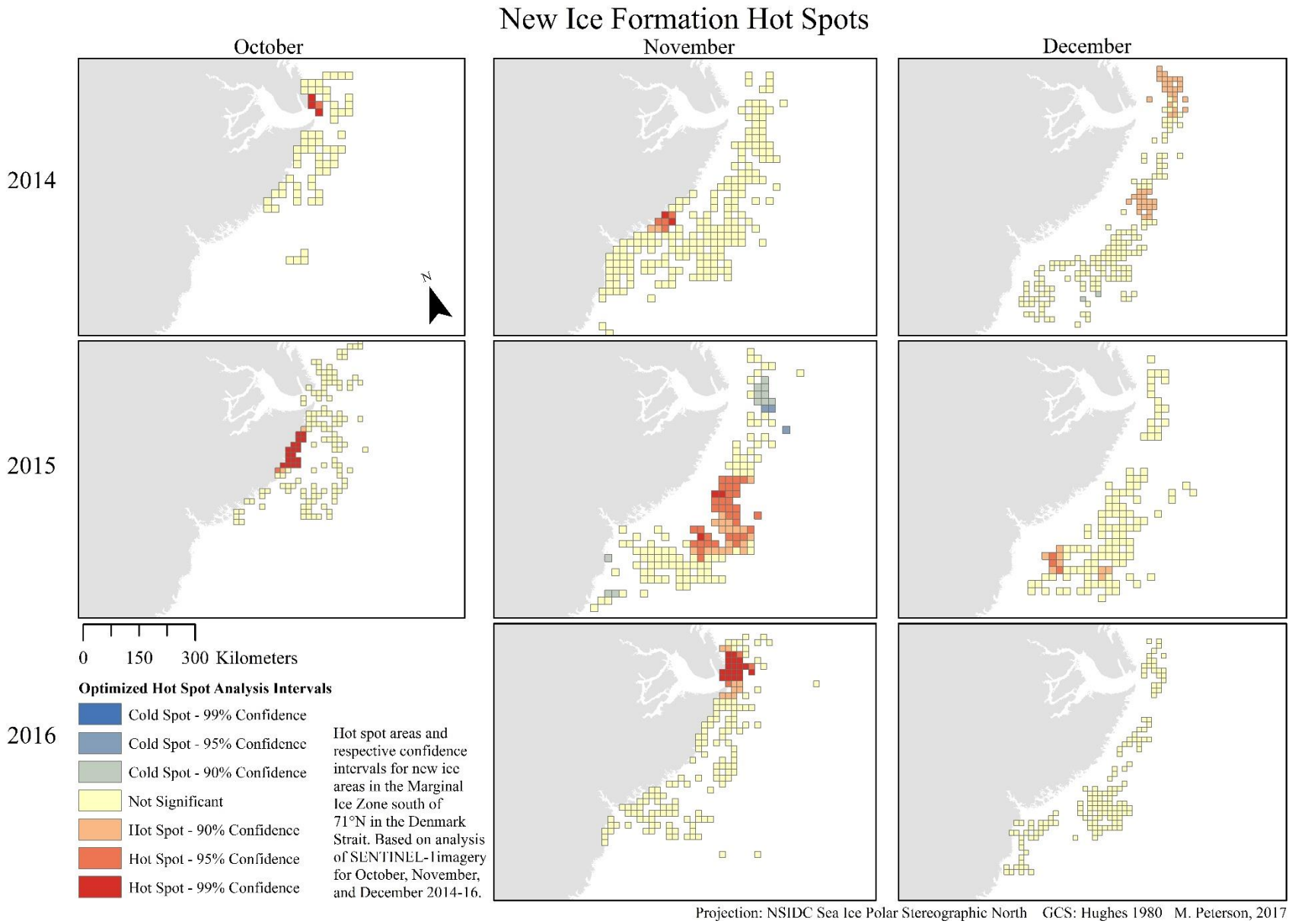


*Figure 30: A comparison of where hot spots of MIZ new sea ice formation occurred across each month of the study period.*

## 5.3 Spatial Analysis

### 5.3.1 Intersections

Intersections were performed to cross separate months with each other to determine which share the greatest spatial MIS new ice formation overlap. Intersections in Table 3 are sorted from greatest to least shared area. October 2015 and November 2016 showed the most overlap, which is interesting because the ice pack descended much later than usual in 2016, with initial descent into the study area occurring at the beginning of November instead of mid-way through October, as occurred in the previous two autumns. This means that new MIZ ice formation in November 2016 displayed behavior similar to new MIZ ice formation in an October. Granted, the study period is short, so this could be normal variation, however the areas of 2016 lagged generally, after getting a late start, so there could be future implications if this pattern persists.

December 2014 and December 2015 had the second-most overlap out of all the monthly intersections. The two years had very similar new ice formation behavior in the MIZ, so this result is expected. Also, both of these months saw substantial formation (compared to the other months in the study), which adds to the area count's rank. The third highest intersection area occurred between November 2014 and November 2016. Unexpectedly, November 2016 occupies two of the top three intersection spots. It is unclear why November 2016 would be more similar to October 2015, November 2014, and October 2014 (where it occupies the fourth highest area as well), than the other months except for that it may have displayed the most spatial variation of all the months. Conversely, December 2016 seems to offer the least commonality with the other months, occupying the bottom half of *Table 3*. December 2016 also had no significant clustering in the Hot Spot Analysis, which portends to the unfavorable climate conditions of that month, and corresponding high variability in the sea ice pack extent and the location of the MIZ.

*Table 3 Area of monthly spatial intersections of new ice formation areas in the MIZ, sorted from most to least shared area.*

| **Monthly Intersect** | **Intersecting Area ($km^2$)** |
|---|---|
| October 2015 and November 2016 | 21545.3 |
| December 2014 and December 2015 | 17722.1 |
| November 2014 and November 2016 | 15176.4 |
| October 2014 and November 2016 | 13186.9 |
| November 2014 and November 2015 | 12908.2 |
| October 2014 and October 2015 | 12301.5 |
| December 2014 and November 2016 | 5327.6 |
| November 2014 and December 2016 | 4935.6 |
| November 2015 and November 2016 | 3411 |
| December 2015 and December 2016 | 2642.1 |
| December 2015 and November 2016 | 2070.6 |
| December 2014 and December 2016 | 1574.2 |
| November 2015 and December 2016 | 1094.3 |

*Figure 31* demonstrates the magnitude of the spatial intersections between the various months. There is a large difference between the months that shared the most and the months that shared the least, which lends questions to why new MIZ ice formation was so weak in December 2016.

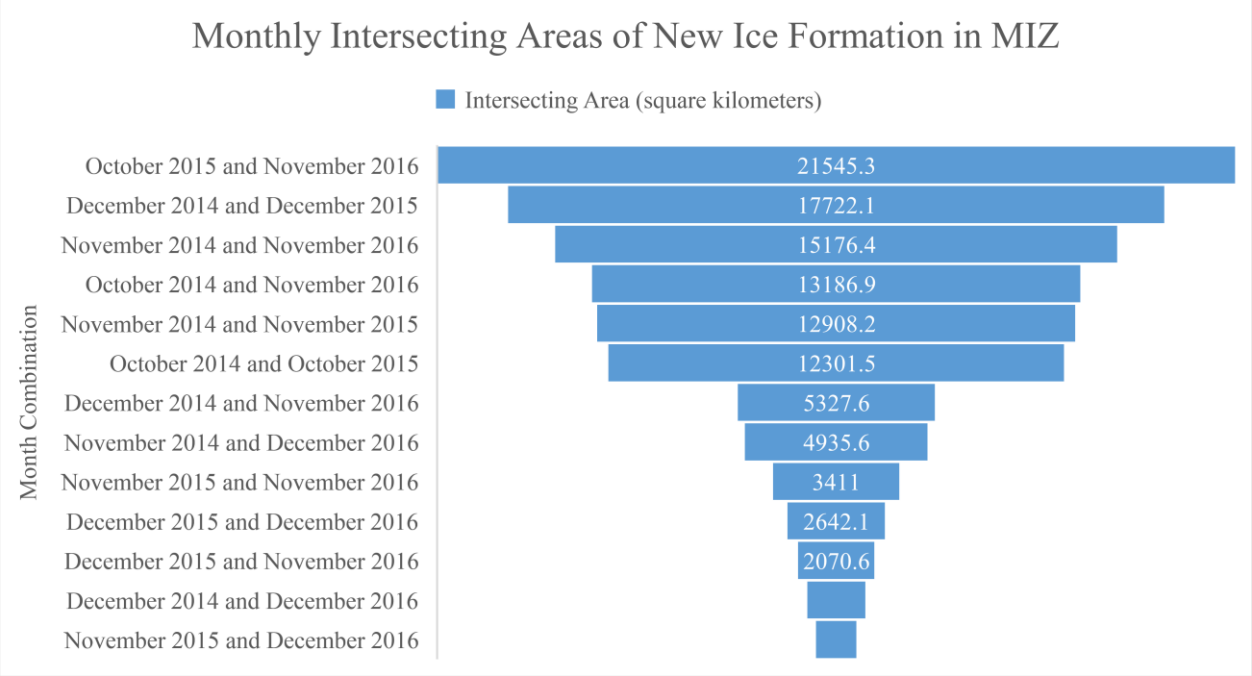


*Figure 31: Shows the quantities of new ice areas shared by each monthly pairing.*

*Figure 32* maps the locations of the six largest intersections. Map 1/6 shows the greatest amount of shared area as well as the greatest spatial coverage. Map 2/6 shows how much of the overlapping formation between December 2014 and 2015 occurred in the southernmost part of the study area, well-separated from the coast by a substantial sea ice pack. In map 3/6, the overlap in the MIZ speaks to the extent of the ice pack, and also to the large variation of new ice formation in November as the pack makes its way southwards. Map 4/6 demonstrates how the new ice formation behavior of November 2016 mimicked that of October 2014 as well as that of October 2015 in map 1/6. Maps 5/6 and 6/6 demonstrate how similar November and October were for the 2014 and 2015 seasons.

*Figure 33* is intended to show where the greatest clustering of intersections occurred. The only significant clustering occurred along the Blosseville Coast, just south of Scoresby Sound, which makes sense because new MIZ ice formation each autumn happens first in that area. Some formation would have been expected at the northern tip of Scoresby, as seen in each year, however, formation does not occur there in the later months of autumn because that area is eventually occupied by sea ice pack for the remainder of the study period. Therefore, very significant formations are likely occurring in the coastal areas south of Scoresby longer into the season. However, this is because of the scope of the study period, as opposed to significant clustering of formation in general.

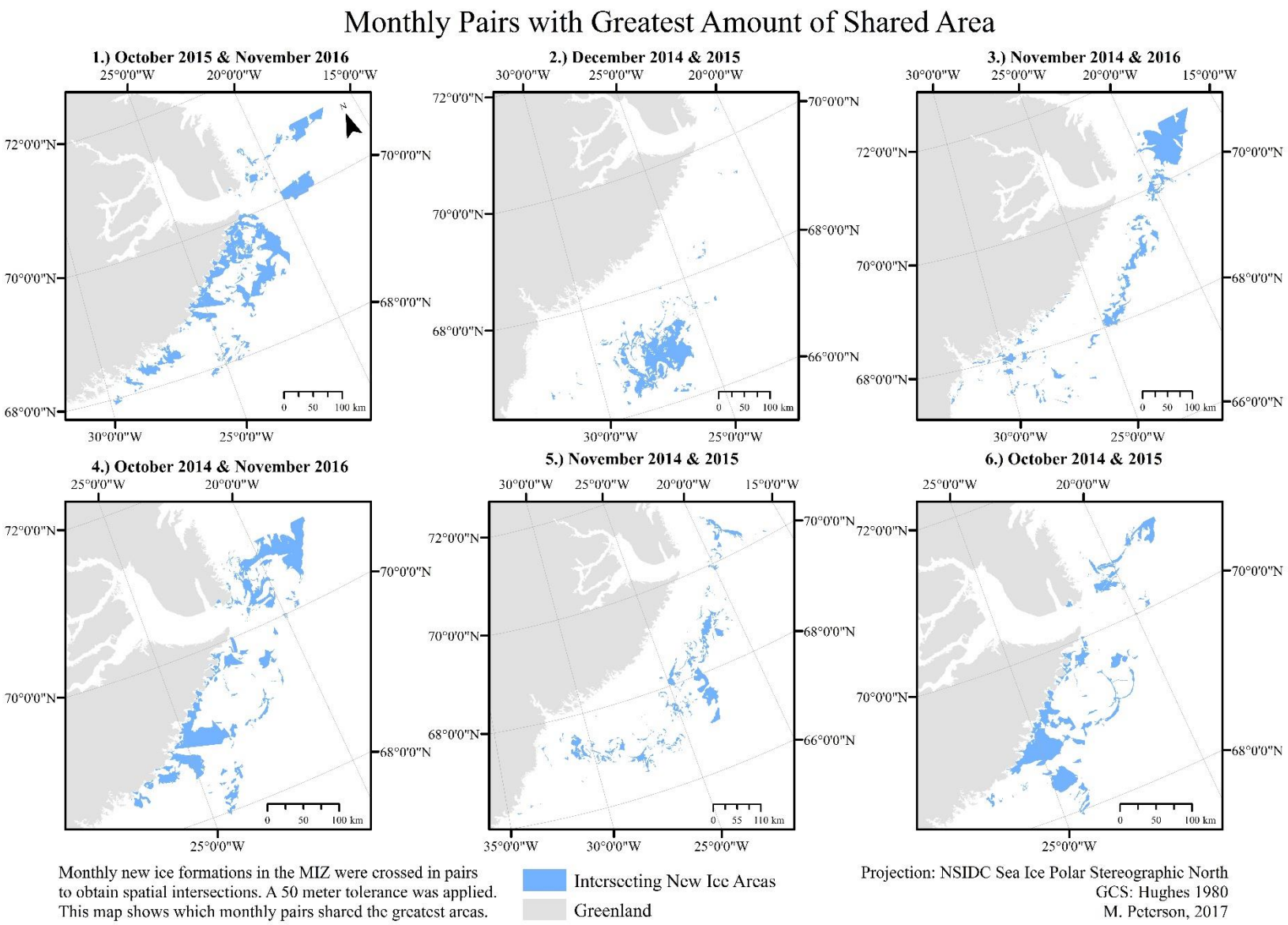


*Figure 32: Maps of the six monthly pairings that shared the most area of new ice formation in the MIZ from greatest to least shared area.*

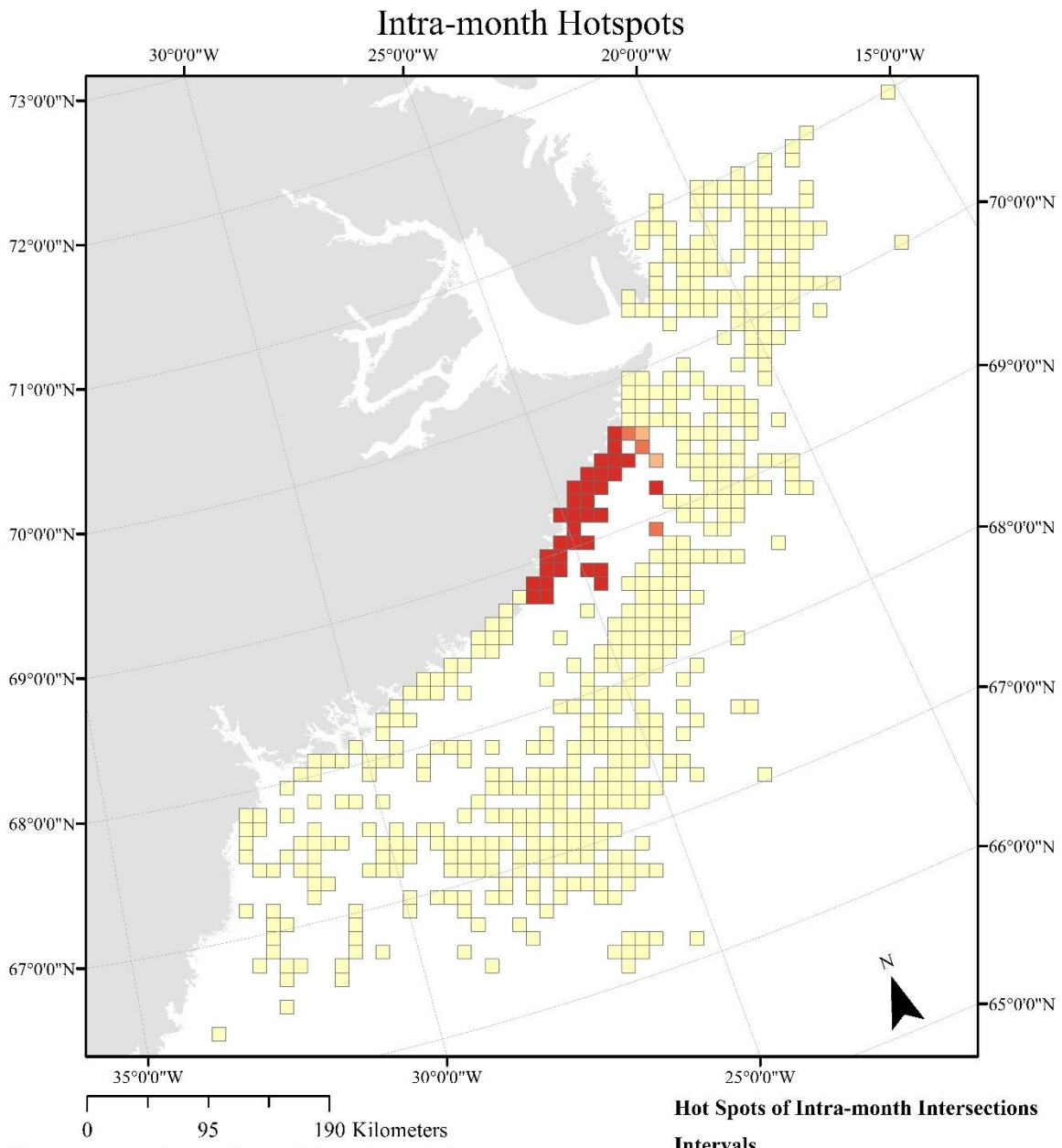


Hot spot areas and respective confidence intervals for new ice areas in the Marginal Ice Zone south of 71°N in the Denmark Strait. Based on analysis of SENTINEL-1 imagery for October, November, and December 2014-16. Includes all new ice areas greater than the 25000 sqare meters polygon threshold.

Months were crossed in pairs to obtain intersections. This map shows where intersections were significant across all years between monthly pairs.

Fishnet records number of incidences in a region from centroids of digitized new ice areas, and calculates the statistical signficance of the hot spot.

*Figure 33: Map showing the clustering between the different monthly intersections. The most statistically-significant clustering is found where ice first forms in the MIZ as freeze-up occurs.*

## Weather deformation

The end of November 2015 is an example of why it is important to study new ice formation in the Denmark Strait. Throughout November 2015, sea ice was moving steadily further south as the weeks passed. In the series of analyzed SAR imagery (*Figure 34*), on November 26th, 2015, the open ocean seems to be subject to high surface roughening, which appears to be a mesoscale storm system because of the uniformity of the pattern over most of the study area. This weather event was confirmed by optical imagery and wind data. Wind speeds went up to 40 knots mid-coast. The next day of available SAR imagery for the study area was for November 28th, 2015. The new ice formation on November 28th varies spatially from the last available day before the storm, which was November 24th, 2015.

At the northernmost boundary of the study area, the ice edge had migrated towards the shoreline nearly sixty-one kilometers between November 24th and November 28th, 2015. This means that large swaths of open ocean are freed of sea ice because of young ice deformation and compaction during the storm. Thus, after the conclusion of the storm, the ocean and atmosphere can more freely interact, allowing oceanic heat and moisture transport back to the much cooler atmosphere. The spatial disparity between the ice extents is most pronounced near the mouth of Scoresby Sound and the 67°N latitude line.

While storms in the cold seasons are important in the preconditioning of the ocean for sea ice formation by cooling the surface ocean at deeper layers (Wadhams, 2000), winter storms can also precondition strong summer melting by deforming ice irreversibly in that season (Itkin et al., 2016). It is worth noting that the concentration of thick, strong, MY ice has dwindled in recent years (Vizcarra, 2017b). This means more of the ice that is present in the Denmark Strait is constituted of FY or otherwise young ice, much of which is new ice forming in the Strait, itself. Mass freeze-up in the Strait is important enough to warrant study for maritime safety purposes, as conducted by the DMI and the IMO. Large expanses of very young and FY ice formations are present in the area, and what ice formed in the Arctic Ocean may be weakened by warmer sea surface temperatures and air temperatures as they drift to more southern locations. Thus, when strong winds from storms compact ice floes, more ice deformation can be expected than occurred previous to the 21st century because there is much more young ice; and young ice does not have the mechanical strength and melt-resistance of MY ice floes, as described by Wadhams (2000).

While deformation is not observed explicitly in this study, it can be inferred. Storms can be counted in the imagery when there are excessively high winds in the study area. Roughening of the ocean surface by excessive winds can be confirmed by wind records from ASCAT and from optical imagery. On days where there are storms, which often last for a few days, ice extent ceases to grow, and just after the storms ceases, the next image will have a reduced sea ice pack extent, on order of kilometers.

This phenomenon can be observed on the dates December 19-21, 2016. On the day after the storm has ceased, the pack extent is measurably reduced at the mouth of Scoresby Sound. The lateral shift along the 70° North parallel is 43 kilometers from the day before the storm. This is significant, because while the area becomes preconditioned for new ice freeze-up, the reduced pack extent exposes tens or hundreds of square kilometers to ocean-atmosphere interactions. If, for instance,

air temperatures have increased, this exposes the ocean to potential surface warming which can melt present ice and prevent new ice formation.

Another observation from this specific storm, is that sea ice extent does not decrease everywhere. It actually increases at the 69° North parallel. However, this is likely from the sea ice pack from the 70° North parallel relocating because of north and northeasterly wind-caused ice buildup on the coast. The ice on the edges of the last image are also banded out in ice streamers so the pack is less uniform and ice is more likely to drift into the Strait, dependent on wind and ocean current conditions.

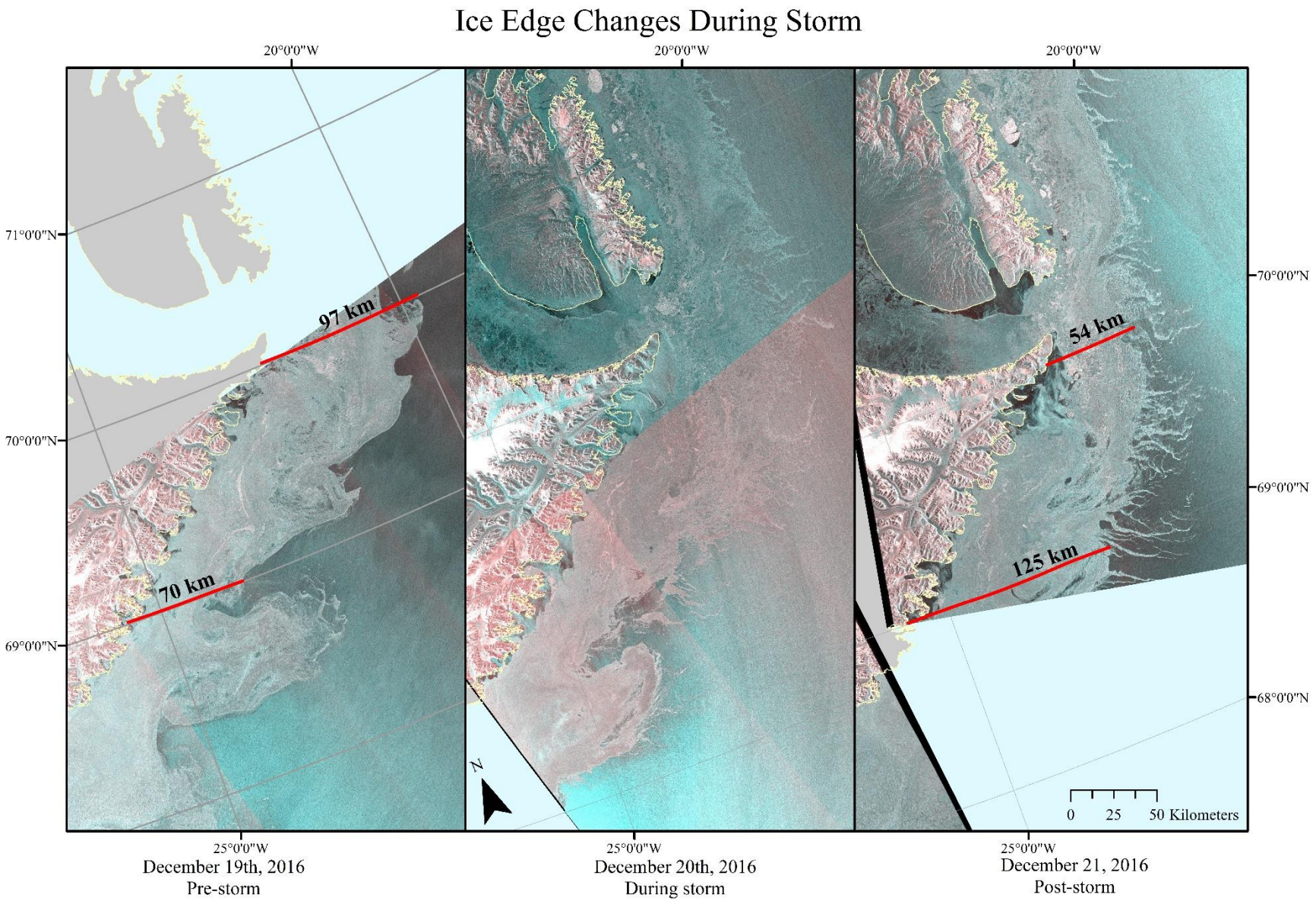


*Figure 34: Maps showing how sea ice edge and extent can be modified by storm and wind activity.*

### 5.3.2 Extent by year

Another way to visualize the spatial variations between the three autumns is to look at the end-of-season extents. The map in *Figures 35* and *36* show the extents of the sea ice pack edge on December 21st of each of the study years, and for the last decade, respectively. December 21st is the first day of astronomical winter, when the pack should be expanding at the most rapid rates because of suppressed air temperatures and cooling sea surface layer temperatures. The data for the ice edges were provided by the NIC.

The last three years show large latitudinal variations. At the northernmost part of the image, 2015 has the furthest eastern extent, followed by 2016, and trailed by 2014. The light pink line shows the extent of the northernmost portion of the 2016 extent. Between the 68th and 69th parallels, the extents are nearly the same for all three years. However, there is substantial variation again in the southern part of the study area, with 2016 having the greatest extent at about 66.5 ° North, to be overtaken in the south by 2014 and 2015.

This result seems counterintuitive to the new ice portion of the study, because 2014 showed the greatest growth in the MIZ. However, the ice extents contain both new and all other ice types, so 2015 and 2016 had a higher influx of ice from north of the study area by December 21st.

In *Figure 35*, of the December 21st extents from the last decade, there is a lot of variation. The start year, 2006, the end year, 2016, and the year of the sea ice record minimum (2012) were emphasized to show that the fluctuations are bi-directional, not just showing lesser extents each year. However, using the NSIDC's Sea Ice Index tool to compare the median monthly sea ice extents over the last decade to the median ice edge from 1981-2010, there are negative sea ice extent differences occurring in the study area (Fetterer et al., 2016). The changes in the Autumn indicate a negative trend in the ice extent over the decade. Anomalies in sea ice concentrations in the study area were more interannually variable at the beginning of the decade with both positive and negative deviations from the normal, but express only negative concentration anomalies over the course of the study period.

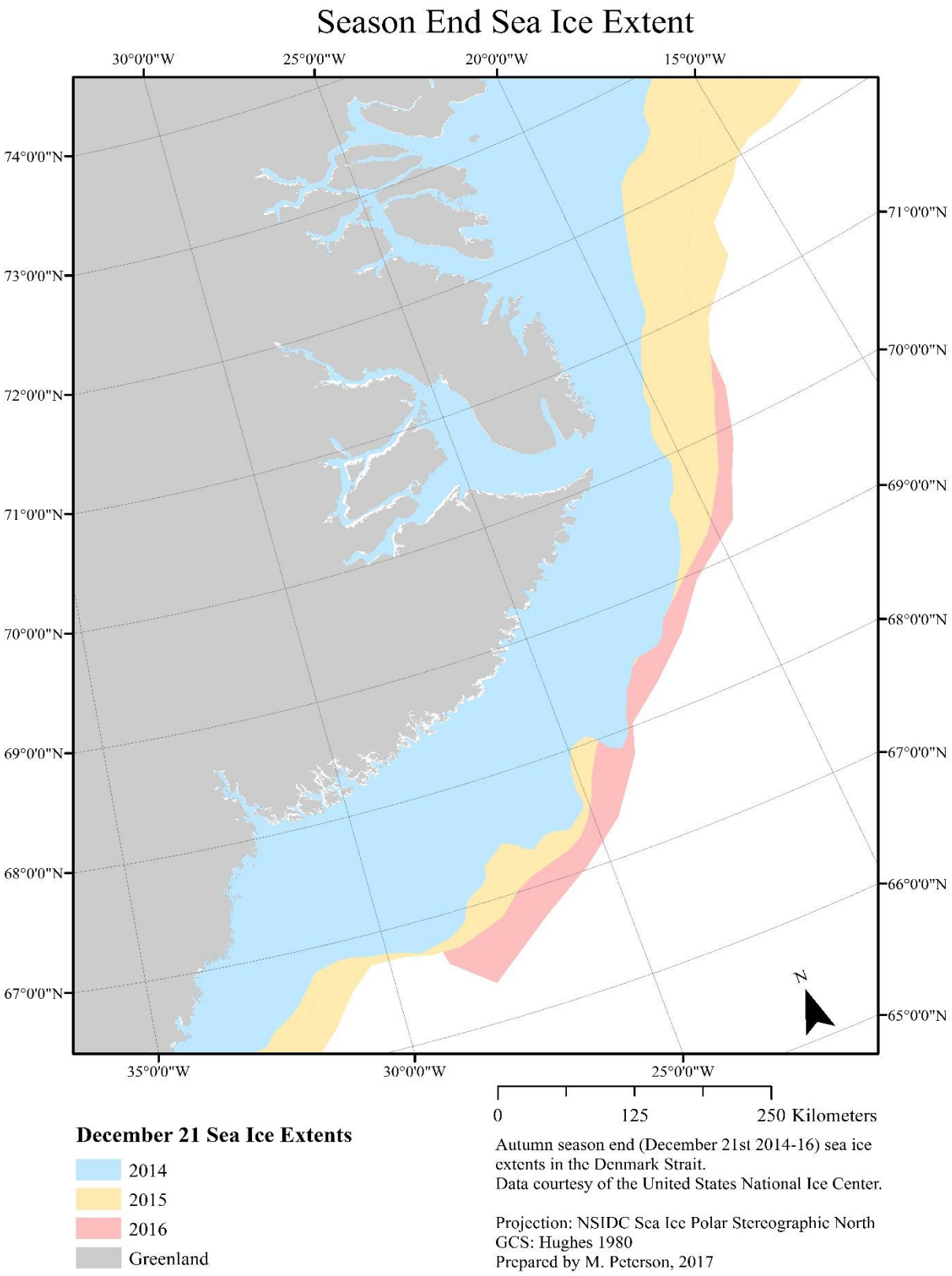


*Figure 35: Sea ice extents for the end of the winter season for the three years of study, according to National Ice Center ice edge shapefiles.*

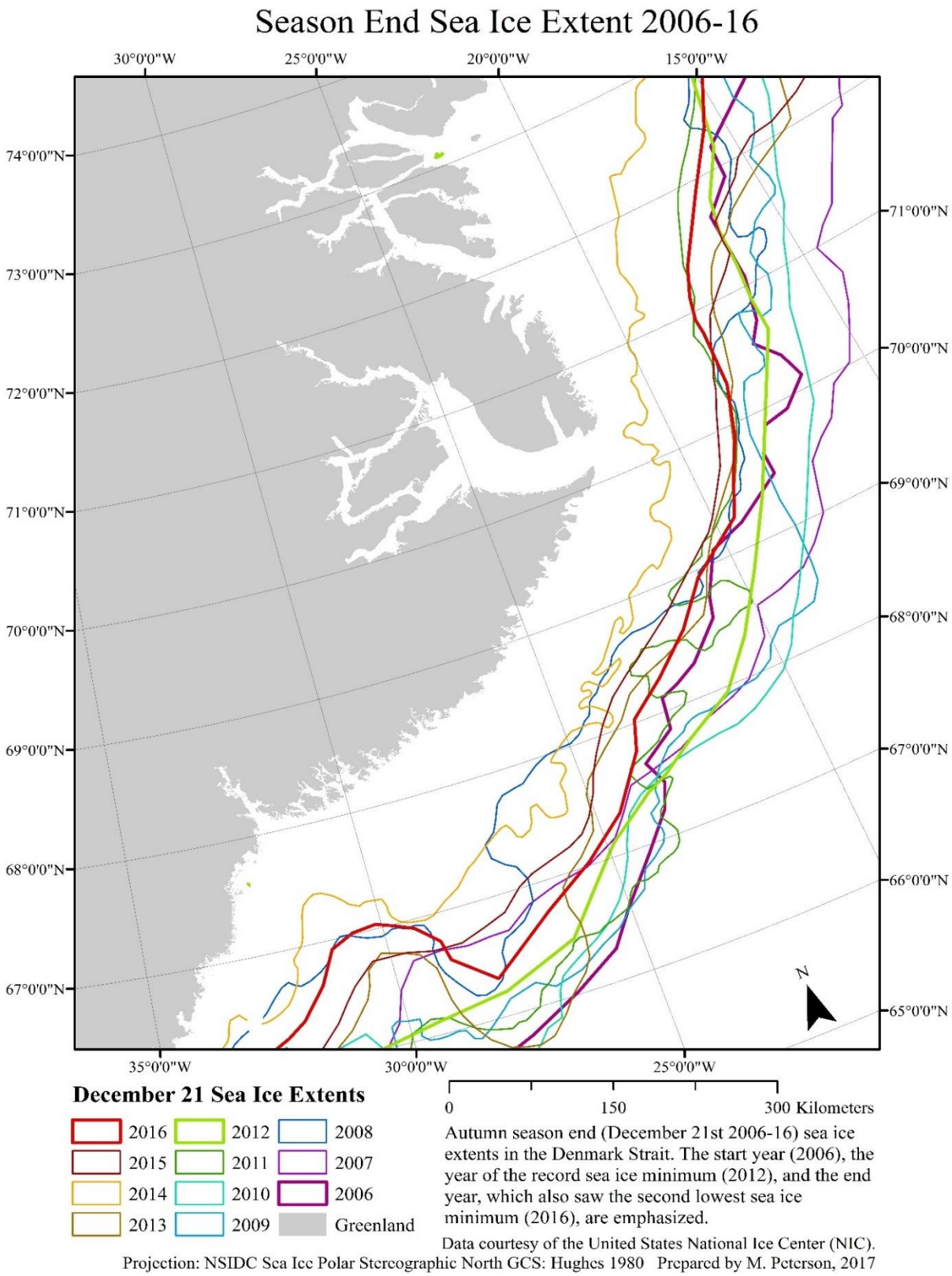


*Figure 36: End of autumn season extents from 2006-2016 shows interannual variability of sea ice pack extent, but a trend towards less area.*

## 5.4 Climate Pre-conditioning

A narrative begins to take shape when the climate variables over the three year period are considered. Daily and monthly temperatures were acquired for stations in areas around the Denmark Strait. Via NOAA GHCN, historical daily data for air temperatures in Tasiilaq, Greenland and Scoresby Sound (at Ittoqqortoormiit, Greenland) were acquired. Air temperatures for Tasiilaq are found in *Table 6 (appendix)* and are given in Fahrenheit (freezing point of water is 0°C/32° Fahrenheit, sea ice formation occurs at -1.8°C/28.7°F)

During October 2016, air temperatures in Tasiilaq did not dip below freezing from October 1 to October 26. The average minimum temperature in October 2016 was 2.2°C/36°F, and the average maximum temperature was 6.6°C/44°F. Maximum temperatures remained above freezing the entire month. These air temperatures corresponded with no sea ice pack present in the study area, and no new ice formation. Usually, by mid-October, air temperatures are dropping and allowing for the sea surface layer to cool enough for some minor new ice formation. The graph in *Figure 37a* demonstrates how both the average minimum and maximum air temperatures were higher than normal in October 2016. *Figure 37b* shows how few days with temperatures below freezing occurred in October 2016, and *Figure 37c* shows how there were no days in October 2016 that remained entirely below freezing.

*Table 7 (appendix)* gives the daily observation of air temperature at Ittoqqortoormiit, Greenland (located in Scoresby Sound), as well as wind direction and velocity, whether there was ice formation and an example of preconditioning of new ice formation.

*Table 4* and the graph in *Figure 38* show the proportion of days below freezing and the average monthly air temperature at Scoresby Sound. Some data values are missing because of indications that data quality for those dates (including all of December 2016) could not be verified. This is unfortunate, because it would be interesting to understand how air temperatures in Scoresby Sound corresponded to the large new ice formation in November 2014 and strange new ice formation behavior in December 2016

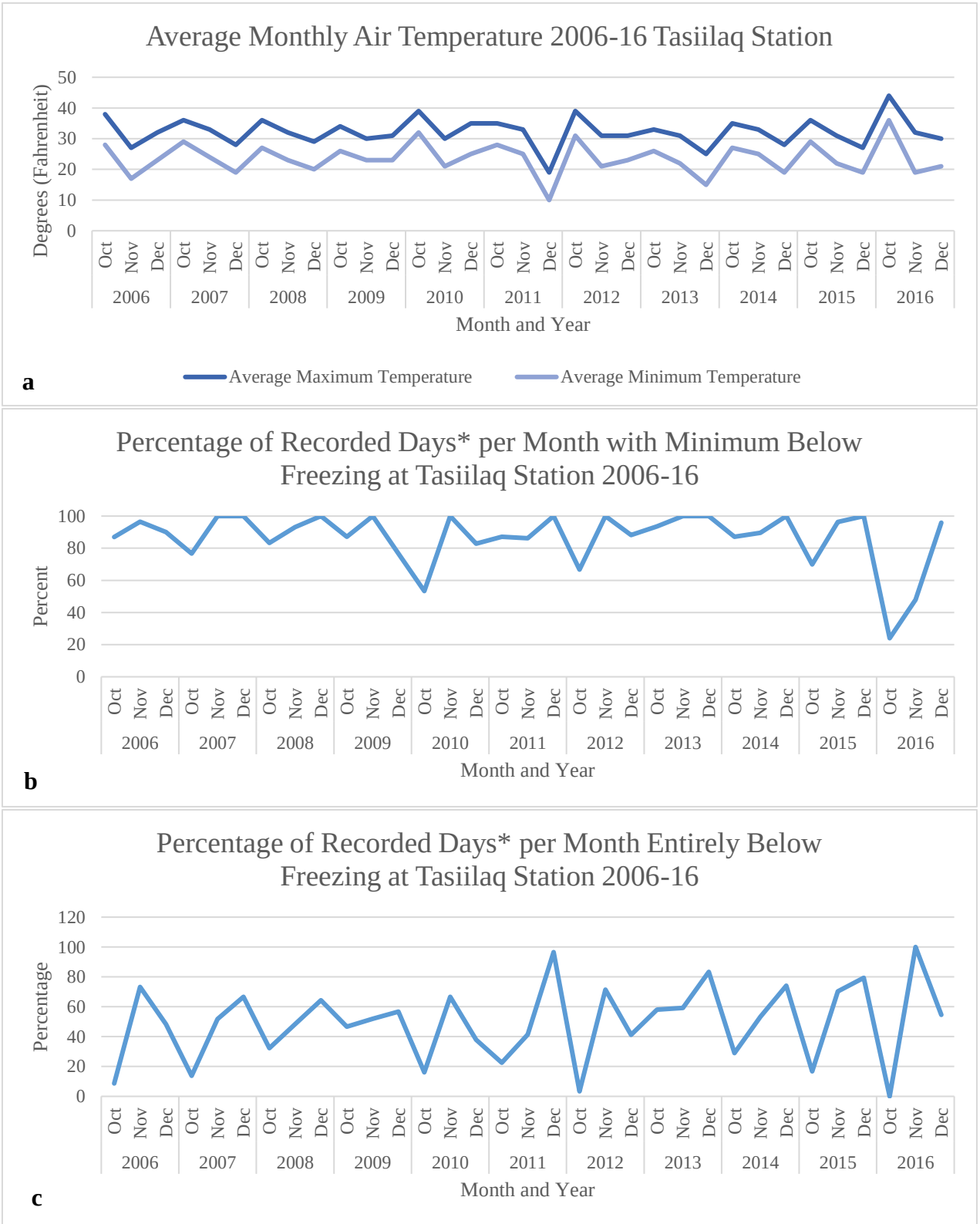


*Figure 37: (a) Graph showing the monthly average air temperatures at Tasiilaq, and (b) the percentage of days with minimum temperatures below freezing temperature (0 ° C, 32 ° F). Figure 37 (c) shows the percentage of days with sustained daily temperatures below freezing.*

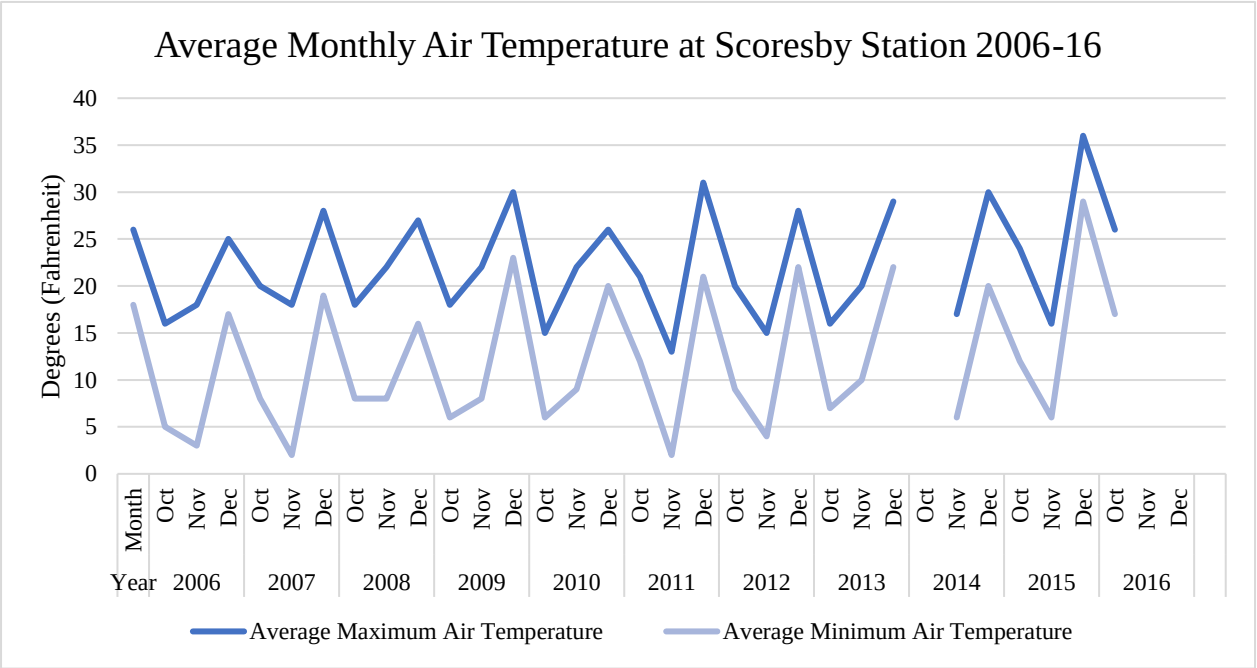


*Figure 38: Graph of monthly air temperatures at Ittoqqortoormiit and the interannual variability.*

*Table 4: Fraction of days with reliable observations at Ittoqqortoormiit station with minimum air temperatures at or below freezing, and days entirely below freezing. Dates with unconfirmed data quality from NOAA GHCN were omitted.*

| Year | Month | Days with minimum Air T at or below freezing** | Days entirely below freezing |
|---|---|---|---|
| 2014 | Oct | 28/29 | 20/29 |
| 2014 | Nov | 4/4 | 2/3 |
| 2014 | Dec | 21/21 | 21/21 |
| 2015 | Oct | 31/31 | 18/31 |
| 2015 | Nov | 30/30 | 27/30 |
| 2015 | Dec | 31/31 | 30/31 |
| 2016 | Oct | 25/25 | 4/29 |
| 2016 | Nov | 22/22 | 14/20 |
| 2016 | Dec | * | * |
| | | *Data not available<br>**Only confirmed quality data included | |

Daily wind observations were recorded from interpretation of regions from archived ASCAT maps (*Table 8, appendix*). Dates with missing data indicate that data was not available, and some observations were taken from the earlier or latter part of the day, if there was not an observation around the time that the SAR image was acquired. The most prevailing winds in the study area are northeasterly winds, and local katabatic westerlies near the coast of Greenland. Storms are identifiable, typically where wind speeds exceed 35 knots. Where many wind directions are indicated may signify a low pressure system moving through the area(where the winds are high, >30) or very calm winds where the winds (are very low, <10 knots).

Sea surface temperatures were also read from archived maps and the lowest reading in the general region was recorded in *Table 9, appendix*. This was done so that if temperatures decreased anywhere in the study region within the freezing threshold for sea ice, it would be indicated. However, the spatial resolution of the CLASS Global SST product is very coarse, at 50 kilometers, so localized areas of further suppressed sea surface temperatures were considered possibilities where there appeared to be clear formation on the Sentinel-1 imagery and air temperature agreement. Unfortunately, the product was discontinued in 2016, so there are not readings for the year when the new sea ice formation seemed to lag behind the other two years.

All of the climate variables were considered together with the imagery and a qualitative interpretation was made, along with a determination of whether there was any preconditioned new ice formation in the MIZ. The qualitative log is found in *Table 10, appendix*. The days that were considered preconditioned are listed in *Table 11, appendix* and an overall tabulation of the preconditioning of the three autumns is given in *Table 5*.

Overall, preconditioning for new MIZ ice in the study area appears most closely related with air temperatures suppressed under 30° Fahrenheit/ -1° Celsius and minimum daily air temperatures below 20° Fahrenheit/-2° Celsius. Also, more new ice formation was associated with months that had a greater proportion of days entirely below freezing. Unsurprisingly, the largest formations were associated with calm winds, less than 10 knots, although formation still occurred through approximately 25 knots. It is worth noting that a major form of pre-conditioning for sea ice formation, however, is the presence of preexisting sea ice itself, however that is inherent in this study.

*Table 5: Counts of climate pre-conditioned days during the study period, compared to the number of image days analyzed in the study for each year.*

| **Pre-conditioned Day Analysis** | | |
|---|---|---|
| **Year** | **Pre-conditioned days** | **Images Assessed for Season** |
| 2014 | 15 | 43 |
| 2015 | 21 | 46 |
| 2016* | 10 | 35 |
| *shorter season because freeze-up not until November | | |

## 5.5 Drift

Variations in backscatter responses in MY ice allow for specific parcel identification and tracking. Some studies (Muckenhuber, Korosov, & Sandven, 2016) have been working to automate the process of tracking ice drift directions and velocities, as well as the volumes of ice which are exported through areas of interest, such as the Fram Strait, well-north of the study area. The conclusions of these studies are interesting inputs for research on the Denmark Strait, because Fram Strait is the largest export area of Arctic sea ice, and imports sea ice into the study area. A sub-component of this study sought to continue drift ice direction and volume tracking efforts.

In the early autumn, as the sea ice first passes south of Scoresby Sound, it is very difficult to differentiate between discrete ice blocks because of how pulverized the southward moving ice has become on its journey. This tends to taper off later in the season, however remains an issue the further south one desires to analyze. South of Scoresby Sound, when air temperature conditions permit, allows for freeze-up of surface ocean into new ice between discrete parcels of FY and MY ice that have been advected southwards. In autumn, it is common for a freeze-thaw cycle to dominate as air temperatures fluctuate with the changing weather (apparent in the temporal patterns over the course of each year). Ice can become increasingly broken into smaller parcels because of freeze-thaw, particularly in combination with the mechanical forces exerted in the ice gyres that form in the EGC south of Scoresby, and deformation from storm and strong wind compaction activity.

Deformation is apparent in autumn, when even unique, recognizable floes north of Scoresby Sound can become indistinguishable from surrounding ice within a matter of days, as evidenced in *Figure 39*. Previous studies (Muckenhuber et al., 2016) formally identified that drift ice tracking was not pursued in the autumn season, because of the amount of deformation the sea ice pack undergoes in that season. The best seasons for monitoring drift ice are when the ice is fully-formed and at its strongest during the winter and the spring seasons. During summer, passive microwave sensors confuse surface melt signatures on the pack ice with that of open water because of the similarities in spectral response, and in the autumn sea ice is very broken-up, with floes breaking-up beyond recognition during storms and in the gyres of the EGC against the Blosseville Coast. This study sought to use consecutive images on a weekly basis to track sea ice as it passed south of Scoresby Sound and to monitor floe direction and velocity. The sub-study was not successful, however, because of the reasons established in Muckenhuber et al (2016). Break-up of the sea ice pack was very pronounced in the three autumn study periods, particularly in the part of the study area which is south of Scoresby Sound. Individual MY floes could rarely be identified in multiple consecutive image time series, as further evidenced in *Figure 40*.

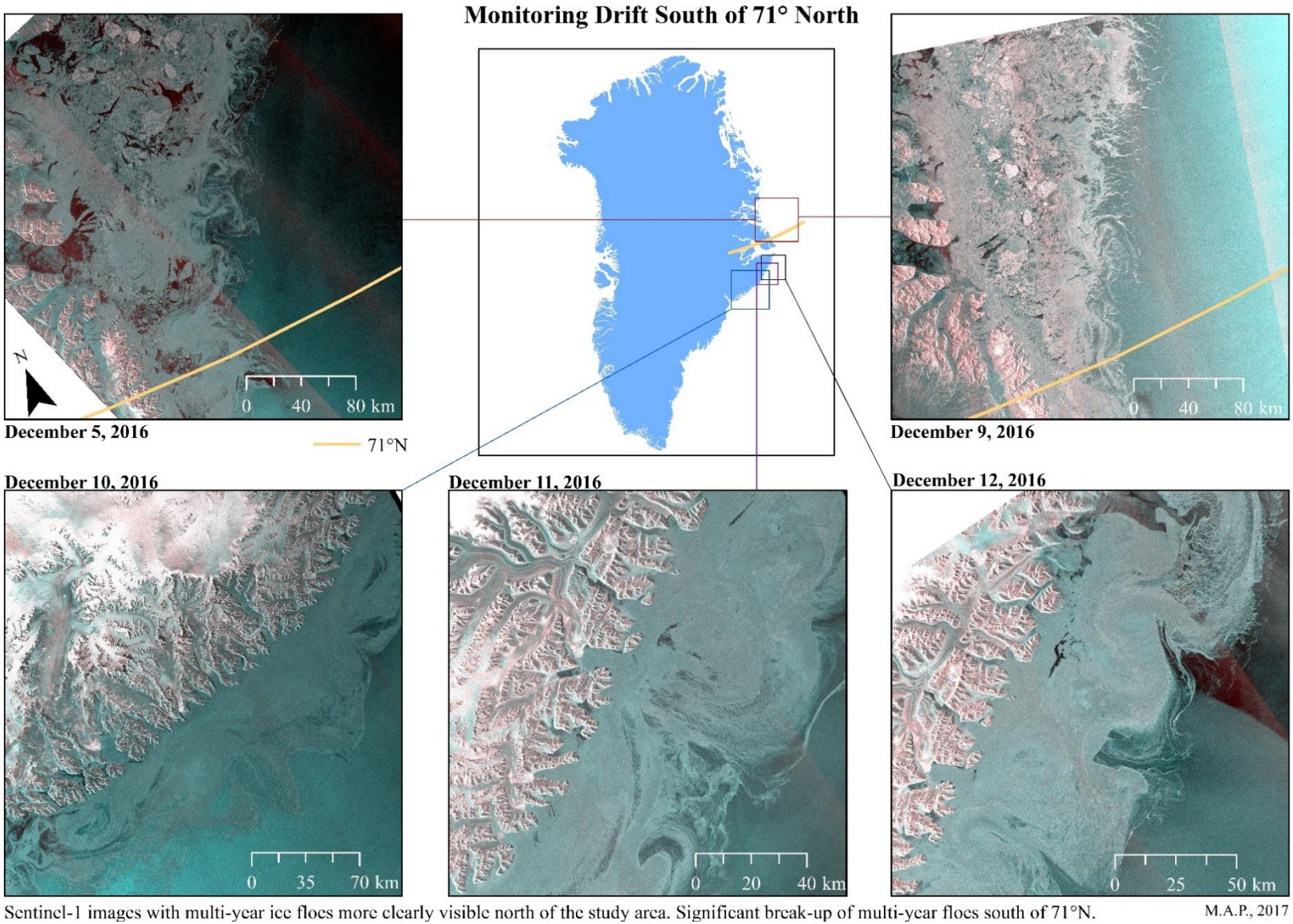


*Figure 39: Example of how it can be difficult to monitor drift south of Scoresby Sound because of the break-up that the sea ice pack undergoes there during the autumn season.*

In *Figure 39*, MY ice floes with distinctive features are visualized in the top of the image. However, once these floes pass into the study area, through the light yellow line representing 71 ° North, they become increasingly indistinguishable over the next few days. As the ice travels southwards, it deforms into smaller and smaller floes, until the unique MY floe markings have disintegrated into an unidentifiable portion of the well-processed sea ice pack. In winter, with decreasing air and sea temperatures, MY floes can survive in the study area, but that is outside the scope of this study.

On occasions of very cold temperatures in the study area and rapid revisit times, several parcels were tracked for single image pairs. However, so few instances were confidently recorded, that an analysis on drift velocities and drift directions cannot be made as expected and results cannot be confirmed with statistical significance because the sample size is too small. *Figure 40* shows an image pair from late in the study period in 2016. Taken just one day earlier, the large, easily identifiable MY floe coming out of Scoresby Sound has disappeared.

The conclusion is that it is very difficult to identify a significant sample of ice floes and track their drift during autumn south of 71° North because of subjection of sea ice to extreme Autumn break-up.

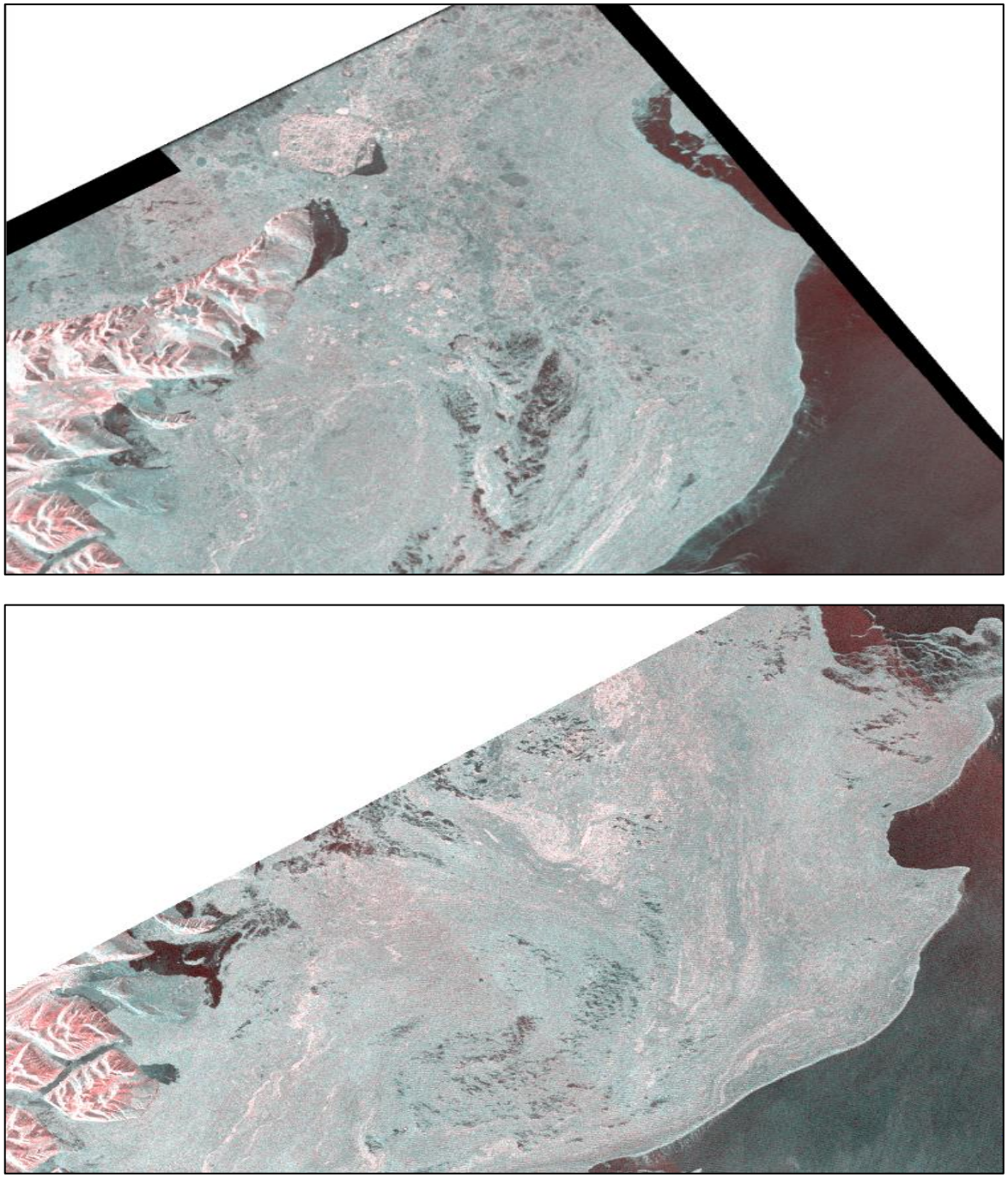

*Figure 40: Sentinel-1 images of December 18 (top) and 19 (bottom), 2016. Very clear ice floes with distinctive markings are present in the December 18th image. Within one day, those parcels of ice have been rendered all but unrecognizable by deformation processes.*

# 6 Discussion

The objectives of the study involved testing Sentinel-1 imagery to determine how useful it is for independent classification and in combination with other climate variables. While classifying the new ice parcels was successful, particularly with the addition of climate information and additional imagery sources, new ice formation often occurs on very rapid times scale, on the order of hours or days. While the polar revisit time for Sentinel-1 is very high, missing images can prevent new ice from being identified as it formed. It is likely that the images available during the study period missed substantial formation. To compensate for this, young-looking ice was marked "N" for "Not confident" where it appeared to be very recently formed.

Another issue with the new ice portion of the study, is that, because of varying data availability, and the desire to capture all the possible new formation, a formal sampling scheme was not used. This is partially because of the availability of images over the course of the months is not consistent, and also because the available imaging dates may not have been representative of the overall conditions. While the study was performed as accurately as possible with the available imagery, a more regular temporal resolution would have been preferable.

In the study area, ice deformation presents a challenge to monitoring drift ice from Sentinel-1 imagery. In the autumn, the warm ocean water, variable air temperatures, and intermittent storms can inhibit sea ice growth. The force of winds and the East Greenland Current drive sea ice into the coast of Greenland south of Scoresby Sound. The autumn sea ice pack making the southward journey becomes increasingly broken-up until unique features from MY floes are no longer distinguishable. While it is clear sea ice is abundant in the area, individual floes become lost in the pack during the study period and make manual, let alone, automated tracking, difficult. Beneath a certain size, mixed-ice parcels and floes of varying types in the pack appears too homogeneous to specifically track and interpret. Typically, discrete parcels of sea ice are clearly visible and distinguishable based on their varying backscatter signals to the sensor. Spatial resolution of satellite imagery is certainly high enough to distinguish parcels based on new, first, or MY ice classifications, as well as to discern surface characteristics by which to track the drift of the ice parcel, and to automate these procedures through algorithms and machine learning. This is possible north of Scoresby Sound in autumn, winter, and spring; but because of conditions south of the Scoresby Sound, the homogeneity of autumn sea ice makes identification tedious, offering a limited sample size.

While the optimized hot spot analysis achieves spatially and statistically significant results, it is worth pointing out that the discrete boundaries of the digitized polygons are overlooked in such an analysis. The hot spot analysis requires the input of points, and thus, centroids were calculated for each polygon representative of new ice formation in the study area. Depending on the method of calculating the hot spots, whether via aggregation in a fishnet or snapping to weighted neighborhood points, the instances of overlap of the far edges of polygons are not accounted for. Thus, presence and absence is not accurate in the hot spot analysis output. In order to compensate for the spatial discrepancy (between counting instances of center points instead of all overlapping instances), additional spatial analysis was carried out to determine locations which produced the greatest quantity of new ice formation across combinations of months. This analysis is interesting, but because of

sampling error due to image availability and because some polygons did not have the confidence of the analyst, it would be beneficial to run additional statistical analyses as more autumn seasons are imaged by Sentinel-1.

Another issue in the hot spot analysis is the breaking up of larger polygons, and either skewing the analysis by increasing polygon counts, or ignoring the weight of large areas by digitizing them as a single polygon represented by one centroid point. Ideally, to address the issue of underestimating the influence of larger new ice areas, or overestimating clusters where there are mostly small area formations, new ice polygons should be divided into somewhat even areas (within an area range) when they are digitized so that more expansive formations will carry representative weight across a spatial extent. This could prove difficult, because the smallest bound should be at the minimum threshold of 2500 $m^2$, but many new ice formations far surpass that area and would be extremely tedious to digitize into potentially hundreds of smaller polygons.

Alternatively, a polygon layer, such as a fishnet, could be created where all instances of any area of a polygon (above a minimum threshold value) would register as a single instance in any cell that it overlaps. The accumulated counts from the cell over a series of days, months, or seasons could then be translated as a field to a centroid point for each fishnet polygon and a hot spot analysis could be carried out with a more representative sample. In this case, the analysis field would be the accumulated instance count from the original fishnet polygon mesh.

In order to make a more concrete analysis on how the climate records relate to the spatial instances of new MIZ ice formation, spatial statistics should be applied to combine the data sets and model a quantitative relationship. The next steps to approach this would be to find complete climate data sets for each image date, and ensuring that there is not a data level difference where there are changes in the data set. For instance, if sea surface temperatures could be collected for Autumn 2016 and combined with the CLASS SST Global 50 km dataset, the two data sets would need to be translated to the spatial resolution of the coarser data set. Also, downloadable data sets for spatial SST, air temperature, air pressure, and wind data sets would need to be located and cleaned for use in analysis. Correlation and regression in R would provide a more quantitative climate-new MIZ ice relationship for the Denmark Strait.

To address the delays in freeze-up onset it would be worth further examining interannual variability. One possible extension to address this would be to perform a raster-based cell count of sea ice presence and absence on a weekly time scale throughout the Autumn season for the last decade, using NIC ice edge data. Thus, the probability of sea ice presence can be determined week-by-week.

Weekly spatial intersections instead of monthly spatial intersections would also be worth examining to gain more precise insight on the similarities and differences over the Autumn periods of new sea ice formation in the MIZ. With the further collection of sea ice imagery from Sentinel-1 in the coming years, a longer, more robust record will be available to assessing freeze-up spatial and temporal patterns, and the associated climate conditions in the Denmark Strait.

# 7 Conclusions

SAR imagery from Sentinel-1 already has three years of data which are freely available online through the Copernicus Program. Sentinel-1 imagery provides high resolution, all-weather, all-illumination imagery for use in sea ice mapping applications. The Denmark Strait is a highly traversed marine corridor, which means that sea ice behavior must be monitored at frequent intervals for safety purposes. This study tested how independent classification and demarcation of new sea ice areas in the MIZ from Sentinel-1 images compared to classification with the assistance of climate data and supplemental imagery (from passive microwave, and optical sensors, when available). The difference in confidence and the number and area of polygons digitized when climate variables were included in the analysis was substantial. This indicates that automating new ice classification of Sentinel-1 imagery without other data inputs may be difficult.

The study also finds that over the course of three astronomical autumn seasons, 2014-2016, there were changes in the spatial and temporal patterns of new ice formation in the Denmark Strait. The years 2014 and 2015 were similar in new sea ice formation in the MIZ, however, 2016 differed substantially, with no formation in October of that year, and less than normal new ice formation through the rest of the season. As evidenced through spatial intersections of MIZ new ice areas, it seems that November 2016 exhibits a pattern more like October of the two previous years, and December 2016 shows very little spatial resemblance to any other month analyzed in the study period. Autumn 2014 saw the most growth out of the study period, per the images available.

A hot spot analysis was carried out to determine where statistically significant clusters of new MIZ ice formation occurs. The largest hot spots in the initial and the secondary analyses occurred on the northern side of Scoresby Sound, and at around 68 ° North 25 ° West. Significant clustering was present in all months with new ice formation, except for during December 2016. These results are interesting when considering the difficulty the sea ice pack had in reaching normal extents in Autumn 2016, breaking the minimum monthly sea ice extent records for October, November, and December.

A qualitative analysis of climate variables, as they corresponded to new ice formation in the Sentinel-1 images, was carried out and days with substantial formation were assessed for climate indicators. Pre-conditioned days were noted, and forty-six days over the three autumns were identified as having preconditions for favorable new MIZ ice formation. 2015 had the most pre-conditioned days out of the three study seasons.

At the end of the astronomical autumn season, on December 21$^{st}$, the sea ice extents in the Denmark Strait for the three study seasons (2014-16) were compared to those of the last decade. The last three years had some of the lowest sea ice extents out of the decade, even lower than the year with the record minimum sea ice extent (2012). While interannual fluctuations in sea ice extent are normal, due to the dynamic nature of the phenomenon and the variability of the atmospheric and ocean conditions which control its production and survival, there is a visible decrease in autumn sea ice extent in the Denmark Strait since 2006 (Fetterer et al., 2016).

Sea ice drift directions and velocities are interesting to monitor as well, to get an understanding of how wind conditions and currents are controlling the sea ice pack. Sea ice

parcel tracking was attempted with MY floes in the autumns of 2014, 2015, and 2016 using Sentinel-1 image pairs of consecutive days. Similar to the findings of studies such as Muckenhuber et al. (2016) where autumn ice pack was not considered for feature tracking because of extensive pack deformation, autumn sea ice pack deformation south of Scoresby Sound is so pronounced that no significant drift results are reported from this study.

Sentinel-1 offers high resolution, openly accessible, frequent revisit, all-weather/solar illumination, polar and sub-polar imagery which makes it an excellent choice for use in sea ice monitoring. However, more work will need to be carried out to determine how to best model new MIZ sea ice formation and how to automate classification from SAR imagery for use in maritime safety and in climate monitoring. This serves as a preliminary study on new ice formation in an era of decreasing multiyear ice concentration and record low sea ice extents. It is worth studying new ice formation in zones of seasonal sea ice cover because the results may have implications for the future of an increasingly younger Arctic sea ice cover. More areas will be seasonally ice free in the Arctic, and seasonally ice-covered areas can give insight into spatial and temporally freeze-up patterns.

While this is a preliminary study on the utility of Sentinel-1 imagery applications to sea ice monitoring, there are further studies that can be conducted to extend use of Sentinel-1. In a further extension of the study, it would be informative to use spatially-linked climate data and statistical analysis to assess a possible quantitative relationship between new sea ice production and how it is explained spatially by a variety of variables, including the addition of the depth of the surface ocean, drift speeds, and above-ice temperatures.

Eventually, it would be beneficial to have automatically-derived Sentinel-1 sea ice classifications for ice types and ice concentrations with further development in Sentinel-1 pattern recognition and training. Automatically-derived Sentinel-1 sea ice products would add spatial resolution to the steady legacy of passive microwave derived products. This study provides support that such a task would be best supplemented with ancillary data, at least in the identification of possible new ice formation areas.

# References


Arctic Circle Secretariat. (2016). Arctic Circle conference panel: Global economic interests of Arctic change. The Arctic Circle. Retrieved from https://vimeo.com/188430739

Bader, J., Mesquita, M. D. S., Hodges, K. I., Keenlyside, N., Østerhus, S., & Miles, M. (2011). A review on Northern Hemisphere sea-ice, storminess and the North Atlantic Oscillation: Observations and projected changes. *Atmospheric Research*, *101*(4), 809–834. http://doi.org/10.1016/j.atmosres.2011.04.007

Beitler, J. (2016). Sea ice hits record lows. Retrieved December 5, 2016, from http://nsidc.org/arcticseaicenews/2016/12/arctic-and-antarctic-at-record-low-levels/

Beitler, J. (2017). Another record, but a somewhat cooler Arctic Ocean. Retrieved May 2, 2017, from http://nsidc.org/arcticseaicenews/2017/04/another-record-but-a-somewhat-cooler-arctic-ocean/

Bekryaev, R. V., Polyakov, I. V., Alexeev, V. A., Bekryaev, R. V., Polyakov, I. V., & Alexeev, V. A. (2010). Role of Polar Amplification in Long-Term Surface Air Temperature Variations and Modern Arctic Warming. *Journal of Climate*, *23*(14), 3888–3906. http://doi.org/10.1175/2010JCLI3297.1

Cabedo-Sanz, P., Belt, S. T., Jennings, A. E., Andrews, J. T., & Geirsdóttir, A. (2016). Variability in drift ice export from the Arctic Ocean to the North Icelandic Shelf over the last 8000 years: A multi-proxy evaluation. *Quaternary Science Reviews*, *146*, 99–115. http://doi.org/http://doi.org/10.1016/j.quascirev.2016.06.012

Carsey, F. D., Barry, R. G., & Weeks, W. F. (1992). Microwave remote sensing of sea ice. In F. Carsey (Ed.), *Microwave Remote Sensing of Sea Ice* (pp. 1–7). Washington, DC: American Geophysical Union. Retrieved from https://books.google.is/books

ESRI. (2017). How Hot Spot Analysis (Getis-Ord Gi*) Works. Retrieved May 3, 2017, from http://pro.arcgis.com/en/pro-app/tool-reference/spatial-statistics/h-how-hot-spot-analysis-getis-ord-gi-spatial-stati.htm

European Space Agency. (2017). User Guides - Sentinel-1 SAR - Sentinel Online. Retrieved April 15, 2017, from https://sentinel.esa.int/web/sentinel/user-guides/sentinel-1-sar

Fetterer, F., Knowles, W., Meier, W., & Savoie, M. (2016). Sea Ice Index, Version 2. Boulder, Colorado, USA: NSIDC: National Snow and Ice Data Center. http://doi.org/10.7265/N5736NV7

Gerland, S., Haas, C., Hall, R., Holfort, J., Hansen, E., Loyning, T. B., & Renner, A. (2006). Spring sea ice thickness in the western Fram Strait: Preliminary results. In P. Wadhams & G. Amanatidis (Eds.), *Artic Sea Ice Thickness: Past, Present and Future* (pp. 158–164). Luxembourg: European Commission.

Getis, A., & Ord, J. K. (1992). The Analysis of Spatial Association by Use of Distance Statistics. *Geographical Analysis*, *24*(3), 189–205. Retrieved from http://www.csiss.org/gispopsci/workshops/2005/PSU/docs/castro_getis.pdf

Holt, B. (2004). SAR Imaging of the Ocean Surface. In C. R. Jackson & J. R. Apel (Eds.), *Synthetic Aperture Radar Marine User's Manual* (pp. 25–80). Washington, DC: U.S. Department of Commerce. Retrieved from http://www.sarusersmanual.com/

Icelandic Met Office. (2017). Sea ice around Iceland. Retrieved May 1, 2017, from http://en.vedur.is/sea-ice/

Itkin, P., Spreen, G., Cheng, B., Doble, M., Girard-Ardhuin, F., Haapala, J., … Wilkinson, J. (2016). Thin ice and storms: a case study of sea ice deformation from buoy arrays deployed during N-ICE2015. *J. Geophys. Res.*, *Submitted*(NICE2015 special issue). http://doi.org/10.1002/2016JC012403

Jayne, S. R. (2015). Marginal Ice Zone. Retrieved May 3, 2017, from http://sjayne.whoi.edu/marginal-ice-zone/

Jónsdóttir, I. (2006). Historical variation in sea-ice extent off Iceland. In *International Ice Charting Working Group*. Helsinki: Finnish Institute of Marine Research. Retrieved from ftp://sidads.colorado.edu/pub/projects/noaa/iicwg/IICWG-2006/1_Monday/Sea Ice monitoring/iicwg__07.pdf

Jónsdóttir, I., & Sveinbjörnsson, E. (2007). Recent variations in sea-ice extent off Iceland. *Jökull*, *57*(57), 61–70.

Jónsson, S. (2017). Ocean currents. Retrieved May 3, 2017, from http://www.fisheries.is/ecosystem/oceanography/ocean-currents/

Kang, D., Im, J., Lee, M.-I., & Quackenbush, L. J. (2014). The MODIS ice surface temperature product as an indicator of sea ice minimum over the Arctic Ocean. *Remote Sensing of Environment*, *152*, 99–108. http://doi.org/10.1016/j.rse.2014.05.012

Kumar, A., Perlwitz, J., Eischeid, J., Quan, X., Xu, T., Zhang, T., … Wang, W. (2010). Contribution of sea ice loss to Arctic amplification. *Geophysical Research Letters*, *37*(21), n/a-n/a. http://doi.org/10.1029/2010GL045022

Kwok, R. (2014). Declassified high-resolution visible imagery for Arctic sea ice investigations: An overview. *Remote Sensing of Environment*, *142*, 44–56. http://doi.org/10.1016/j.rse.2013.11.015

Kwok, R., Cunningham, G. F., & Pang, S. S. (2004). Fram Strait sea ice outflow. *Journal of Geophysical Research: Oceans*, *109*(C1), C01009. http://doi.org/10.1029/2003JC001785

Lynch, P. (2016, July 19). 2016 climate trends continue to break records. Retrieved May 2, 2017, from https://www.nasa.gov/feature/goddard/2016/climate-trends-continue-to-break-records

Mann, M. E. (2002). Little Ice Age. In M. C. MacCracken, J. S. Perry, & T. Munn (Eds.),

*Encyclopedia of Global Environmental Change* (Vol. 1, pp. 504–509). Chichester: John Wiley & Sons, Ltd. Retrieved from http://www.meteo.psu.edu/holocene/public_html/shared/articles/littleiceage.pdf

McCandless Jr., S. W., & Jackson, C. R. (2004). Principles of Synthetic Aperture Radar. In C. R. Jackson & J. R. Apel (Eds.), *Synthetic Aperture Radar Marine User's Manual* (pp. 1–24). Washington, DC: U.S. Department of Commerce. Retrieved from http://www.sarusersmanual.com/

Muckenhuber, S., Korosov, A. A., & Sandven, S. (2016). Open-source feature-tracking algorithm for sea ice drift retrieval from Sentinel-1 SAR imagery. *Cryosphere*, *10*(2), 913–925. http://doi.org/10.5194/tc-10-913-2016

National Snow and Ice Data Center. (2017). Cryosphere Glossary. Retrieved May 3, 2017, from https://nsidc.org/cryosphere/glossary/term/marginal-ice-zone

Ogilvie, A. E. J., Hill, B. T., & Jónsson, T. (2011). Sea Ice as Enemy and Friend: The Case of Iceland and Labrador/Nunatsiavut. In *6th NRF Open Assembly* (pp. 1–18). Hveragerdi: Northern Research Forum. Retrieved from https://www.rha.is/static/files/NRF/OpenAssemblies/Hveragerdi2011/proceedings/finalastridogilvienrf2011paper.pdf

Ogilvie, A. E. J., & Jónsdóttir, I. (2000). Sea Ice, Climate, and Icelandic Fisheries in the Eighteenth and Nineteenth Centuries, *53*(4), 383–394. Retrieved from http://pubs.aina.ucalgary.ca/arctic/Arctic53-4-383.pdf

Ogilvie, A. E. J., Woollett, J. M., Smiarowski, K., Arneborg, J., Troelstra, S., Kuijpers, A., … Mcgovern, T. H. (2009). Seals and Sea Ice in Medieval Greenland. *Journal of the North Atlantic*. Retrieved from http://www.nabohome.org/meetings/glthec/materials/ogilvie/OgilveetalSealsPaper.pdf

Onstott, R. G., & Shuchman, R. A. (2004). SAR Measurements of Sea Ice. In C. R. Jackson & J. R. Apel (Eds.), *Synthetic Aperture Radar Marine User's Manual* (pp. 81–116). Washington, DC: U.S. Department of Commerce. Retrieved from http://www.sarusersmanual.com/

Overland, J. E., & Wang, M. (2013). When will the summer Arctic be nearly sea ice free? *Geophysical Research Letters*, *40*(10), 2097–2101. http://doi.org/10.1002/grl.50316

Potter, S., Cabbage, M., & McCarthy, L. (2017, January 18). NASA, NOAA data show 2016 warmest year on record globally. Retrieved May 2, 2017, from https://www.nasa.gov/press-release/nasa-noaa-data-show-2016-warmest-year-on-record-globally

Rigor, I. G., & Wallace, J. M. (2004). Variations in the age of Arctic sea-ice and summer sea-ice extent. *Geophysical Research Letters*, *31*(9), n/a-n/a. http://doi.org/10.1029/2004GL019492

Sea Ice Atlas. (2017). Glossary. Retrieved May 3, 2017, from http://seaiceatlas.snap.uaf.edu/glossary

Shuchman, R., Onstott, R. G., Johannessen, O. M., Sandven, S., & Johannessen, J. A. (2004). Processes at the Ice Edge --The Arctic. In C. R. Jackson & J. R. Apel (Eds.), *Synthetic Aperture Radar  Marine User's Manual* (pp. 373–396). Washington, DC: U.S. Department of Commerce. Retrieved from http://www.sarusersmanual.com/

Stroeve, J., Serreze, M., Drobot, S., Gearheard, S., Holland, M., Maslanik, J., … Scambos, T. (2008). Arctic Sea Ice Extent Plummets in 2007. *Eos, Transactions American Geophysical Union*, *89*(2), 13. http://doi.org/10.1029/2008EO020001

Strong, C., & Magnusdottir, G. (2009). Modeled winter sea ice variability and the North Atlantic Oscillation: a multi-century perspective. *Climate Dynamics*, *34*(4), 515–525. http://doi.org/10.1007/s00382-009-0550-7

Strong, C., & Rigor, I. G. (2013). Arctic marginal ice zone trending wider in summer and narrower in winter. *Geophysical Research Letters*, *40*(18), 4864–4868. http://doi.org/10.1002/grl.50928

Tang, Q., Zhang, X., Yang, X., & Francis, J. A. (2013). Cold winter extremes in northern continents linked to Arctic sea ice loss. *Environmental Research Letters*, *8*(1), 14036. http://doi.org/10.1088/1748-9326/8/1/014036

U.S. National Ice Center. (2017). Daily Ice Analysis Products. Retrieved April 20, 2017, from http://www.natice.noaa.gov/products/daily_products.html

University of Washington Applied Physics Laboratory. (2017). Atmosphere-Ice Coupling in the Evolving MIZ. Retrieved from http://www.apl.washington.edu/project/project.php?id=miz

Vihma, T. (2014). Effects of Arctic Sea Ice Decline on Weather and Climate: A Review. *Surveys in Geophysics*, *35*(5), 1175–1214. http://doi.org/10.1007/s10712-014-9284-0

Viking Society for Northern Research. (1981). *Saga-Book* (Vol. XX). London: University College London. Retrieved from http://www.vsnrweb-publications.org.uk/Saga-Book 1-22 searchable/Saga-Book XX.pdf

Vinje, T., & Finnekasa, O. (1986). *The Ice Transport through the Fram Strait*. Oslo, Norway: Norsk Polarinstituut.

Vinje, T., Løyning, T. B., & Polyakov, I. (2002). Effects of melting and freezing in the Greenland sea. *Geophysical Research Letters*, *29*(23), 44-1-44–4. http://doi.org/10.1029/2002GL015326

Visbeck, M. H., Hurrell, J. W., Polvani, L., & Cullen, H. M. (2001). The North Atlantic Oscillation: past, present, and future. *Proceedings of the National Academy of Sciences of the United States of America*, *98*(23), 12876–7. http://doi.org/10.1073/pnas.231391598

Vizcarra, N. (2017a). Arctic sea ice maximum at record low for third straight year. Retrieved May 5, 2017, from http://nsidc.org/arcticseaicenews/2017/03/arctic-sea-ice-maximum-at-record-low/

Vizcarra, N. (2017b). Warm Arctic, cool continents. Retrieved May 10, 2017, from https://nsidc.org/arcticseaicenews/2017/05/warm-arctic-cool-continents/

Wadhams, P. (2000). *Ice in the Ocean*. Amsterdam: Gordon and Breach Science Publishers.

Wang, M., & Overland, J. E. (2009). A sea ice free summer Arctic within 30 years? *Geophysical Research Letters*, *36*(7), n/a-n/a. http://doi.org/10.1029/2009GL037820

Wang, M., & Overland, J. E. (2012). A sea ice free summer Arctic within 30 years: An update from CMIP5 models. *Geophysical Research Letters*, *39*(18). http://doi.org/10.1029/2012GL052868

Widell, K., Osterhus, S., & Gammelsrod, T. (2003). Sea ice velocity in the Fram Strait monitored by moored instruments. *Geophysical Research Letters*, *30*(19).

Zege, E., Malinka, A., Katsev, I., Prikhach, A., Heygster, G., Istomina, L., … Schwarz, P. (2015). Algorithm to retrieve the melt pond fraction and the spectral albedo of Arctic summer ice from satellite optical data. *Remote Sensing of Environment*, *163*, 153–164. http://doi.org/10.1016/j.rse.2015.03.012

# Appendix

*Table 6: Daily air temperatures for the study period taken at Tasiilaq, Greenland weather station (in degrees Fahrenheit). NOAA GHCN.*

Daily Air Temperatures* Tasiilaq

| Year | **Month** | **Day** | **Max T** | **Min T** |
|---|---|---|---|---|
| **2014** | October | 12 | 38 | 27 |
| | | 18 | 36 | 27 |
| | | 21 | 33 | 27 |
| | | 24 | 30 | 24 |
| | | 26 | 34 | 20 |
| | | 30 | 31 | 19 |
| | | 31 | 37 | 21 |
| | November | 2 | 31 | 25 |
| | | 3 | 32 | 21 |
| | | 5 | 25 | 22 |
| | | 6 | 28 | 18 |
| | | 7 | 29 | 20 |
| | | 9 | 24 | 19 |
| | | 12 | 34 | 19 |
| | | 14 | 46 | 31 |
| | | 17 | 34 | 29 |
| | | 20 | 32 | 31 |
| | | 22 | 37 | 21 |
| | | 23 | 37 | 33 |
| | | 24 | 36 | 31 |
| | | 25 | 31 | 21 |
| | | 26 | 36 | 21 |
| | | 27 | 37 | 29 |
| | | 29 | 29 | 25 |
| | | 30 | 29 | |
| | December | 1 | | 13 |
| | | 2 | 22 | 12 |
| | | 3 | 30 | 14 |
| | | 4 | 29 | 15 |
| | | 6 | | 16 |
| | | 7 | 33 | 18 |
| | | 8 | 34 | 20 |
| | | 12 | 26 | |

**Table continued on next page**

| | | | | |
|---|---|---|---|---|
| | | 13 | | 12 |
| | | 15 | 25 | 10 |
| | | 16 | 25 | 19 |
| | | 17 | 32 | 15 |
| | | 18 | 32 | 20 |
| | | 19 | 31 | 24 |
| **2015** | October | 2 | 35 | 26 |
| | | 3 | 39 | 26 |
| | | 7 | 38 | 34 |
| | | 9 | 41 | 34 |
| | | 14 | 40 | 30 |
| | | 16 | 40 | 33 |
| | | 19 | 34 | 27 |
| | | 21 | 27 | |
| | | 25 | 35 | 19 |
| | | 26 | 38 | 23 |
| | | 27 | 44 | 32 |
| | | 28 | 42 | 37 |
| | November | 2 | 30 | 28 |
| | | 4 | 37 | 21 |
| | | 7 | | 21 |
| | | 8 | 33 | 19 |
| | | 11 | 26 | 20 |
| | | 12 | 28 | 18 |
| | | 14 | 24 | 17 |
| | | 16 | 24 | 20 |
| | | 17 | 23 | 17 |
| | | 18 | 40 | 13 |
| | | 19 | 56 | 18 |
| | | 20 | 58 | 37 |
| | | 21 | 41 | 32 |
| | | 22 | 40 | |
| | | 23 | | 26 |
| | | 24 | 29 | 23 |
| | | 26 | | 13 |
| | | 28 | 27 | 17 |
| | December | 1 | 30 | 24 |
| | | 2 | 31 | 21 |
| | | 4 | | 19 |
| | | 5 | 29 | 17 |
| | | 6 | 38 | 21 |
| | | 11 | 19 | 14 |
| | | 12 | 20 | 11 |

**Table continued on next page**

| | | | | |
|---|---|---|---|---|
| | | 13 | 21 | 17 |
| | | 15 | 21 | 17 |
| | | 17 | 17 | 12 |
| | | 18 | 18 | 7 |
| **2016** | November | 1 | 37 | 30 |
| | | 3 | 35 | |
| | | 6 | 29 | |
| | | 7 | 38 | |
| | | 8 | 30 | 23 |
| | | 13 | 37 | 21 |
| | | 15 | 33 | |
| | | 18 | 27 | 20 |
| | | 19 | 27 | 20 |
| | | 22 | 26 | 18 |
| | | 23 | | 18 |
| | | 25 | 20 | -8 |
| | | 27 | 38 | 31 |
| | | 28 | 36 | |
| | | 30 | 29 | 21 |
| | December | 1 | | 22 |
| | | 2 | 33 | 27 |
| | | 3 | 30 | |
| | | 4 | | 19 |
| | | 5 | | 29 |
| | | 9 | 29 | 10 |
| | | 10 | | 22 |
| | | 11 | 41 | 34 |
| | | 12 | 36 | 32 |
| | | 13 | | 26 |
| | | 14 | 38 | |
| | | 15 | | 21 |
| | | 16 | 33 | 22 |
| | | 17 | 34 | 21 |
| | | 18 | 34 | 26 |
| | | 19 | 29 | |
| | | 20 | 20 | |
| | | 21 | 16 | 10 |

***NOAA Climate Data Online daily summaries where data quality is confirmed**

*Table 7: Daily climate observations (using Ittoqqortoormiit readings) and determination of preconditioning.*

Study Area Daily Observations

| Year | Month | Day | MaxT | MinT | Ice form.? | Favorable wind? | Knots | Direction | Precon. ex? |
|---|---|---|---|---|---|---|---|---|---|
| **2014** | Oct | 12 | 33 | 19 | Y | Y | 5-15 | N | Y |
| | | 18 | 25 | 22 | M | N | 15-30 | N, NE | N |
| | | 19 | | | N | N | >50 | NE | N |
| | | 21 | 27 | 20 | Y | N | | | N |
| | | 24 | 24 | 18 | Y | Y | 5-15 | N, NW | Y |
| | | 26 | 33 | 25 | Y | Y | 5-10 | SE | Y |
| | | 30 | 21 | 10 | Y | M | 5-20 | NE | N |
| | | 31 | 21 | 8 | Y | N | 20-50 | NE | M |
| | | 1 | | | N | N | >50 | NE | N |
| | Nov | 2 | 26 | 17 | Y | N | 15-25 | NE | N |
| | | 3 | 39 | 17 | Y | Y | 0-15 | SE | M |
| | | 5 | | | Y | M | 10-20 | NE | N |
| | | 6 | | | N | N | 30-50 | N | N |
| | | 7 | | | M | N | 30 | S | N |
| | | 9 | | | Y | M | 5-15 | NE | M |
| | | 12 | | | M | N | 25-30 | NE | N |
| | | 13 | | | N | N | >50 | NE | N |
| | | 14 | | | N | N | 10-15 | NE | N |
| | | 17 | | | Y | Y | 5-25 | SW | Y |
| | | 20 | | | Y | M | 10 | SSE | M |
| | | 21 | | | Y | Y | 10-15 | SSE | Y |
| | | 22 | | | N | N | 5-20 | SE | Y |
| | | 23 | | | N | N | 5-20 | SE | N |
| | | 24 | | | Y | M | 10-15 | SSW | N |
| | | 25 | | | Y | M | 10-15 | S | N |
| | | 26 | | | Y | Y | 0-10 | N,S,W | Y |
| | | 27 | | | Y | M | 15-25 | SW | Y |
| | | 29 | | | Y | M | 20-35 | SE | Y |
| | | 30 | | | Y | N | 15-30 | E | N |
| | Dec | 1 | | | Y | N | 25-40 | WSW | N |
| | | 2 | | | Y | N | 5-20 | NW | Y |
| | | 3 | | | Y | N | 20-30 | SW | Y |
| | | 4 | | | Y | N | 30-45 | N | Y |
| | | 6 | | | M | N | 15-30 | NE | N |
| | | 7 | | | Y | N | 25-30 | NE | N |
| | | 8 | | | M | N | 10-25 | N | N |
| | | 12 | 7 | 0 | Y | N | 5-15 | NNW | N |
| | | 13 | 8 | 1 | Y | N | 25 | SE | N |

**Table continued on next page**

| | | | | | | | | | |
|---|---|---|---|---|---|---|---|---|---|
| | | 15 | 14 | 2 | Y | N | 30-35 | NNW | Y |
| | | 16 | 13 | 6 | M | N | 5-15 | SE | N |
| | | 17 | 16 | 10 | Y | N | 10-30 | SE, NE | N |
| | | 18 | 25 | 15 | Y | N | 10-20 | S | N |
| | | 19 | 20 | 12 | Y | N | 10-15 | S | N |
| **2015** | Oct | 2 | 30 | 23 | Y | Y | 0-15 | NW,W,SW | Y |
| | | 3 | 35 | 20 | Y | Y | 0-10 | W | Y |
| | | 7 | 36 | 30 | Y | N | 15-35 | N | N |
| | | 9 | 38 | 28 | Y | N | 10-35 | E, N | N |
| | | 14 | 37 | 15 | Y | M | 10-30 | SW | N |
| | | 16 | 30 | 22 | Y | N | 20-30 | SW | N |
| | | 19 | 33 | 18 | M | N | 20-25 | SW | N |
| | | 21 | 20 | 9 | Y | N | 20-25 | NE | N |
| | | 25 | 22 | 7 | Y | Y | 5-20 | N | Y |
| | | 26 | 22 | 9 | M | N | 20-30 | SE | N |
| | | 27 | 20 | 13 | Y | Y | 0-10 | E, SE, SW | Y |
| | | 28 | 27 | 15 | Y | Y | 10-25 | ENE | M |
| | Nov | 2 | 26 | 17 | Y | N | 15-25 | NE | N |
| | | 4 | 13 | 12 | N | N | 20-40 | NE | N |
| | | 7 | 32 | 23 | N | N | 10-30 | N | N |
| | | 8 | 32 | 25 | N | N | 10-20 | S | N |
| | | 9 | | | N | N | 10-30 | N | N |
| | | 11 | 19 | 8 | Y | N | 15-30 | N | N |
| | | 12 | 25 | 16 | Y | Y | 10-20 | NE | Y |
| | | 14 | 23 | 11 | Y | Y | 15-20 | N | Y |
| | | 16 | 22 | 13 | Y | N | 20-30 | NE | N |
| | | 17 | 17 | 6 | Y | N | 20-30 | N | N |
| | | 18 | 13 | 2 | Y | Y | 20-25 | N | Y |
| | | 19 | 7 | -1 | Y | Y | 10-20 | N, NE | Y |
| | | 20 | 30 | 2 | Y | Y | 10-20 | W | Y |
| | | 21 | 44 | 17 | Y | Y | 10-15 | NW | Y |
| | | 22 | 47 | 23 | Y | Y | 0-10 | S, SE | M |
| | | 23 | 41 | 26 | Y | N | >50 | N | N |
| | | 24 | 29 | 19 | Y | Y | 35-50 | N | Y |
| | | 26 | 16 | 2 | M | N | 30-40 | N | N |
| | | 28 | 18 | 7 | M | N | 30->50 | N | N |
| | | 29 | | | N | N | 35-40 | N | N |
| | Dec | 1 | 16 | 9 | Y | N | 25-30 | N | N |
| | | 2 | 19 | 11 | N | N | 40->50 | N | N |
| | | 3 | | | N | N | 30-40 | N | N |
| | | 4 | 20 | 10 | Y | N | 20-30 | N | N |
| | | 5 | 16 | 6 | Y | Y | 25-40 | N | Y |
| | | 6 | 17 | 5 | Y | Y | 10-20 | W | Y |
| | | 8 | | | N | N | 35-45 | NE | N |

**Table continued on next page**

| | | | | | | | | | |
|---|---|---|---|---|---|---|---|---|---|
| | | 11 | 16 | 5 | Y | Y | 10-20 | WSW | Y |
| | | 12 | 14 | 6 | Y | N | 10-25 | N | N |
| | | 13 | 14 | 6 | Y | N | 20-40 | N | N |
| | | 14 | | | N | N | 30->50 | NE | N |
| | | 15 | 7 | 3 | Y | N | 35-40 | NE | N |
| | | 17 | 6 | -4 | Y | N | 30-45 | N | Y |
| | | 18 | 15 | 4 | Y | M | 10-30 | N | M |
| **2016** | Nov | 1 | 37 | 22 | Y | M | 0-20 | S | M |
| | | 3 | 31 | 24 | Y | N | 30-40 | N | N |
| | | 6 | 39 | 18 | Y | M | 20-40 | SSW | M |
| | | 7 | 41 | 32 | M | N | 20-30 | SSW | N |
| | | 8 | 37 | 23 | Y | Y | 15-30 | SSE | Y |
| | | 13 | 36 | 25 | Y | Y | 10-20 | S, E | Y |
| | | 15 | 31 | 16 | Y | Y | 5-20 | W, N | Y |
| | | 18 | | | Y | N | 30-45 | N | N |
| | | 19 | 29 | 24 | Y | N | 25-30 | N | N |
| | | 21 | | | Y | Y | 0-25 | NNW | Y |
| | | 22 | 19 | | Y | Y | 0-20 | SE | Y |
| | | 23 | 18 | 8 | Y | Y | 0-20 | S | N |
| | | 25 | | | Y | Y | 25-40 | N | N |
| | | 27 | -10 | -17 | Y | Y | 10-15 | SW | Y |
| | | 28 | -12 | -23 | Y | Y | 10-30 | S, N | Y |
| | | 30 | | | Y | N | 20-35 | N | N |
| | Dec | 1 | | | Y | Y | 10-20 | N, NE | N |
| | | 2 | | | Y | N | 20-25 | ENE | N |
| | | 3 | | | Y | M | 0-20 | N | N |
| | | 4 | | | Y | M | 10-25 | N, NE | N |
| | | 5 | | | Y | Y | 5-15 | SW | M |
| | | 9 | | | Y | N | 25-30 | N | N |
| | | 10 | | | Y | Y | 5-30 | E | N |
| | | 11 | | | Y | Y | 5-25 | E, NE | N |
| | | 12 | | | Y | N | 20-40 | N | N |
| | | 13 | | | Y | N | 5-20 | NE | N |
| | | 14 | | | M | N | 10-40 | E, N | N |
| | | 15 | | | Y | N | 25-30 | ENE | N |
| | | 16 | | | Y | N | 20-35 | NW, N | N |
| | | 17 | | | Y | Y | 0-10 | NE, SW | N |
| | | 18 | | | Y | Y | 10-25 | SW | Y |
| | | 19 | | | Y | Y | 20-30 | SW | N |
| | | 20 | | | Y | N | >55 | N | N |
| | | 21 | | | Y | Y | 10 | NE | Y |
| | | | Air temperatures and wind conditions for Scoresby Sound. May differ elsewhere in study area. | | | | | | |

*Table 8: shows the study area broken into three general regions and the predominating winds for that date read from archived ASCAT maps.*

**Daily Wind Observations**

| Year | Month | Day | TQ WindV* | TQ WindD** | KQ WindV | KQ WindD | SB WindV | SB WindD |
|---|---|---|---|---|---|---|---|---|
| **2014** | Oct | 12 | 5-15 | NE | 5-20 | NNW | 5-15 | N |
| | | 18 | 10-20 | NNE | 20-30 | NNE | 15-30 | N, NE*** |
| | | 21 | | | | | | |
| | | 24 | 10-25 | N | 15-20 | NE | 5-15 | N, NW |
| | | 26 | 5-15 | NW | 5-15 | W | 25-35 | N |
| | | 30 | 15-30 | NNE | 15-20 | NE | 5-10 | E |
| | | 31 | 15-50 | NNE | 15-50 | NE | 20-50 | NE |
| | Nov | 2 | 0-5 | NW | 10-25 | NE | 15-25 | NE |
| | | 3 | 5-15 | SW | 5-10 | SE | 5-10 | WSW |
| | | 5 | 20-40 | NNE | 20-30 | NE | 10-15 | N |
| | | 6 | 5-10 | NE | 10-35 | N | 30-50 | N |
| | | 7 | 5-15 | SW | 20-30 | SSW | 30 | S |
| | | 9 | 30-35 | NE | 20-30 | NE | 5-15 | NE |
| | | 12 | 40 | NNE | 35-50 | NE | 25-30 | NE |
| | | 13 | 40-45 | NE | >50 | NE | 30 | N |
| | | 14 | 30-40 | ENE | 25-30 | NE | 10-15 | NE |
| | | 17 | 10-15 | SE | 5-25 | SSE | 10-25 | SW |
| | | 20 | 10-15 | SW | 10-15 | S | 10 | SSE |
| | | 21 | 5-10 | NW | 10-20 | SE | 10-15 | SSE |
| | | 22 | 5-15 | NE | 5-15 | NE | 5-20 | SE |
| | | 23 | 15-45 | E | 10-30 | SE | 5-20 | SE |
| | | 24 | 10-20 | NE | 5-15 | E | 10-15 | SSW |
| | | 25 | 5-15 | SW | 5-20 | W | 10-15 | S |
| | | 26 | 5-15 | NE | 0-10 | NE, S | 0-10 | N,S,W |
| | | 27 | 15-25 | NE | 10-20 | NE | 15-25 | SW |
| | | 29 | 10-25 | SW | 15-25 | S | 20-35 | SE |
| | | 30 | 15-30 | SW | 20-35 | N | 15-30 | E |
| **2014** | Dec | 1 | 10-30 | SW | 10-20 | SW | 25-40 | WSW |
| | | 2 | 20-30 | W | 15-35 | NE | 5-20 | NW |
| | | 3 | 10-35 | W | 10-20 | SSW | 20-30 | SW |
| | | 4 | 5-20 | NE | 20-30 | ENE | 30-45 | N |
| | | 6 | 5-35 | NNW | 25-35 | NE | 15-30 | NE |
| | | 7 | 15-30 | W | 5-15 | NE | 25-30 | NE |
| | | 8 | 20-45 | ENE | 25-35 | NE | 10-25 | N |
| | | 12 | 10-20 | W, SSW | 10-25 | NW | 5-15 | NNW |
| | | 13 | >50 | NW | 20-30 | NE | 25 | SE |
| | | 15 | 20-30 | SE | 10-25 | SE | 30-35 | NNW |

**Table contents continued on next page**

| | | | | | | | | |
|---|---|---|---|---|---|---|---|---|
| | | 16 | >50 | NE | 35-40 | NE | 5-15 | SE |
| | | 17 | 10-35 | NW | 15-35 | NE | 10-30 | SE, NE |
| | | 18 | 5-15 | NE, E, SE | 0-20 | NE, NW,SSE | 10-20 | S |
| | | 19 | 20-25 | SE | 5-25 | E | 10-15 | S |
| **2015** | Oct | 2 | 15-30 | NW | 5-25 | NE, NW | 0-15 | NW,W,SW |
| | | 3 | 20-40 | NE | 10-20 | NE | 0-10 | W |
| | | 7 | 25-39 | NE | 25-30 | NE | 15-35 | N |
| | | 9 | 0-15 | E, SE | 0-15 | E, NW | 10-35 | E, N |
| | | 14 | 0-30 | SW | 10-25 | W | 10-30 | SW |
| | | 16 | 0-15 | NW, NE, S | 0-20 | SW | 20-30 | SW |
| | | 19 | 0-15 | NE, SSW | 0-15 | SSW | 20-25 | SW |
| | | 21 | 10-20 | NE | 15-30 | NE | 20-25 | NE |
| | | 25 | 0-20 | NE | 0-15 | NE | 5-20 | N |
| | | 26 | 15-30 | S | 5-30 | SE | 20-30 | SE |
| | | 27 | >50 | E | 5-20 | ENE | 0-10 | E, SE, SW |
| | | 28 | 5-20 | E | 30-35 | NE | 10-25 | ENE |
| | Nov | 2 | 15-30 | NE | 10-30 | NE | 15-25 | NE |
| | | 4 | 20-35 | NE | 20-30 | NE | 20-40 | NE |
| | | 7 | 30-40 | NE | 30-50 | NE, N | 10-30 | N |
| | | 8 | 5-15 | SW | 10-35 | N | 10-20 | S |
| | | 9 | 10-20 | NE | 10-25 | NE | 10-30 | N |
| | | 11 | 10-40 | NE | 20-30 | NE | 15-30 | N |
| | | 12 | 5-20 | NE | 25-30 | NE | 10-20 | NE |
| | | 14 | 10-25 | NE | 5-20 | NE | 15-20 | N |
| | | 16 | 10-25 | NE | 20-35 | NE | 20-30 | NE |
| | | 17 | 25-45 | NE | 20-35 | NE | 20-30 | N |
| | | 18 | 0-25 | NE | 0-20 | NE | 20-25 | N |
| | | 19 | 10-20 | W | 0-10 | NW | 10-20 | N, NE |
| **2015** | Nov | 20 | 5-25 | W | 10-15 | SW | 10-20 | W |
| | | 21 | 0-20 | W | 0-10 | NE | 10-15 | NW |
| | | 22 | 10-35 | W | 20-30 | NNE | 0-10 | S, SE |
| | | 23 | 10-35 | E | 10-20 | SE | >50 | N |
| | | 24 | 10-25 | NW | <5-25 | NW, NE | 35-50 | N |
| | | 26 | 10-30 | E, W | 15-30 | NE | 30-40 | N |
| | | 28 | 20-30 | NE | 20-30 | NE | 30->50 | N |
| | | 29 | | | 20-30 | NE | 35-40 | N |
| | Dec | 1 | 25->50 | E, NE | 30->50 | NE | 25-30 | N |
| | | 2 | 25->50 | NE | 30-50 | ENE | 40->50 | N |

**Table contents continued on next page**

| | | | | | | | | |
|---|---|---|---|---|---|---|---|---|
| | | 3 | 20->50 | NE | 30-40 | NE | 30-40 | N |
| | | 4 | 30-40 | NE | 20-40 | NE | 20-30 | N |
| | | 5 | 10-30 | E | 0-10 | E | 25-40 | N |
| | | 6 | 15-20 | SW | 5-25 | SE, NE | 10-20 | W |
| | | 8 | >50 | NE | >50 | NE | 35-45 | NE |
| | | 11 | 0-15 | SW | 5-10 | S | 10-20 | WSW |
| | | 12 | 0-10 | SW | 0-15 | E | 10-25 | N |
| | | 13 | 5-30 | All dir. | 10-20 | NE | 20-40 | N |
| | | 14 | 20-40 | NE | 30-35 | NE | 30->50 | NE |
| | | 15 | 10-30 | NE | 10-45 | NE | 35-40 | NE |
| | | 17 | 25-35 | NE | 20-40 | NE | 30-45 | N |
| | | 18 | 10-30 | NE | 15-30 | NE | 10-30 | N |
| **2016** | Nov | 1 | 10-35 | NE, SE | 0-15 | NE | 0-20 | S |
| | | 3 | 20-30 | N | 10-40 | E, NE | 30-40 | N |
| | | 6 | 10-25 | SSW, NE | 5-20 | N, S, E | 20-40 | SSW |
| | | 7 | 20-40 | NW | 0-20 | NW, SW | 20-30 | SSW |
| | | 8 | 5-10 | W | 15-40 | ENE | 15-30 | SSE |
| | | 13 | 25-40 | E | 10-40 | SW | 10-20 | S, E |
| | | 15 | 5-20 | WNW | 5-30 | E | 5-20 | W, N |
| | | 18 | 0-15 | SE | 5-15 | N | 30-45 | N |
| | | 19 | 5-10 | NW | 0-15 | WNW, NE | 25-30 | N |
| | | 21 | 10 | SE | 0-15 | NE | 0-25 | NNW |
| | | 22 | 0-15 | NE | 0-15 | NW, SW | 0-20 | SE |
| | | 23 | 10-25 | NE | 10-20 | ENE | 0-20 | S |
| | | 25 | 5-20 | NW | 0-10 | E, NW | 25-40 | N |
| | | 27 | 10-30 | SW | 10-20 | SE | 10-15 | SW |
| | | 28 | 10-15 | NW | 5-20 | N, SW | 10-30 | S, N |
| | | 30 | 30-40 | NE | 15-30 | NE | 20-35 | N |
| **2016** | Dec | 1 | >50 | NE | 25-40 | NE | 10-20 | N, NE |
| | | 2 | 15-40 | NE | 10-30 | SE, NE | 20-25 | ENE |
| | | 3 | | | 0-20 | NE | 0-20 | N |
| | | 4 | >50 | NE | 20-30 | NE | 10-25 | N, NE |
| | | 5 | | | 0-15 | N, S | 5-15 | SW |
| | | 9 | 30-40 | NE | 25-40 | NE | 25-30 | N |
| | | 10 | | | 20-35 | NE | 5-30 | E |
| | | 11 | | | 20-35 | NE | 5-25 | E, NE |
| | | 12 | 5-10 | NE | 10-15 | SW | 20-40 | N |
| | | 13 | 20-40 | N | 25-40 | NE | 5-20 | NE |
| | | 14 | 5-20 | S | 20-30 | E | 10-40 | E, N |
| | | 15 | | | 25-35 | NE | 25-30 | ENE |
| | | 16 | 0-10 | W | 20-25 | SW | 20-35 | NW, N |

**Table contents continued on next page**

| | | | | | | | |
|---|---|---|---|---|---|---|---|
| | 17 | 25-40 | E | 5-30 | E, N | 0-10 | NE, SW |
| | 18 | 10-25 | SW | 10-35 | SW | 10-25 | SW |
| | 19 | | | 0-10 | SW | 20-30 | SW |
| | 20 | | | 5-15 | SE | >55 | N |
| | 21 | 10-20 | NW | 10-20 | S | 10 | NE |

Regions:
TQ= Tasiilaq
KQ= Kangerdlugssuaq
SB= Scoresby

Key:
*WindV is Wind Velocity in knots
**WindD is Wind Direction (indicates where wind is from)
***Commas indicate difference across area

*Table 9: Sea surface temperatures were read for three generalized regions in the study area. The minimum value in the region was recorded from the CLASS SSTs map for each day, where available.*

**Sea Surface Temperatures* 2014-15**

| Year | Month | Day | Tasiilaq | Kangerdlugssuaq | Scoresby | Likely pre-conditioned |
|---|---|---|---|---|---|---|
| **2014** | October | 12 | 3 | 1 | -0.5 | *** |
| | | 18 | 3 | 1 | -1 | |
| | | 21 | 2.5 | 0 | -1 | |
| | | 24 | 4 | 0 | -1.5 | |
| | | 26 | 3.5 | 0 | -1 | *** |
| | | 30 | | | | |
| | | 31 | 2 | 0.5 | 0 | |
| | November | 2 | | | | |
| | | 3 | 2 | -1.5 | 0 | |
| | | 5 | | | | |
| | | 6 | | | | |
| | | 7 | 2 | -1 | -0.5 | |
| | | 9 | | | | |
| | | 12 | 2 | -1 | -1 | *** |
| | | 14 | 4 | -0.5 | -1 | |
| | | 17 | 3.5 | -1 | -1.5 | *** |
| | | 20 | 3.5 | -1 | -1.5 | *** |
| | | 22 | | | | |
| | | 23 | | | | |
| | | 24 | | | | |
| | | 25 | 2.5 | -1 | -2 | |
| | | 26 | | | | |

**Table contents continued on next page**

| | | | | | | |
|---|---|---|---|---|---|---|
| | | 27 | 3.5 | -1.5 | -1 | *** |
| | | 29 | | | | |
| | | 30 | | | | |
| | December | 1 | | | | |
| | | 2 | 3.5 | -1.5 | -1.5 | |
| | | 3 | | | | |
| | | 4 | 3.5 | -1.5 | -1.5 | *** |
| | | 6 | | | | |
| | | 7 | | | | |
| | | 8 | 3 | -1.5 | -1 | *** |
| | | 12 | 3 | -1.5 | 0 | |
| | | 13 | | | | |
| | | 15 | | | | |
| | | 16 | 3 | -1.5 | 0 | |
| | | 17 | | | | |
| | | 18 | | | | |
| | | 19 | | | | |
| **2015** | October | 2 | 1 | 0 | 0 | |
| | | 3 | | | | |
| | | 7 | 1 | -0.5 | -1.5 | *** |
| | | 9 | 2 | 0 | -1 | |
| | | 14 | 2.5 | 0 | -1 | *** |
| | | 16 | 1.5 | -0.5 | -1 | |
| | | 19 | 1 | -1 | -0.5 | *** |
| | | 21 | | | | |
| | | 25 | 1 | 0 | -0.5 | *** |
| | | 26 | | | | |
| | | 27 | 1.5 | -0.5 | -1 | |
| | | 28 | 2 | -0.5 | -1 | *** |
| | November | 2 | 3 | -1.5 | 0 | *** |
| | | 4 | | | | |
| | | 7 | 2.5 | -1.5 | 0 | *** |
| | | 8 | | | | |
| | | 11 | 3 | -1.5 | -1 | *** |
| | | 12 | 3.5 | -1 | 0 | *** |
| | | 14 | | | | |
| | | 16 | | | | |
| | | 17 | 3 | -1.5 | 0.5 | |
| | | 18 | | | | |
| | | 19 | | | | |
| | | 20 | 3 | -1.5 | 0 | |
| | | 21 | | | | |
| | | 22 | | | | |

**Table contents continued on next page**

| | | | | | |
|---|---|---|---|---|---|
| | 23 | | | | |
| | 24 | 1 | -1.5 | -0.5 | |
| | 26 | 1 | -1.5 | -1.5 | *** |
| | 28 | | | | |
| December | 1 | 1.5 | -2 | 0 | |
| | 2 | | | | |
| | 4 | 3 | -1.5 | 0 | |
| | 5 | | | | |
| | 6 | 2.5 | -1.5 | 0 | *** |
| | 11 | 2.5 | -1.5 | 0 | |
| | 12 | | | | |
| | 13 | | | | |
| | 15 | 2.5 | -1.5 | 0 | |
| | 17 | | | | |
| | 18 | | | | |

***minimum Temperatures in area in °C**

*****taken from closest available dates**

**NOAA CLASS (Sea Surface Temperature (50 KM) (SST50)**

**Product discontinued in 2016**

*Table 10: Qualitative log of analysis combining all available climate information and imagery for each date in order to make an assessment about which days were pre-conditioned by the climate.*

## Qualitative Log

**Observations of Sentinel-1 imagery in combination with archived weather data.**

| Year | **Month** | **Day** | **Observations** | **Pre-conditioned** |
|---|---|---|---|---|
| **2014** | October | 12 | A lot of extensive formations adjacent to Scoresby and just south of pack | * |
| **2014** | October | 18 | Gravity waves and boundary rolls, very little formation | |
| **2014** | October | 19 | No formation, storm with winds >50 knots. Storm visible in Optical imagery (MODIS) | |
| **2014** | October | 21 | High winds, storm, very little formation. | |

**Table contents continued on next page**

| | | | | |
|---|---|---|---|---|
| **2014** | October | 24 | Very extensive calm, cold pools in MIZ. Suspect a lot of formation. | * |
| **2014** | October | 26 | Extensive cold pool south of Scoresby in MIZ. Suspect formation. No formation elsewhere, winds high in open ocean and north. Gravity waves, boundary rolls in south. | * |
| **2014** | October | 30 | Higher winds away from pack. Underwater turbulence and boundary rolls. Likely formation by pack adjacent to Scoresby. | |
| **2014** | October | 31 | Clear formation of varying types. High winds in the north and open ocean. | * |
| **2014** | November | 1 | Big storm, no formation. | |
| **2014** | November | 2 | High winds, very minor formation area in calmest wind zone. | |
| **2014** | November | 3 | Clear weather and cold/calm pools, possible formation, but high air temperatures | |
| **2014** | November | 5 | Formation in south and further into open ocean. | |
| **2014** | November | 6 | Poor conditions in MIZ, likely young, not new, ice. Formation internal to pack where conditions are clear and calm. | |
| **2014** | November | 7 | Stormy and windy in North and open ocean along coast. Calmer in south. | |
| **2014** | November | 9 | Favorable in North. Can see formation between two overlapping images. | |
| **2014** | November | 12 | Very unfavorable, very high winds. Edge of storm. | |
| **2014** | November | 13 | Stormy, winds >40 knots. | |
| **2014** | November | 14 | High winds, unlikely formation. | |
| **2014** | November | 17 | Very calm offshore, in expansive pools. Suspected formation. | * |
| **2014** | November | 20 | Small formation areas, windy conditions off-shore. | |

**Table contents continued on next page**

| | | | | |
|---|---|---|---|---|
| **2014** | November | 21 | Several large formation areas. | * |
| **2014** | November | 22 | Large formation in south. Too windy in north/elsewhere. | * |
| **2014** | November | 23 | No large formation in view, but suspected north of image. Storm in south. | |
| **2014** | November | 24 | Only small formations. Very windy. | |
| **2014** | November | 25 | Some formation in sheltered MIZ, mixed because of moderate winds. | |
| **2014** | November | 26 | Major formation, very variable in open ocean. Clouded, but mostly calm. | * |
| **2014** | November | 27 | Favorable formation in south. Too windy in north. Calmer near shore in the south. | * |
| **2014** | November | 29 | Some formation in south. Low pressure moving past Tasiilaq. | * |
| **2014** | November | 30 | Some formation. Could have been more formation, but not dark enough in south, perhaps a lot of young, not new, ice? | |
| **2014** | December | 1 | Gravity waves, high winds, little formation. | |
| **2014** | December | 2 | Not ideal wind conditions, still some formation, much in south. | * |
| **2014** | December | 3 | Windy conditions, boundary roll, and gravity waves. Some massive, clear formation areas! Upwelling and fishing boats? | * |
| **2014** | December | 4 | Good formation in south. Very high winds in north. | * |
| **2014** | December | 6 | Too windy in most of study area. Major gravity waves. Some large formation connected to north of study area. | |
| **2014** | December | 7 | High winds especially in the north, little formation, but very clear on ice edge, in south. | |
| **2014** | December | 8 | High winds, formations on the edges (lee-side? North) of MIZ. Questionable (unlikely) formation because of winds in south. | |

**Table contents continued on next page**

| | | | | |
|---|---|---|---|---|
| **2014** | December | 12 | Boundary roll, low contrast, not much formation. Mostly forming on MIZ edge, small patch further away from pack. | |
| **2014** | December | 13 | Several large formations . Boundary roll. High winds offshore. Suspect more in south. | |
| **2014** | December | 15 | Large formation, potentially. Expansive pool is in south with calm winds. Unsure how much is formation. Some being mixed by winds that are too high further out into the ocean. Digitized by texture. | * |
| **2014** | December | 16 | Not much clear formation, too windy. | |
| **2014** | December | 17 | To windy for substantial formation . | |
| **2014** | December | 18 | Does not appear calm enough for large formation, some areas look close. May be young ice? Or just cold upwelling on pack edge being mixed by wind? | |
| **2014** | December | 19 | Unsure why formation is low in MIZ (internal formation). Winds likely. | |
| **2015** | October | 2 | Expansive potential formation. Most are likely ice. | * |
| | October | 3 | Formation is strange. Either very large, or algae. Calm winds. | * |
| | October | 7 | Very little pack and formation. Boundary roll visible. Very strong wind gradient with opposing winds. | |
| | October | 9 | Boundary rolls, gravity waves. Not much formation except on the lee-side of coastal areas and a little bit on the lee-side of pack which is flush with North Scoresby. VIS shows storm in north. | |
| | October | 14 | A lot of coastal formation. Lee side of southwesterly winds. | * |
| | October | 16 | Windy near pack area. Formation disrupted in north and on leeward coast. South of images it's calmer. | |

**Table contents continued on next page**

| | | | | |
|---|---|---|---|---|
| | October | 19 | Weather features in south, not really ice-indicative. Boundary of a weather front more likely than formation. | |
| | October | 21 | Clear skies, high winds, very little MIZ formation. Leeward coastal formation. | |
| | October | 25 | Large formation in south. | * |
| | October | 26 | No good MIZ formation, big gyres. May have recently frozen. Low contrast. | |
| | October | 27 | Huge amounts of potential formation. | * |
| | October | 28 | Formation North of study area (except a little bit) and in North Iceland (Iceland not digitized). High winds south of Scoresby. Boundary roll. | |
| | November | 2 | High winds, very little recently frozen ice present. | |
| | November | 4 | No ice formation, very high winds. | |
| | November | 7 | Gravity waves, high winds. Formation only in pack. | |
| | November | 8 | Boundary layer, no formation. | |
| | November | 9 | Too windy for formation. | |
| | November | 11 | Very limited formation because of winds. | |
| | November | 12 | Some formation, mostly limited, one nice area with locally favorable winds. | * |
| | November | 14 | Large area of formation. Localized low winds and cold air temperatures. | * |
| | November | 16 | Limited formation. Not much contrast, especially in North where there are high winds. | |
| | November | 17 | Very little, or young, not new, formation. Large upwelling near Jan Mayen? | |
| | November | 18 | Nice sized MIZ formation. Winds slower where the formation is. | * |

**Table contents continued on next page**

| | | | | |
|---|---|---|---|---|
| | November | 19 | Large formation in south, winds very calm where ice formed. | * |
| | November | 20 | Some pre-conditioned, formation areas where winds are low. | * |
| | November | 21 | Very pre-conditioned. Very large potential formation areas along Blosseville Coast. One very questionable storm in south, south of image. Ships and upwelling? | * |
| | November | 22 | Very calm in north. Fairly large edge formations, however poor contrast. Winds look turbulent at edge, and high winds in open ocean. | * |
| | November | 23 | Several recently frozen patches mark 'N'. High winds in open ocean. Calm spot near pack. Huge storm in north. Boundary roll and gravity waves in north and open ocean. | |
| | November | 24 | NIC confirms large ice areas. Very calm wind in formation area. Very high winds in north. My analysis lined up perfectly with NIC MIZ edge. | * |
| | November | 26 | Very low contrast. Ice in north looks recently frozen. Huge boundary rolls and gravity waves. | |
| | November | 28 | Very strong wind conditions. Weak formation, if truly any. | |
| | November | 29 | Very low contrast. No visible formation. | |
| | December | 1 | Recently frozen ice. Really strong winds, and thin, recent formations. | * |
| | December | 2 | No new ice, high winds, and boundary rolls. | |
| | December | 3 | No new formation, very strong winds. | |
| | December | 4 | Some formation. Surprising because winds are high (although data is 6 hours off). | * |
| | December | 5 | Large expanses of formation in south. Boundary rolls, wind streaks visible, local calm. Excessive winds north of study area. | * |

**Table contents continued on next page**

| | | | | |
|---|---|---|---|---|
| | December | 6 | Some recently frozen. Huge formation in MIZ and in middle of Strait (in the southernmost image) | * |
| | December | 8 | No new formation, high winds. | |
| | December | 11 | Suspect large formation in south, not much in north because of high winds. Very calm, glimpses of formation south of study area. | * |
| | December | 12 | Huge southern MIZ formations. Higher winds in north. Calm in south. Boundary rolls. Confusing open ocean areas outside of NIC zone, and marked 'N' since they could contain ice. | * |
| | December | 13 | Higher winds in north. Formation in south limited to shelter near pack. But strong where it is. | |
| | December | 14 | Recently frozen in North, not marking. | |
| | December | 15 | Intense boundary layer and gravity waves in north (no formation. Still excessive wind in northern image. Limited southern formation, newly frozen, marked 'N'. | |
| | December | 17 | Large, clear formations. Some recently frozen (unmarked). Very unfavorable winds, but very cold air temperatures. | * |
| | December | 18 | Some large formation areas, clearer in north. Boundary roll in south and area of calm in middle of Strait. | * |
| | December | 20 | No formation. | |
| **2016** | November | 1 | Large cold pool areas, air temperatures may be too warm for mass formation. | |
| | | 3 | Mostly coastal leeward cold pools. | |
| | | 6 | A little coastal formation where sheltered. Conditions good because formation north of area. | * |
| | | 7 | Only coastal formation, winds too strong. | |

**Table contents continued on next page**

| | | | | |
|---|---|---|---|---|
| | | 8 | Boundary roll and gravity waves. High winds, and very limited but likely (mostly coastal) formation. | |
| | | 13 | Substantial formation south of Scoresby, where winds are slowest <10 knots. | * |
| | | 15 | Appears to be weather by Scoresby. Mix of calm and gusts (5 and 20 knots, respectively) | |
| | | 18 | Formation in North Scoresby (morning). Formation south of Scoresby in the evening. Slows to 10 knots. Boundary layer and high winds all day, moving southwards. | * |
| | | 19 | Some very small formation patches (more in north of area) | |
| | | 21 | Massive calm area, large areas with winds from 5-10 knots. | * |
| | | 22 | Large potential areas. Very calm expanses. Unsure about largest area, out of NIC zone. | * |
| | | 23 | Boundary roll, large calm area and calm winds, some formation. Winds increase in South. | |
| | | 24 | Too windy for formation. | |
| | | 25 | Only very little formation. Too windy in north, not sure why in south. | |
| | | 27 | Large formation areas. Calm and cold so ice is likely. | * |
| | | 28 | Boundary roll visible. Favorable wind conditions and substantial formation in south. | * |
| | | 30 | Gravity waves, high winds, random southern formation. Formation not digitized near Iceland. | |
| | December | 1 | Very minor formation. Should be more in north. Winds high in south. | |
| | | 2 | Large formation just north of area. Little in area. | |

**Table contents continued on next page**

| | | | | |
|---|---|---|---|---|
| | | 3 | Small formations, some along coast, expect more with calm winds in many areas. | |
| | | 4 | Boundary rolls in morning. Some southern formation. Expect more in Scoresby. | |
| | | 5 | Massive boundary roll and waves. Followed MIZ when digitizing because the new ice boundary is unclear. Favorable winds. | |
| | | 9 | Recently frozen formations. High winds. | |
| | | 10 | Very tiny, maybe recently frozen formations. High winds in south. Possible formations in north of image where winds are 5-10 knots. | |
| | | 11 | Turbulence, boundary roll, below-surface waves. Expect formation north of image where winds are lower. | |
| | | 12 | Boundary roll. Appears to be high winds. Some formation where winds are calmer in south. | |
| | | 13 | Many small formation areas. Calm in north corresponds to small formation areas in morning. Winds get too strong for formation in evening image. | * |
| | | 14 | High winds, suspicious formation. Calm area too far from Scoresby to mark. May be formation off of Iceland, also not marked. | |
| | | 15 | Appears too wind for substantial formation. | |
| | | 16 | Too windy, especially in north. Boundary rolls and gravity waves. | |
| | | 17 | Gravity waves, boundary rolls. Expect more formation with calm conditions in the north of image. | |
| | | 18 | Good formation in calm areas. Most areas limited by extreme wind further east. | * |
| | | 19 | Much recently frozen. Should be more formation in south, south of image. | * |

**Table contents continue on next page**

| | | | | |
|---|---|---|---|---|
| | | 20 | High winds in open ocean, only formation is pack-protected. Major gravity waves. | |
| | | 21 | Boundary roll, calmer in northern half in second half of day. Morning in north, too windy and no formation. | |

*Table 11: List of climate pre-conditioned freeze-up days, according to analysis of Sentinel-1 imagery combined with historical climate data and supplemental imagery.*

| Pre-conditioned Days | | |
|---|---|---|
| **2014** | **2015** | **2016** |
| 10/12/2014 | 10/2/2015 | 11/6/2016 |
| 10/24/2014 | 10/3/2015 | 11/13/2016 |
| 10/26/2014 | 10/14/2015 | 11/18/2016 |
| 10/31/2014 | 10/25/2015 | 11/21/2016 |
| 11/9/2014 | 10/27/2015 | 11/22/2016 |
| 11/17/2014 | 11/12/2015 | 11/27/2016 |
| 11/21/2014 | 11/14/2015 | 11/28/2016 |
| 11/22/2014 | 11/18/2015 | 12/13/2016 |
| 11/26/2014 | 11/19/2015 | 12/18/2016 |
| 11/27/2014 | 11/20/2015 | 12/19/2016 |
| 11/29/2014 | 11/21/2015 | |
| 12/2/2014 | 11/22/2015 | |
| 12/3/2014 | 11/24/2015 | |
| 12/4/2014 | 12/1/2015 | |
| 12/15/2014 | 12/4/2015 | |
| | 12/5/2015 | |
| | 12/6/2015 | |
| | 12/11/2015 | |
| | 12/12/2015 | |
| | 12/17/2015 | |
| | 12/18/2015 | |